Estimation of contaminant losses

Mill Creek catchment, Lake Hayes

Prepared for Otago Regional Council

December 2023

Prepared by:
Neale Hudson, Annette Semadeni-Davies, Reza Moghaddam

For any information regarding this report please contact:

Scott Larned
Chief Scientist – Freshwater
+64 3 348 8987
scott.larned@niwa.co.nz

National Institute of Water & Atmospheric Research Ltd
PO Box 11115
Hamilton 3251

Phone +64 7 856 7026

Revision	Description	Date
Version 1.0	Final version sent to client	22 December 2023

Quality Assurance Statement		
	Reviewed by:	Dr Andrew Hughes
	Formatting checked by:	Rachel Wright
	Approved for release by:	Dr Scott Larned

Contents

Tables

Figures

Executive summary

In collaboration with the community and stakeholders, Otago Regional Council (ORC) has established water quality objectives for the region. In the case of Lake Hayes, persistently poor water quality led to development of a Lake Management strategy in 1995, with the objective of *"…improving the water quality of Lake Hayes, to achieve a standard suitable for contact recreation year round and to prevent further algal blooms"*

Subsequent investigations have identified several potential management actions, including reduction of nutrient inflow load, enhanced flushing of the lake using water sourced from the Arrow River (including a scenario involving hypolimnetic withdrawal of lake water), artificial aeration, and chemical dosing. Model predictions have indicated that catchment load reduction was central to achieving positive lake water quality outcomes.

In this report, we have estimated loads of key contaminants (nitrogen, phosphorus and suspended sediment) entering Lake Hayes over the period for which data exist. Data exist for:

- the Mill Creek at Fish Trap site (continuous discharge, and water quality data derived from flow-related event sampling, as well as routine grab samples):

- the inflow to the lake (Mill Creek at Lake Hayes site) - grab samples including event-related samples, as well as water quality surrogate measurements with a turbidity sensor, and a nitrate sensor:

- Mill Creek at Hunter Road, which represents contaminant loads entering the upper Mill Creek catchment, and which has a continuous turbidity sensor as well.

In addition to our data, ORC has collected a set of water quality samples from sites located across the catchment in a series of comprehensive water quality surveys (henceforth referred to as synoptic surveys).

Stream contaminant loads were estimated using several methods as follows:

- By relating measured concentration samples to discharge estimates, and using calibrated models to predict stream flow concentrations, and contaminant loads at daily, monthly and annual intervals.

- Calibrated statistical models were developed in Microsoft Excel using the "Solver" regression-fitting technique and in Python using an open-source regression modelling library (the Least Squares Optimisation tool).

- Using the LOADEST software modelling tool developed by the USGS. The modelling tool selected the "best" model for the purpose using in-built processes based on several statistical criteria.

- Multiple load estimation techniques were applied to water quality data derived from routine grab samples, event-related grab samples, and surrogate data (which represented suspended sediment and nitrate-N).

Data exist for total phosphorus (TP), dissolved reactive phosphate (DRP), nitrate plus nitrite N (NNN), total suspended sediment (TSS), as well as two surrogates: nitrate-N (measured continuously using

an optical sensor), and turbidity (a measure of water cloudiness, which can be used as a surrogate for TSS concentration and visual clarity).

Long term contaminant load estimates

Key results derived from the Mill Creek at Fish Trap site include:

- a 20% reduction in the 1994 TP load has been achieved since 1996, and annual loads have been less than a third of the 1994 values consistently since 2002.

- The annual TP load was 3.0 t in 1994, and the annual average load over the three year period 2018-202 was 0.6 t (a 79% decrease).

- The decrease in TP load estimated over time is primarily related to rainfall and runoff. The period 1994-2000 was characterised by having five of the seven largest annual discharge estimates measured between 1984 and 2021, whereas more recently, rainfall has been more "typical" of the long term period.

- When the estimated TP load data were separated into pre-2003 and post 2003 groups, seasonal patterns in the magnitude of TP load were similar between the two periods, but loads were considerably lower in all months during the post-2003 period. When estimated over the two periods, the median TP load/month decreased approximately 50%, from approximately 73 kg TP/month in 1984-2002, to approximately 36 kg TP/month in the period 2003-2021. During 2020, the estimated TP load varied from approximately 20 t TP in May to a maximum of 177 t TP in August.

- For NNN, annual loads decreased from more than 10 t/year in 1994 to an average of approximately 5 t/year over the period 2018-202 (a decrease of 51%).

The estimated NNN load at the Fish Trap site has a strong seasonal pattern, with a minimum in February and a maximum in spring. For the post-2002 period, the maximum monthly load occurred in September. In 2020, the minimum estimated monthly NNN load (280 kg) occurred in June, and the maximum estimated NNN load was observed in September (738 kg).

Predicted TSS loads were more variable in the pre-2002 period that other contaminants, and the magnitude of the estimated load was sensitive to the estimation technique. Using the LOADEST estimations, pre-2002 annual load estimates ranged from 230 t/year (1990) through to 2,100 t/year (1994 and 1995). Post 2002, seasonal loads have been generally lower and more consistent, ranging from 932 t in 2002 to a low of 120 t/year in 2017. A strong seasonal pattern was evident in both periods, but with considerably fewer very high estimates of TSS load in the latter period.

A substantial set of flow-related grab samples (representing dissolved and particulate forms of nitrogen and phosphorus) exist for the Mill Creek at Lake Hayes site. The following annual contaminant loads were estimated at this site (Table i):

Table i: **Annual contaminant loads for the Mill Creek at Lake Hayes site.**

Year	Load (kg/year)				Load (t/year)
	DRP	NNN	TN	TP	TSS
2018	29.88	5458.9	6126.5	642.1	396.8
2019	89.69	5207.7	8909.7	743.7	409.7

Year	Load (kg/year)				Load (t/year)
	DRP	NNN	TN	TP	TSS
2020	146.01	5683.9	10171.4	1371.3	850.1
2021	62.64	5900.2	4128.0	913.4	480.0

Use of surrogate measurements to estimate contaminant loads.

Nitrate-N instantaneous load (flux) estimates were obtained for the Mill Creek at Lake Hayes site as the product of concentration derived from a TriOS sensor (measured at 15 minute intervals), and discharge measured at the same frequency; annual loads derived from these estimates are compared with those derived from modelling in Table ii. Within the limitations imposed on the LOADEST method by available calibration data, there is reasonable concordance between these estimates.

Table ii: **Comparison of annual load estimates derived from two approaches. ,**

Year	Annual load per estimation method (kg)	
	TriOS-nitrate	LOADEST NNN
2019	6951	5126
2020	8023	5841

Several approaches were explored to estimate TSS and TP loads at the "Mill Creek at Hunter Road" and "Mill Creek at Lake Hayes" sites using turbidity as a surrogate metric. Regression equations were derived, and model fit was evaluated using several performance metrics. Monthly and annual loads were derived for both water quality variables at both sites. The reliability of these estimates was influenced by several factors, including: amount of surrogate measurement record (proportion of theoretical total amount of data); the extent of extraneous record (e.g., interference with the optical method of measurement); the number of grab samples available for calibration of regression models; and the nature of grab sample data available for the Hunter Road site (regular monthly frequency vs. flow-proportional samples, collected during flood events).

Synoptic survey results

We were able to compare the DRP and TP concentrations and fluxes measured at seven sites in the Lake Hayes catchment at two time periods: 1997, and over the three year period 2018-2020.

Median TP concentrations increased at three sites since 1997 (McMullan Ck at Malaghan Road, Mill Creek at Hunter Road, and at the inflow to Lake Hayes), and median DRP concentrations increased at the latter two sites and at the "Dan O'Connell Ck 300 m u/s" site over this period. At other sites, concentrations remained the same or decreased.

The synoptic survey data collected from 2018-2020 show consistent spatial patterns in the magnitude of instantaneous load for several water quality variables:

- Relatively small contaminant loads were evident at all sites in the upper catchment compared to the loads from the lower catchment.

- A step-change in both concentration and flux of nitrogenous material was evident at the Hunter Road site, suggesting that nitrogen was entering Mill Creek in runoff or groundwater from adjacent land, or from unmonitored tributaries upstream of this site.

- A similar step change was evident for DRP and particularly TP, which was accompanied by a significant step change in median TSS flux. These results indicate that TSS entering Mill Creek upstream of Hunter Road is likely to contribute the bulk of the TP load.

- The DRP and TP flux increases slightly downstream of Hunter Road, suggesting that the bulk of phosphorus load enters Mill Creek upstream of Hunter Road.

The bulk of nitrogenous material enters Mill Creek in the reach downstream of Hunter Road (as indicated by flux estimates). Available information suggests that the bulk of the nitrogen load is derived from surface runoff or shallow groundwater that discharges to Mill Creek, and not to the deeper groundwater system that discharges to the lake via the spring.

The results from the synoptic surveys represent both base and event sized flows, and should be used with caution because they are relatively few.

Seasonality of contaminant loads

Estimated loads demonstrate a consistent seasonal pattern, with smaller loads in late summer/autumn, and the bulk of the load transported in late winter/spring period. The bulk of the contaminant load is therefore transported during high-flow conditions (either during rain events or during snowmelt). From the data available, it is not possible to differentiate between rainfall or snowmelt events.

Land use and catchment modelling

Catchment modelling indicates that land use has remained relatively constant since 1996. The dominant land cover classes may be considered pasture (ca. 55%), tussock (ca. 18%) and native and exotic forest (ca. 23%). Collectively, these cover classes currently comprise ca. 95% of the catchment, with urban land cover comprising 5% of the Lake Hayes catchment (an increase from 66 to 242 hectares between 1996 and 2018). The spatial variations in nutrient loads predicted by catchment modelling is consistent with the synoptic survey results:

- The bulk of the TP load that subsequently reaches Lake Hayes enters Mill Creek upstream of the Hunter Road site (56%), an additional 25% in the reach between Hunter Road and Waterfall Park, and the remaining 19% in the reach between Waterfall Park and the lake.

- The CLUES model predicts that a smaller proportion of the total TN load enters Mill Creek upstream of the Hunter Road site (39%), with the balance entering upstream of Waterfall Park (40%) and the lake inflow (31%).

Mitigation actions

Assessment of land cover, catchment modelling and load estimation indicates that the bulk of N, P and sediment load enters Mill Creek in the reach downstream of Hunter Road. The bulk of the contaminant loads enter the stream under elevated flow conditions. Land cover types contributing both N and P are dominated by pasture, and soil P comprises approximately one third of the total P load at each of the Hunter Road, Waterfall Park and lake inflow reaches.

We recommend that mitigation options identified in earlier investigations be reviewed. These included maintaining and restoring existing wetlands and riparian buffers, constructing sediment traps along the main stem of Mill Creek to capture total suspended solids and total phosphorus, and

which may also buffer storm- and snowmelt flows, establishing a constructed wetland, livestock exclusion (particularly in the upper catchment), and channel restoration in the lower catchment to slow movement of water and reduce bank erosion. Buffer condition could be improved by re-establishing riparian vegetation.

1 Introduction

1.1 Background to Lake Hayes and catchment

In collaboration with the community and stakeholders, Otago Regional Council (ORC) has established water quality objectives for the region. These are described in the Regional Plan: Water (2004). The regional plan has been through several iterations in response to community input and changes in national water resource management approaches. Currently, ORC is incorporating the outcomes of a 2018 review of the Water Plan into a Land and Water Regional Plan (LWRP), which is scheduled to be notified by 31 December 2023.[1] In addition to giving effect to recent changes in national policy, specifically the National Policy Statement for Freshwater Management 2020 (New Zealand Government 2020a; 2023) and associated National Environmental Standards (e.g., New Zealand Government 2020b), the LWRP provide the legal framework for policy and regulatory tools "to promote the sustainable management of Otago's water resources. To achieve this, the plan has policies and methods (including rules) to address issues of use, development and protection of Otago's freshwater resources, including the beds and margins of water bodies."[2]

Historical monitoring has identified that some catchments are subject to particular water quality issues. This led to specific investigations and the development of management plans for individual catchments including the Lake Hayes and the Mill Creek catchment, which is the focus of this report. Lake Hayes was used as a case study in a report prepared for the Ministry for the Environment (MfE) concerning the impact of land use on freshwater (Larned *et al.* 2018). Stressors to water quality outlined in Larned et al (2018) include historical deforestation, the introduction of exotic plant and fish species, the introduction and intensification of pastoral farming, land drainage and associated loss of wetlands, increasing use of fertilisers, and discharge of food processing waste to Mill Creek. Land use change across the catchment was accompanied by increased sediment and nutrient (particularly phosphorus) levels in the lake. Citing earlier work, Caruso (2000) described the Lake Hayes catchment as "a good example of a high-country agricultural/pastoral catchment in New Zealand where P is thought to be the primary cause of eutrophication of the lake in the past". There have been a series of responses aimed at addressing the deterioration of water quality or condition in Lake Hayes, including:

- publication of a Lake Management strategy in 1995, with the objective of *"…improving the water quality of Lake Hayes, to achieve a standard suitable for contact recreation year round and to prevent further algal blooms"* (ORC and QLDC 1995)

- preparation of a "Lake Hayes Restoration and Monitoring Plan" for the Friends of Lake Hayes Inc (Schallenberg and Schallenberg 2017)

---

[1] https://orc.govt.nz/plans-policies-reports/regional-plans-and-policies/water
[2] https://orc.govt.nz/plans-policies-reports/regional-plans-and-policies/water

- review of the Schallenberg and Schallenberg (2017) report in 2018 for ORC, including a detailed review of four lake remediation options and recommendations (Gibbs 2018), and

- preparation of the report "Scoping of diffuse pollution mitigation options for Mill Creek" for Friends of Lake Hayes Society, Inc., Otago Regional Council, Queenstown Lakes District Council, Department of Conservation (Goeller *et al.* 2020).

Potential mitigation strategies proposed to improve lake water quality include:

- food web manipulation to reduce the growth and prevalence of nuisance algae (Schallenberg and Schallenberg 2017),

- chemical dosing of the lake inflow or lake water surface to reduce mobilisation of phosphorus (P) from lake sediments (Gibbs 2018; Gibbs and Hickey 2018),

- increased flushing of the lake, using excess irrigation water from the Arrow River to remove nutrients from the lake water column (Gibbs 2018; Goldsmith and Hanan 2019),

- preferential withdrawal of nutrient rich waters from the bottom of the lake (hypolimnetic withdrawal) (Schallenberg and Schallenberg 2017; Goldsmith and Hanan 2019), and

- artificial destratification of the lake, to keep the lake fully mixed while also increasing oxygen concentrations in the lake, thereby reducing P release from sediments and decreasing algal biomass (Gibbs 2018).

A consistent recommendation from these investigations was that inputs of nutrients to Lake Hayes from the surrounding catchment should be reduced as part of an overall lake management or restoration response. Gibbs (2018) clearly linked the likely success of in-lake restoration actions to accompanying "catchment management strategies reducing the external carbon, nutrient and suspended solids loads to the lake".

McBride et al (2019) developed a physical-biogeochemical model (DYRESM-CAEDYM) for Lake Hayes that simulated the major in-lake physical and biogeochemical processes. This model was used to assess the likely efficacy of four of five of the mitigation strategies listed above: reduction of nutrient inflow load, enhanced flushing of the lake using water sourced from the Arrow River (including a scenario involving hypolimnetic withdrawal of lake water), artificial aeration and chemical dosing. Although all candidate mitigation actions were predicted to have a beneficial impact on lake water quality, model predictions indicated that catchment load reduction was central to achieving positive lake water quality outcomes.

To update their understanding of the current status of contaminant loading to the lake, ORC commissioned NIWA to repeat some of the work previously done, using more recent data and a range of methods for load estimation. In particular, ORC wished to understand whether one of the key objectives of the 1994 strategy was being achieved, namely, were the policy, regulatory actions and mitigation action undertaken by agencies and stakeholders having measurable beneficial impacts on lake water quality and lake condition.

The strategy made provision for periodic review of its effectiveness at five yearly intervals or less. This review would include assessment of changes to the quantity of phosphorus entering Lake Hayes from the surrounding catchment, chemical composition of the lake and changes in lake trophic state. If algal blooms occurred in the lake after a 20% reduction in the total annual phosphorus load to Lake Hayes was achieved (relative to 1994 figures), and/or in-lake phosphorus concentration was consistent with a specified water quality class, ORC would (in consultation with the community) consider additional mitigation strategies, including the in-lake treatment methods listed above.

1.2   Report scope

NIWA was commissioned to characterise contaminant concentrations and long-term changes in those concentrations, and to quantify contaminant loads at multiple points in the Lake Hayes catchment, using existing data. The contaminants of interest are total phosphorus (TP), dissolved reactive phosphorus (DRP), nitrate+nitrite-N (NNN), total N (TN), and total suspended solids (TSS).

Subject to limitations of available data, specific tasks agreed with ORC included:

A. Assessment of the use of continuous monitoring data when estimating N and P loads, including:

  – correlating continuous turbidity records (Fish Trap and Hunter Road sites) to estimated loads of contaminants,

  – use of proxy metrics such as turbidity to estimate the difference in loads between the upstream and downstream sites (where continuous sensors are deployed), for TSS, TN and TP, where a substantial proportion of the contaminant load is associated with particulate material,

  – correlating the NNN load derived from the continuous nitrate sensor record (at the Fish Trap site) with the load estimated using conventional regression techniques.

B. Comparison of estimated loads derived from continuous data against those estimated from:

  – grab samples and continuous stream flow records (using regression modelling) that provide concentration *vs* discharge relationships, and

  – grab samples and gauged flows obtained at the time of sampling (as undertaken by Caruso in 1999).

C. Characterising contaminant loads entering the lake under specific conditions, such as:

  – 'Below median' and 'higher flow' conditions (including estimation of the proportion of annual load entering the lake under these and other conditions, such as seasonally).

  – Using this information to better understand when (and under which conditions) the majority of the P, N and suspended sediment load enter the lake, and using this information to identify mitigation actions that could reduce contaminant inputs to the lake.

D. Determining the likely source and magnitude of nutrient load from the catchment, i.e., apportion the total inflow load to identifiable sub-catchment reaches.

E. Compare contemporary P loads with those estimated for 1994, to assess whether the 20% reduction in P loadings to the lake has been achieved, an objective of the Lake Hayes Management Strategy (ORC and QLDC 1995).

   – Options for estimating contaminant loads would be explored, and where possible, time-series of loads derived from these models would be used to compare loads estimated at annual, seasonal or over other periods of time.

   – Ensure that sensitivity of load estimation to hydrological conditions and annual rainfall was recognised in load estimation processes.

F. Use the Catchment Land Use for Environmental Sustainability (CLUES) model to assess land use impacts and the effects of land use change on annual TN and TP loads.

It should be noted that the data used in the above tasks were used "as received" – there was no expectation or allowance for undertaking data quality assurance or removal or editing of data that might be considered of poor quality or questionable. These aspects are particularly important with regard to data derived from high frequency water quality sensors, which provide surrogate estimates of specific water quality variables.

1.3   Report structure

Section 2 overviews the methodology followed to estimate and model contaminant loads and gives a brief description of the catchment, land uses and historical and contemporary water quality monitoring. Additional details of specific methods and processes applied in the assessment are also summarised in the appendices.

Section 3 summarises the outcomes from CLUES modelling, historical and contemporary hydrology and the results from comprehensive water quality surveys, referred to here as synoptic surveys. This term was used by Caruso (2000; 2001) to describe a series of samples collected from multiple locations with the Mill Creek/Lake Hayes catchment within a short time period (i.e., all sites sampled on the same day). Section 3 also presents the results derived from several load estimation approaches.

Section 4 discusses the results from the different load assessment techniques, and seasonal characteristics of contaminant loads.

Section 5 evaluates the results of this work against the requirements identified in Section 1.2.

2 Methods

2.1 Catchment description

The Hayes Creek catchment is covers approximately 50 km^2 northeast of Queenstown. Hayes Creek is a tributary of the Kawarau River, and incorporates Lake Hayes and the principal inflow to Lake Hayes, Mill Creek. There is also a perennial spring inflow to Lake Hayes which discharges groundwater near to the northwest shoreline of the lake.

Lake Hayes is believed to have been formed following separation from the ancestral Lake Wakatipu by outwash from the Shotover River. The catchment has steep to moderately steep mountain slopes to the north, rising to Coronet Peak, the highest point (1600 m). The Lake lies within a floodplain that comprises fans and terraces with moderately steep rolling hills around the perimeters of the catchment, shown in Figure 2-1.
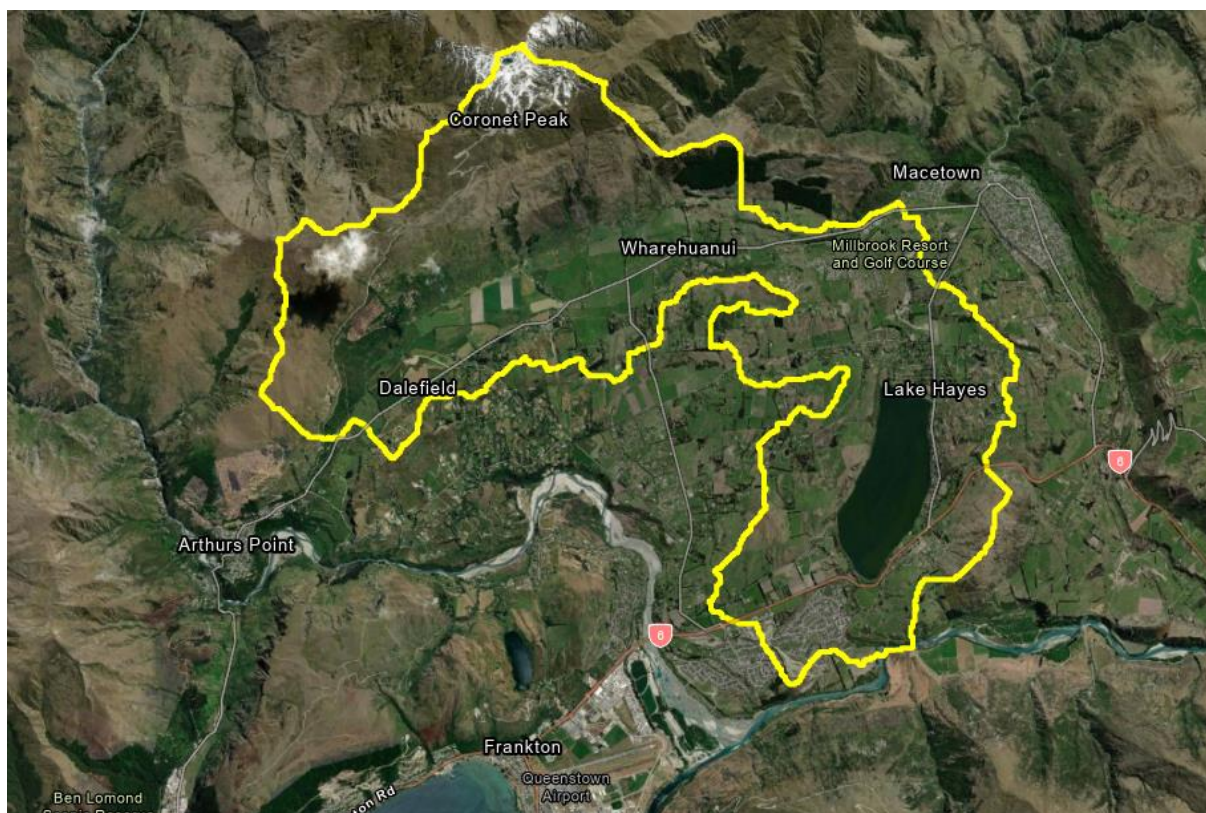
Figure 2-1:   Lake Hayes, Mill Creek inflow and Hayes Creek discharge to the Kawerau River to the south.
The surface water drainage network is detailed in Figure 2-2.

The original native tussock vegetation in the catchment has been replaced on the lowlands by pasture and crops, with sward grass predominating on the poorer soils in the valley and on the low altitude steep faces. The major land use classes are farming (46 %) and tussock (19%). Urban land use accounts for around 3% of the catchment area. Change in land use since the mid-1990s is discussed in Section 4.1.

2.2 CLUES modelling

The Catchment Land Use for Environmental Sustainability model (CLUES: Elliott *et al.* 2016) is a steady-state model that brings together three existing freshwater quality models and a national geo-database consisting of publicly available spatial data within a geographic information system (ArcMap) to predict water quality at the catchment scale. CLUES incorporates customised versions of SPARROW (Elliot *et al.* 2005; Schwarz *et al.* 2006); OVERSEER (Wheeler *et al.* 2014; latest release version 6.3, 2018), and the Soil Plant Atmosphere System Model (SPASMO; Rosen *et al.* 2004). The current version of CLUES has been calibrated nationally (Semadeni-Davies *et al.* 2019; Semadeni-Davies *et al.* 2020).

Catchment modelling was undertaken using the River Environment Classification (REC; Snelder and Biggs 2002; Snelder *et al.* 2010) version 2.5 digital stream network. In this network, the catchment consists of 105 river segments that have a combined length of 75 km. Lake Hayes covers an area of 2.74 km^2. CLUES is semi-distributed with the smallest spatial unit being the REC reach sub-catchment. Spatial data are lumped within each subcatchment.

Land use[3] is represented by the proportion of each sub-catchment covered by each of 19 land use classes and water (or diffuse sources) within the model, while the other spatial data (e.g., slope, soil drainage and climate) are represented by the spatially weighted average for the sub-catchment area. The baseline land use data in CLUES has the reference year 2018 and was derived from the Manaaki Whenua-Landcare Research Land Cover Database v5 (LCDB5) and the AsureQuality Agribase agricultural database. Land use classes within the catchment are given in Section 3.2.1.

The CLUES load calculation method has been described by Elliott *et al.* (2005) and Elliott *et al.* (2016). In brief, contaminant loads from diffuse sources (i.e., land use classes) are calculated for each reach sub-catchment as the product of the source area and associated source yield. The phosphorus load includes soil erosion as an additional source. The generated load is then reduced by a catchment attenuation factor that is a function of soil drainage class, and the mean annual rainfall and temperature for each subcatchment. Where there are known point sources, these are added to the delivered load (there are no known point sources in the Lake Hayes catchment). Once delivered to the stream network, the total loads for each contaminant are routed downstream such that the instream load for a reach is the total of the upstream load and the reach load, less stream attenuation (modelled as a function of stream length and estimated mean annual flow) and reservoir losses (modelled as a function of lake volume and estimated overflow rates)

2.3 Water quality monitoring

There are nine stream monitoring sites and one lake monitoring site in the Lake Hayes catchment (Table 2-1, Figure 2-2). Three of the stream monitoring sites, Hayes Creek at Lake Hayes Estate, Lake Hayes Spring at Lake Hayes and Mill Creek at Fish Trap, are located in the same REC stream subcatchment. With the exception of Hayes Creek at Lake Hayes Estate, all of the stream sites are located upstream of Lake Hayes.

Although turbidity is essentially a measure of the cloudiness of water, turbidity may be used as a surrogate of total suspended solids concentration on a site-specific basis by developing a relationship between turbidity and suspended sediments.

---

[3] Here land use refers to a specific enterprise or activity type (e.g., sheep and beef farming) while land cover refers to classes of land use (e.g., pasture, wooded).

Continuous or high frequency water quality data were provided by sensors deployed at specific sites. A TriOS[4] hyperspectral sensor was deployed at the Mill Creek at Lake Hayes site. The TriOS is a spectroscopic sensor that utilises strong absorbance by nitrate-N of light in the UV region of the electromagnetic spectrum, with peak absorbance at 220 nm, to provide surrogate estimates of nitrate N concentrations. Further information and guidance regarding the use of high frequency sensors was provided in a review undertaken for regional councils by NIWA (Hudson and Baddock 2019).

Table 2-1: **Monitoring sites in the Hayes Creek catchment ordered from upstream to downstream.** The location of site numbers are shown in Figure 2-2. Synoptic = sites used for spatial surveys. Continuous = sites where high frequency water quality sensors are deployed. Discharge = continuous flow monitoring.

Site name	Site no.	REC segment	Upstream catchment area (ha)	Monitoring purpose
Dan O'Connell Creek at Coronet Station 300m Upstream	1	14218389	620	Synoptic
Dan O'Connell Creek at Coronet Station	2	14218146	328	Synoptic
Station Creek at Coronet Station	3	14217895	342	Synoptic
McMullan Creek at Malaghans Road	4	14217446	313	Synoptic
Mill Creek at Hunter Road	5	14218014	2143	Routine grab samples, Event samples, Continuous discharge, continuous turbidity measurement
Mill Creek at Waterfall Park	6	14217470	3062	Synoptic
Mill Creek at Fish Trap	8	14218737	4144	Routine grab samples Discharge
Mill Creek at Lake Hayes	7	14218737	4144	Routine grab samples Event samples, Continuous water quality measurements – nitrate-N and turbidity
Lake Hayes Spring at Lake Hayes	9	14218737	4144	Synoptic
Lake Hayes				Routine grab samples
Hayes Creek at Lake Hayes Estate	10	14220755	4890	Routine grab samples

---

[4] http://www.TriOS.de/en/products/sensors.html
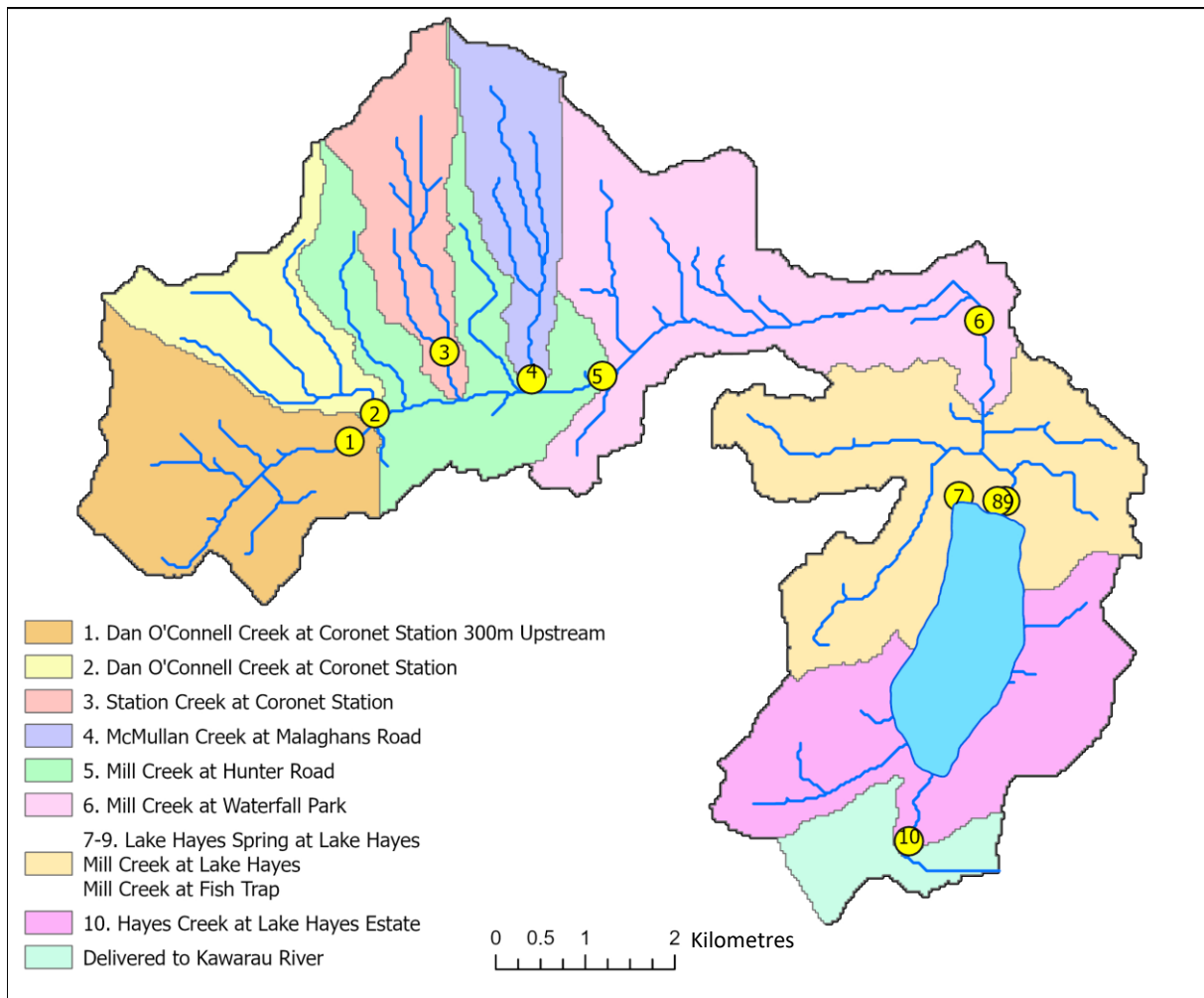
Figure 2-2: **Monitoring site locations within the Hayes Creek catchment.** Headwater streams (first order) are not shown.

2.4   Grab sample and discharge analysis

Discrete water samples were collected manually and by automatic samplers. All are termed "water samples" or "grab samples", and were submitted to laboratories for subsequent water quality analysis.

Streamflow and concentration data were merged using date/time values and look-up functions in Excel or Python to align data from different files. For event-related water quality samples collected using automatic samplers, it was sometimes necessary to adjust the time of sample collection to the nearest time of discharge measurement. The extent of these adjustments were limited to ± 60 minutes maximum. In most cases, adjustments were made within a window of ±5 minutes. We checked for missing values and outliers in the data using the graphical analysis and statistical methods. Records with missing discharge values were patched using interpolation. Negative values in surrogate time series records were omitted from the assessment.

Annual discharge from 1983 to 2022 was derived from streamflow data collected by ORC at the gauging station located at the Fish Trap site. Discharge was recorded at 15 minute intervals and was aggregated to hourly or daily average flows as required. Discharge values were summed for each year to calculate total annual discharge in cubic metres for that year.

2.5   Estimation of contaminant loads

A review of methods for contaminant load estimation is given in Appendix A. We used six approaches in this study, each chosen to best suit the available data:

i.   For sites and time periods when infrequent concentration and discharge estimates exist, **instantaneous loads or flux estimates** (mass/unit of time) were obtained as the product of concentration and discharge at the time of sampling, adjusting units as required. This approach was useful when estimating and discussing the results of "synoptic surveys" as described by Caruso (2000; 2001).

Instantaneous estimates were also made for sites where more extensive discharge or grab sample concentration measurements existed. These estimates were unaffected by errors and uncertainties arising from statistical or process-based models. However, instantaneous estimates are still subject to errors arising from sample collection and handling, laboratory test methods, as well as discharge measurements.

ii.   Application of **rating table regression methods** for several sites for which continuous discharge and moderately frequent grab sample concentration data existed.

iii.   Application of regression methods using the LOAD ESTimator **(LOADEST)** tool (Runkel *et al.* 2004; Gao *et al.* 2021)[5], [6], for the sites where both continuous discharge and moderately frequent grab sample concentration data exist.

iv.   Where nitrate-N was continuously estimated using a TriOS hyperspectral sensor, nitrate-N load was estimated as the product of the TriOS estimate and discharge at the time measurement, summed over the desired time period. These estimates were compared with estimates derived from grab samples, as well as from the LOADEST model.

v.   Application of rating table regression methods for several sites for which continuous discharge and moderately frequent grab sample concentration data existed, as well where the concentration of one or more water quality variable or surrogate were measured at high frequency, typically at the timestep of discharge measurement. The TriOS nitrate sensor provided estimates of nitrate-N concentrations at the Mill Creek at Lake Hayes site, and turbidity was measured at both the Mill Creek at Lake Hayes, and Mill Creek at Hunter Road sites.

The methods used to estimate loads for the different contaminants are described in more detail in the following sections. These apply specifically to fitted concentration vs. discharge regression methods, and methods that use surrogates to estimate TP or TSS loads, or continuous nitrate-N measurements.

The data for three sites (Mill Creek at Fish Trap, Mill Creek at Lake Hayes and Mill Creek at Hunter Road) were sufficient for estimating contaminant loads using multiple approaches for comparison.

Estimated contaminant loads were typically expressed as kg/d, kg/month or tonnes/year.

---

[5] https://github.com/USGS-R/rloadest - LOADEST implemented in the R modelling framework.
[6] In the Aqualinc (2014) report, NZ researchers mentioned use of LOADEST, which was incorrectly named "LowDesk".

3   Results

3.1 Historical nutrient inputs to Lake Hayes

Caruso (2000; 2001) published a detailed assessment of the magnitude and sources of phosphorus in the Lake Hayes catchment. During 1997, grab samples were collected from six sites across the lake catchment. The location of these sites is shown in Figure 2-2, and the results of the 1997 sampling programme are summarised in Table 3-1.

Caruso's analysis of data collected at sites in the Mill Creek catchment during 1997 revealed a strong correlation between hydrological events and TP concentrations, but no clear seasonal patterns in the magnitude of TP concentrations. At a site representing the inflow to Lake Hayes, he apportioned the annual load of TP entering the lake to baseflow (47%), snowmelt (30%), and a single 26-hour long flood event (23%). Spatial analysis of the data suggested that the lower half of the catchment delivered 72% of the total annual total P load to the lake (Caruso 2000).

Caruso also assessed the sources of TP concentrations and fluxes through the Mill Creek catchment, and suggested that a substantial proportion of the TP in Mill Creek (and therefore of P entering the lake) originated from a relatively small sub-catchment in the upper catchment called O'Connell Creek, and from the lower catchment (Caruso 2001). After analysing critical source areas he concluded that "the combination of intensity of cattle and sheep grazing, fertilizer usage, bank erosion and location in the worst subareas outweighed the fact that the worst farms [were farthest] from the lake" (Caruso 2001).

Table 3-1:   Summary of TP and DRP concentration statistics, Mill Creek catchment, 2000. Median values highlighted. From Table 2 of Caruso (2000).

Variable	Statistic	Sample location, number of samples and concentration statistics (concentrations in mg/L).						
		U/S O'Connell	O'Connell	Station	McMullan	Hunter	Fish Trap	Hayes
	n	7	6	6	7	14	15	6
	Mean	0.051	0.061	0.011	0.017	0.03	0.065	0.041
TP	Median	0.036	0.064	0.009	0.014	0.03	0.026	0.047
	Minimum	0.015	0.015	0.005	0.009	0.012	0.013	0.01
	Maximum	0.18	0.098	0.018	0.035	0.047	0.614	0.056
	n	7	6	6	7	14	14	6
	Mean	0.006	0.009	0.003	0.005	0.004	0.007	0.012
DRP	Median	0.004	0.007	0.003	0.005	0.004	0.004	0.01
	Minimum	0.002	0.002	0.001	0.002	0.002	0.001	0.001
	Maximum	0.02	0.017	0.004	0.009	0.008	0.042	0.026

When providing advice to local authorities and the community about where wetlands and other potential mitigation devices could be sited in the Lake Hayes catchment, Goeller et al (2020) estimated annual contaminant yields at the Fish Trap site for the period 1988 to 2019 (inclusive). They also used data derived from samples collected at the same sites sampled by Caruso in 1997 to characterise stream loads for several water quality variables. In Table 3-2 we compare TP load estimates from Goeller et al (2020) with those of Caruso (2000). The load estimates reported by

Caruso should be regarded as indicative – they were derived from single grab samples and flow measured at each site on the sample day. Despite limited data, the 1997 and 2019 data sets indicate consistent spatial pattern of TP loads –relatively small in the upper catchment (with the exception of O'Connell Creek, identified as a major source of P by Caruso), and considerably greater in the lower half of the catchment.

Table 3-2:   Comparison of TP load estimates, 1997 vs 2019. Results from 1997 derived from single sample and flow gauged at the time of sampling (Caruso 2000). Results from 2019 derived from 8 or 10 samples, with exception of the Hunter Road site (4 samples). Results from 2019 from Goeller et al (2020).

Sampling location	Subcatchment area (km²)	TP load (g/d)	
		1997	2019
Dan O'Connell Creek at Coronet Station 300m upstream	1.7	18	20
Dan O'Connell Creek at Coronet Station	5.6	40	130
Station Creek at Coronet Station	1.0	14	20
McMullan Creek at Malaghans Road	3.7	53	170
Mill Creek at Hunter Road	18.24	134	930
Mill Creek at Fish Trap	48.7	474	660

3.2   CLUES modelling

3.2.1   Land use representativity

Figure 3-1 shows the percentage cover of the CLUES land use classes in the sub-catchment upstream of each stream monitoring site. Note that for clarity, wooded land uses have been aggregated into a single group, and minor land uses, such as crops, have also been grouped.
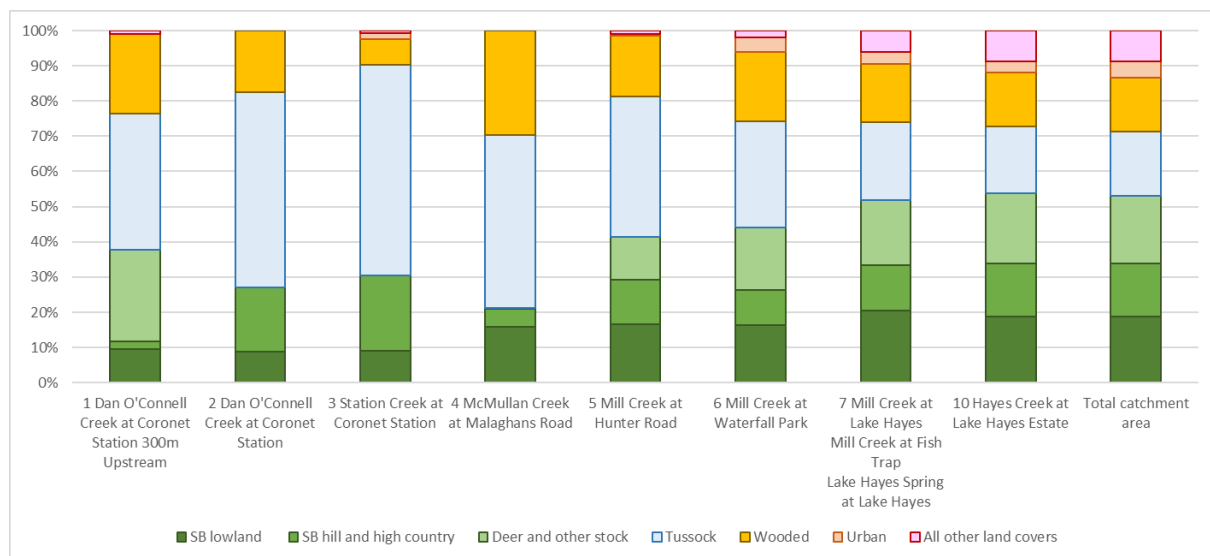
Figure 3-1:   Percentage area of CLUES land use classes upstream of each monitoring site for the baseline year of 2018. Note that hill and high country sheep and beef (SB), forest and scrub (wooded) and minor land use classes (other) have been grouped in the chart. The sites are numbered with reference to Figure 2-2 and Table 2-1.

Table 3-3 gives the total and percentage area for each of the LCDB land cover classes in the Lake Hayes catchment, and Figure 3-2 shows the changes in land cover aggregated into broad classes. There has been very little change in land cover between 1996 for all land cover classes except urban land, which more than trebled in area between 1996 (66 ha) and 2018 (242 ha). However, this represents a relatively minor increase in the percentage of the total catchment area covered by urban land (from about 1% to 5%). Around half of the current urban area consists of parks and open space, and the urban land cover also includes the Coronet Peak Ski field amenities (e.g., carparks). For all time periods, just over half the catchment area is covered by pasture (high and low producing grassland, 54-58%), 18-19% by tussock and 23% by forest (exotic and native) and scrub for all the reference years. The remaining land cover includes Lake Hayes, rivers, and land used for crops and horticulture. The location of the different land cover classes is shown for LCDB5 in Figure 3-3.

Given the limited change in land use over the past two decades (see Table 3-3 and Figure 3-2), we did not create an historic land use scenario under the assumption that all else being equal, changes in loads delivered to Lake Hayes and the Kawarau River would be minor.

Table 3-3: **Land cover area (ha) from Land Cover Database records.** The proportion of total catchment area for each land cover class is given in parentheses. Source https://lris.scinfo.org.nz/layer/104400-lcdb-v50-land-cover-database-version-50-mainland-new-zealand/

Land cover class	Land cover area (ha) and proportion of total catchment area (%)				
	LCDB5 2018	LCDB4 2012	LCDB3 2008	LCDB2 2001	LCDB1 1996
Deciduous Hardwoods	131.4 (2%)	150.8 (3%)	150.8 (3%)	153 (3%)	153 (3%)
Exotic Forest	241.6 (5%)	222.4 (4%)	211.8 (4%)	194.6 (4%)	167.9 (3%)
Forest – Harvested	9.5 (0%)	0 (0%)	0 (0%)	5.2 (0%)	0 (0%)
Gorse and/or Broom	6.2 (0%)	6.2 (0%)	5.3 (0%)	5.3 (0%)	5.3 (0%)
Herbaceous Freshwater Vegetation	2.1 (0%)	2.1 (0%)	2.1 (0%)	2.1 (0%)	2.1 (0%)
High Producing Exotic Grassland	2207 (42%)	2222.4 (44%)	2283.5 (45%)	2356.2 (46%)	2367.8 (47%)
Indigenous Forest	29.5 (1%)	29.5 (1%)	29.5 (1%)	29.5 (1%)	34.8 (1%)
Lake or Pond	296.7 (6%)	296.7 (6%)	295.7 (6%)	295 (6%)	293.3 (6%)
Low Producing Grassland	553.1 (10%)	553.1 (11%)	553.8 (11%)	551.1 (11%)	551.1 (11%)
Manuka and/or Kanuka	9.1 (0%)	9.1 (0%)	9.1 (0%)	9.1 (0%)	9.1 (0%)
Matagouri or Grey Scrub	8.3 (0%)	8.3 (0%)	8.3 (0%)	8.3 (0%)	8.3 (0%)
Mixed Exotic Shrubland	335.6 (6%)	361.9 (7%)	373.4 (7%)	373.4 (7%)	373.4 (7%)
Orchard, Vineyard or Other Perennial Crop	16.9 (0%)	16.9 (0%)	16.9 (0%)	16.9 (0%)	5.6 (0%)
River	4.9 (0%)	4.9 (0%)	4.9 (0%)	4.9 (0%)	4.9 (0%)
Short-rotation Cropland	58.2 (1%)	58.2 (1%)	58.2 (1%)	58.2 (1%)	69.5 (1%)
Tall Tussock Grassland	922.2 (17%)	924.6 (18%)	925.6 (18%)	942.8 (19%)	962 (19%)
Built-up Area (settlement)	117.9 (2%)	102.4 (2%)	96.6 (2%)	19.8 (0%)	17.5 (0%)
Urban Parkland/Open Space	124.1 (2%)	104.8 (2%)	48.9 (1%)	48.9 (1%)	48.9 (1%)
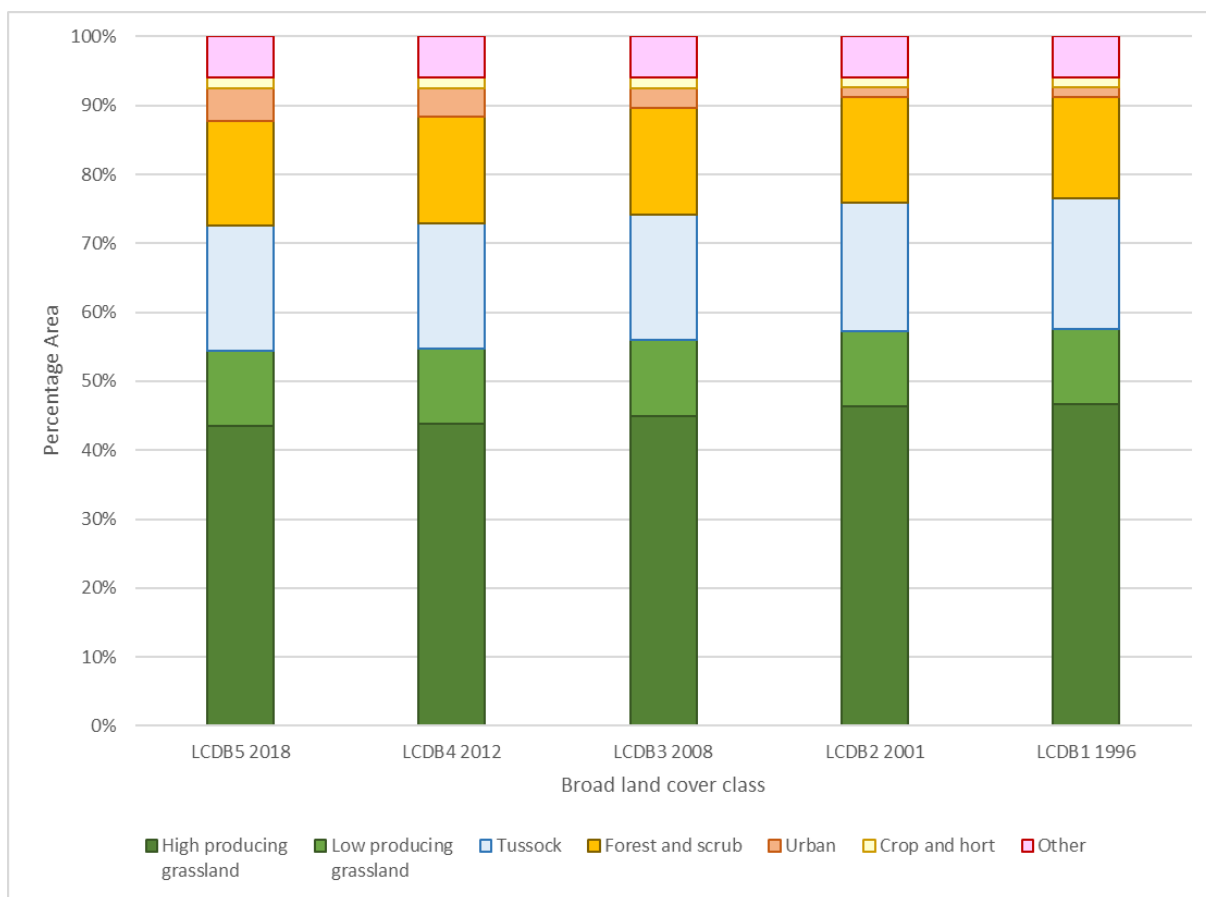
Figure 3-2: **Proportion of land cover by broad class in each assessment period.** Source
https://lris.scinfo.org.nz/layer/104400-lcdb-v50-land-cover-database-version-50-mainland-new-zealand/
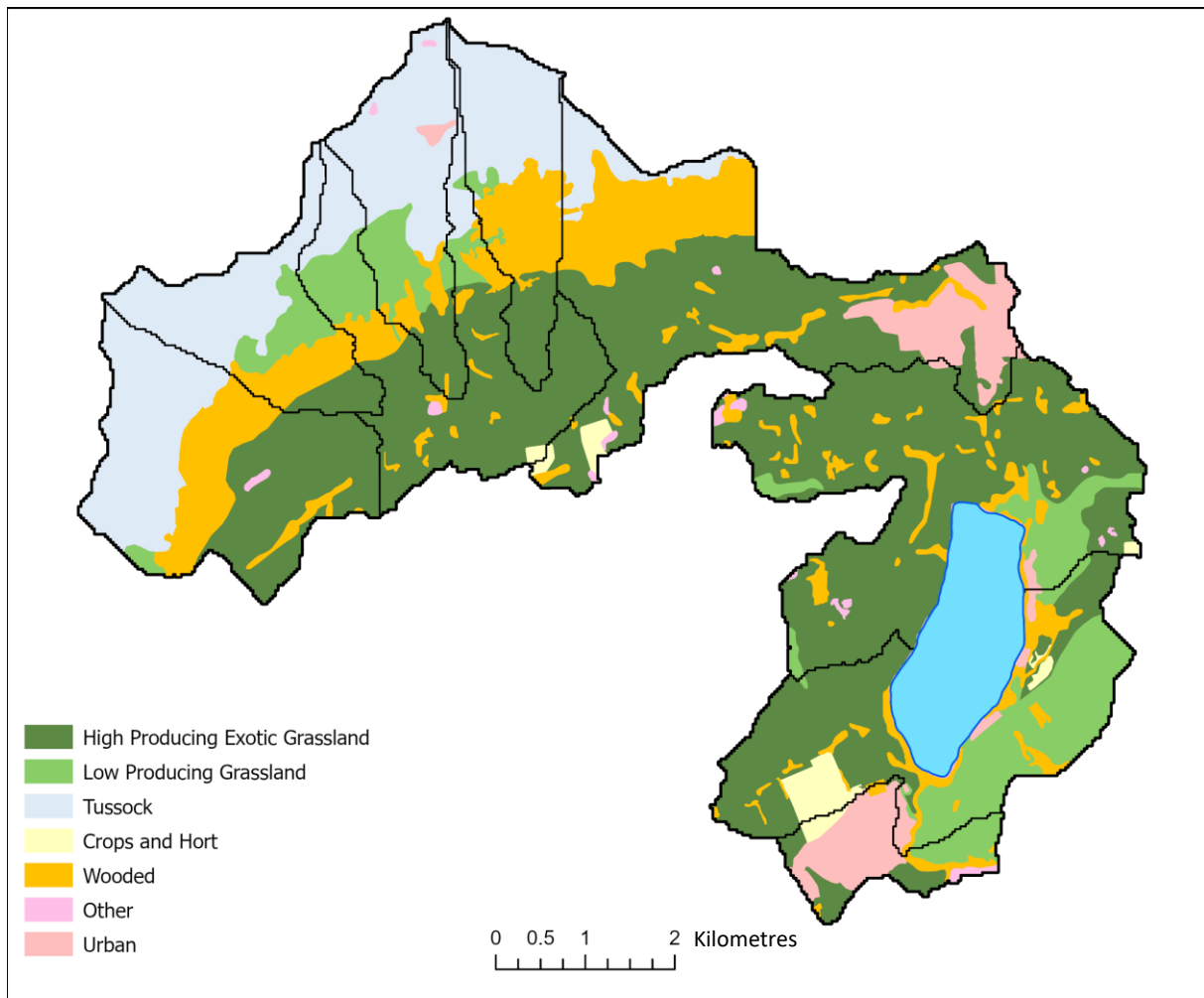
Figure 3-3:   Map showing distribution of broad land cover classes across the Hayes Creek at Hayes Estate site for the reference year 2018. Source: LCDB5. The monitoring site catchment areas are shown for reference.

3.2.2   Nutrient load estimation

CLUES was used to estimate the mean annual loads and area-specific yields of TN and TP for the reference year 2018. The loads and yields estimated for the monitoring sites are given in Table 3-4 and the load estimated by land use is plotted in Figure 3-4 for TN and Figure 3-5 for TP. The highest nutrient loads from diffuse sources come from pastoral land uses, however, the predicted TP loads from soil erosion are also high. This source is estimated in CLUES based on sediment loads modelled by the New Zealand Sediment Yield Estimator (Hicks *et al.* 2018)

There is a substantial decrease in the magnitude of TN and TP loads downstream of Lake Hayes due to attenuation (e.g., sediment deposition) in the lake (Table 3-4).

Table 3-4: Mean annual total nitrogen (TN) and total phosphorus (TP) loads and specific yields as determined by CLUES

Site	TN Load (t/y)	TN Specific yield (t/km²/y)	TP Load (t/y)	TP Specific yield (t/km²/y)
McMullan Creek at Malaghans Road	0.67	0.21	0.15	0.05
Station Creek at Coronet Station	0.62	0.18	0.17	0.05
Dan O'Connell Creek at Coronet Station	0.42	0.13	0.18	0.06
Dan O'Connell Creek at Coronet Station 300m Upstream	1.93	0.31	0.24	0.04
Mill Creek at Hunter Road	6.22	0.29	0.98	0.05
Mill Creek at Waterfall Park	11.08	0.36	1.42	0.05
Delivered to lake*	16.13	0.39	1.76	0.04
Hayes Creek at Lake Hayes Estate	7.76	0.16	0.31	0.01
Delivered to Kawarau River	8.81	0.17	0.41	0.01

*Mill Creek at Lake Hayes, Mill Creek at Fish Trap, Lake Hayes Spring at Lake Hayes
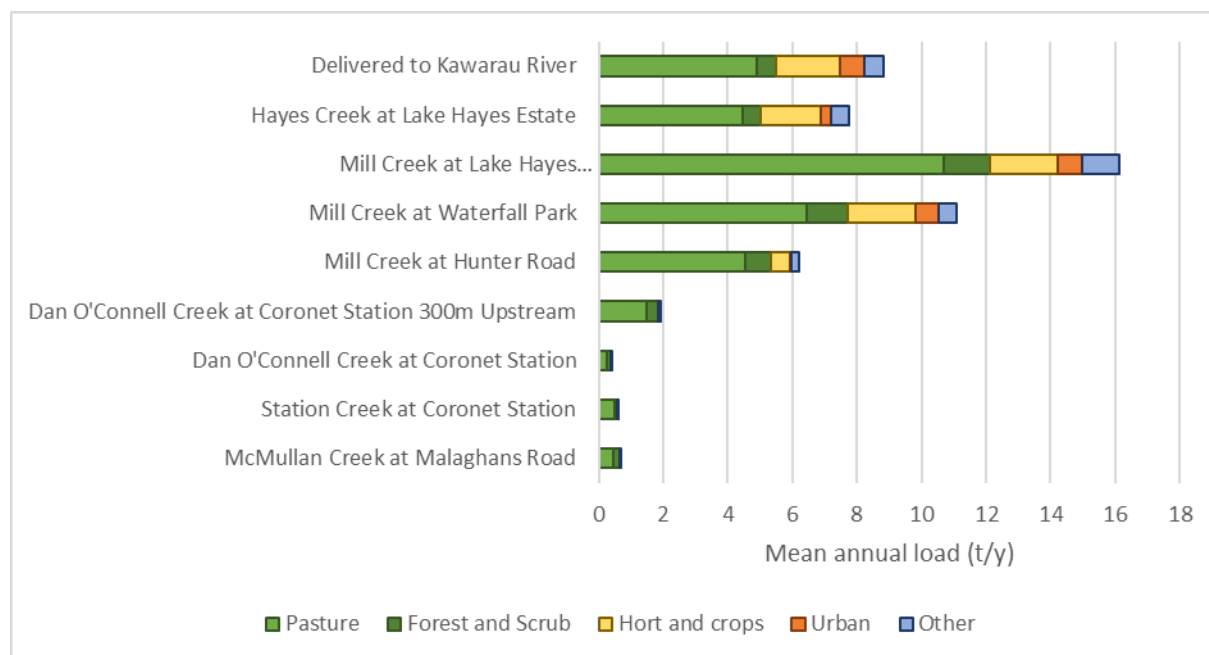
Figure 3-4: Estimated mean annual TN loads subdivided by land use for each monitoring site and for the whole Lake Hayes catchment.
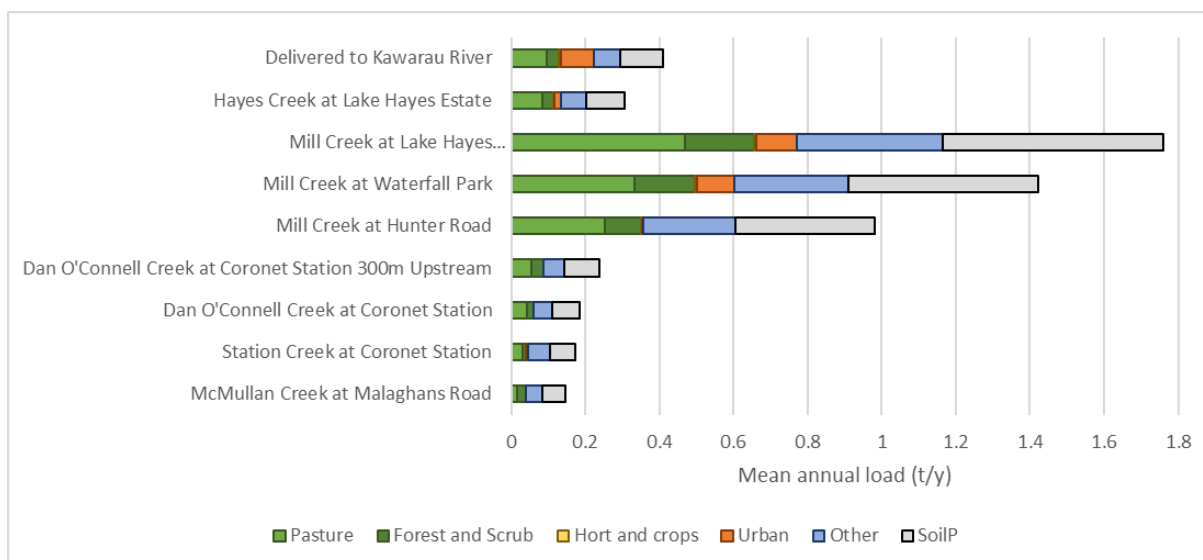
Figure 3-5: **Estimated mean annual TP loads subdivided by land use for each monitoring site and for the whole Lake Hayes catchment.**

3.3 Instantaneous and cumulative discharge – Mill Creek at Fish Trap site

The range of discharge values observed in each calendar year at the Fish Trap gauging station is shown in Figure 3-6 (A). Although Figure 3-6 (A) does not suggest a strong trend in discharge over time, mean hourly discharge was elevated in 1994 and 2000. Figure 3-6 (B) indicates a moderate seasonal patten in discharge generally consistent with a previous assessment (Caruso 2000). Annual discharge (Figure 3-7) confirms that discharge in 1994 was unusually high, and the period 1994 to 2010 had five of the six largest annual discharges for the 38-year period of data shown.

Flows at the Fish Trap site exceeded 228 L/s 95% of the time, and 300 L/s 75% of the time. Stream discharge summary statistics and a flow duration curve are provided in Appendix C for the entire record.

The distribution of flows observed in selected years are summarised in Figure 3-8. These distributions were used when comparing the annual TP mass load during selected assessment periods.
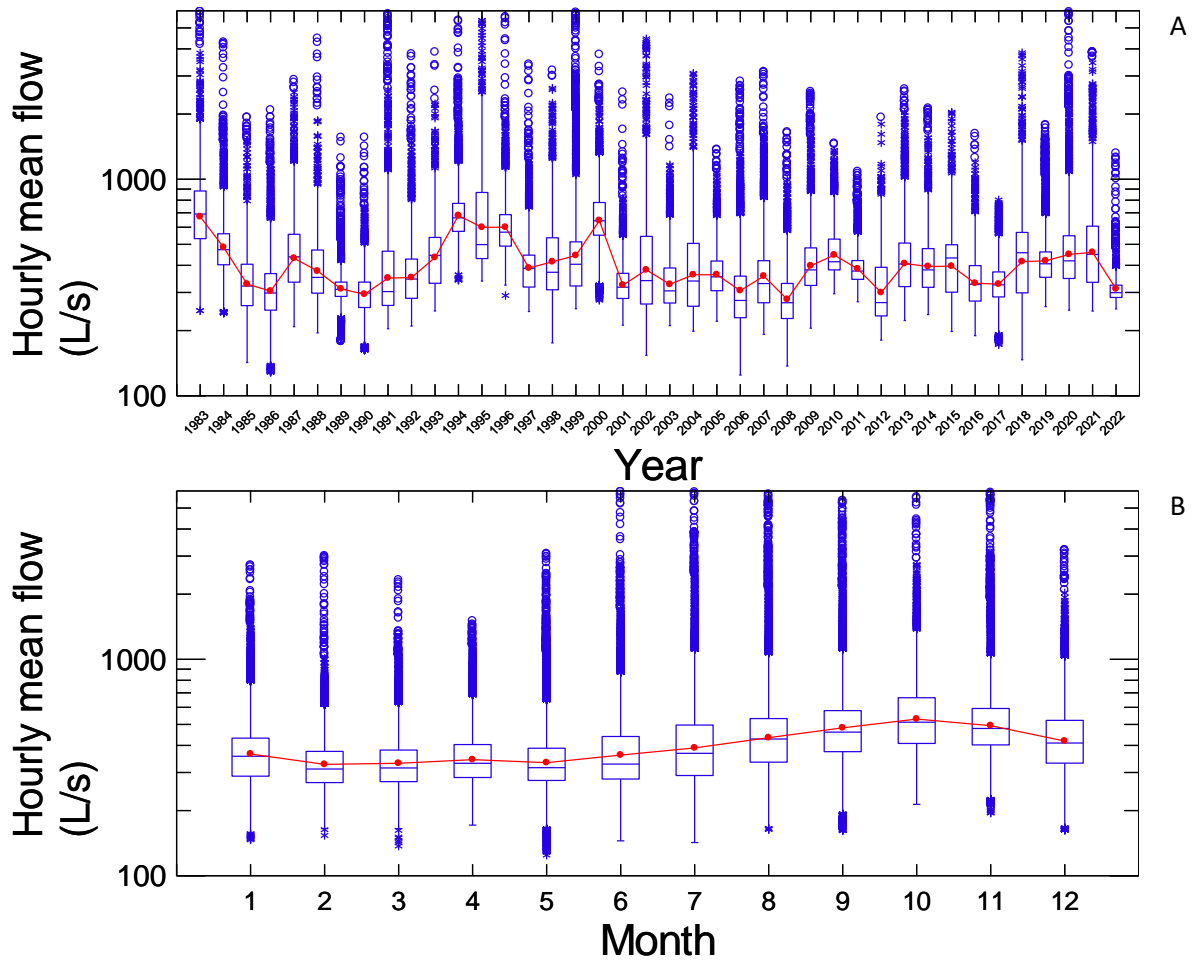
Figure 3-6:   Variation in discharge at the Fish Trap gauging station by year (A) and by month for the entire record (B). Note y-axes have log_{10} scale. The red dot is the average hourly mean flow per aggregation period. Box plot components: horizontal lines are medians, boxes indicate interquartile ranges, whiskers indicate 1.5x the interquartile range, asterisks indicate values between 1.5 and 3x the interquartile range, open circles indicate values > 3x the interquartile range.
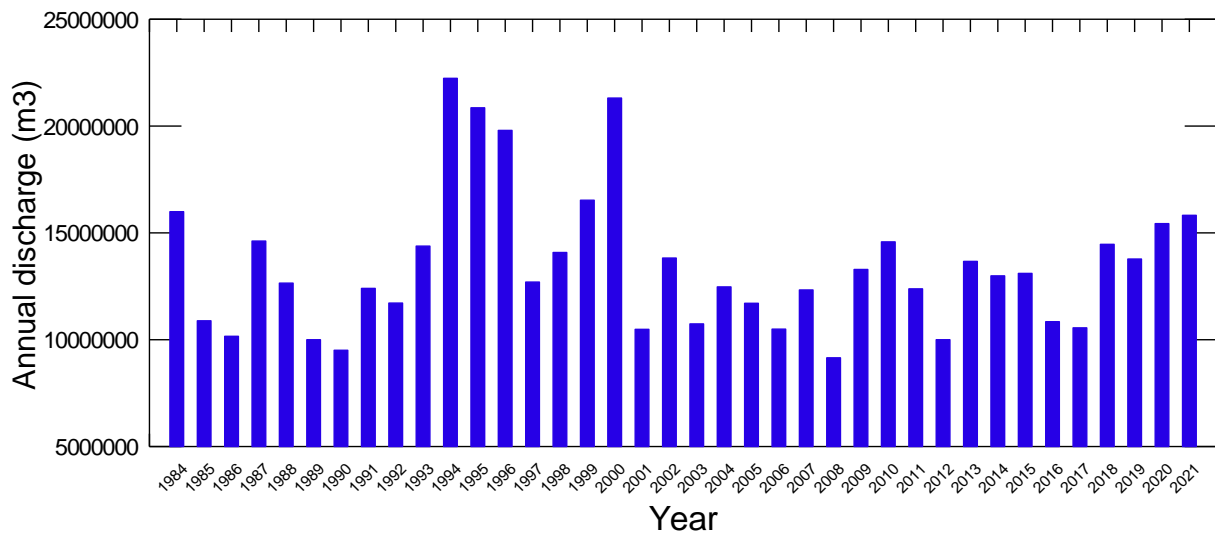
Figure 3-7: Total annual discharge at Fish Trap site between 1984 and 2021.
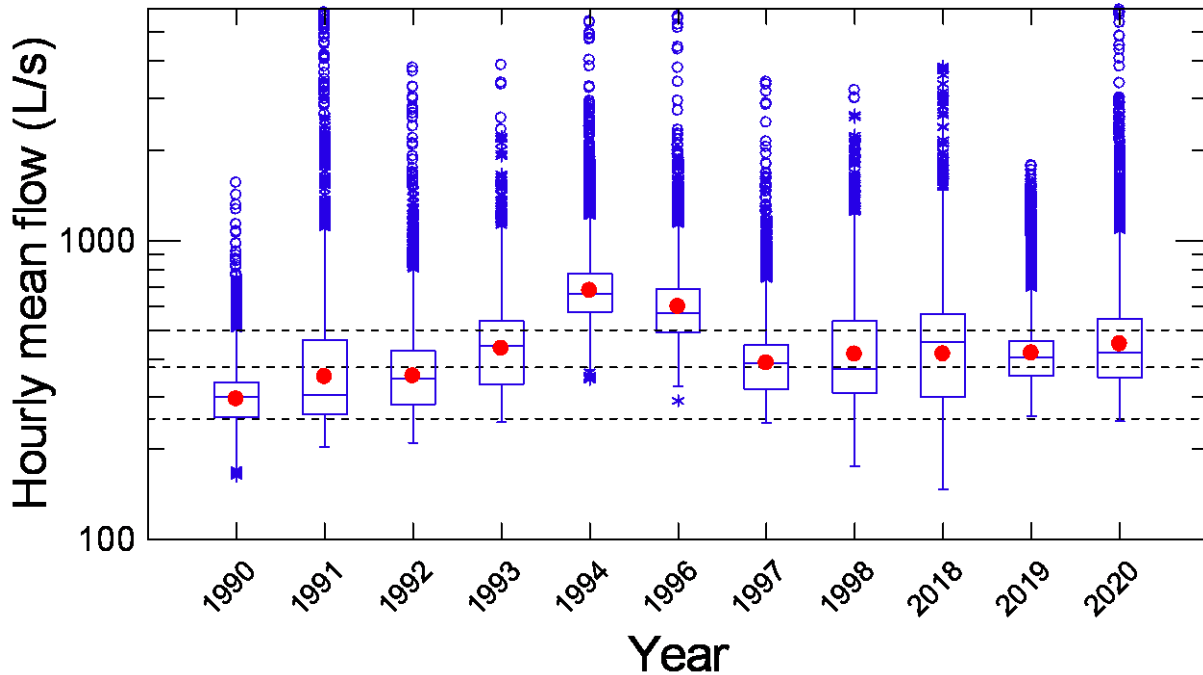
Figure 3-8: Annual hourly discharge data for Mill Creek at Fish Trap for <u>selected years</u>. Dotted lines indicsate long-term 10th percentile (253 L/s), median (285 L/s) and 75th percentile (501 L/s) values. See Figure 3-6 for explanation of box plot components. Red dots indicate annual average values.

3.4 Spot flow gauging

Table 3-5 shows selected summary statistics of the measured flow rates for nine different sites, where spot flow gaugings were carried out. Statistics derived from the long-term flow record at the Fish Trap site are included, as a comparison with the spot gauging values for this site suggest that the synoptic surveys undertaken during 2017/18 represented slightly higher than typical discharge conditions, which is consistent with data presented in Figure 3-7 and 3.8.

3.5 Synoptic survey results

The synoptic survey results were derived from sampling runs in 1997 (DRP and TP only), and additional sampling runs at the same locations in the period 2018-2020 (NNN, TN, DRP, TP, TSS). Details about sample numbers collected in the four assessment periods are in Appendix D and E.

These synoptic surveys provided an indication of changes in DRP and TP concentrations across the Mill Creek catchment over time. Relatively few data are available for the 1997 period, which limits our ability to detect and be certain about possible changes in water quality since that year. Table 3-6 indicates that median DRP concentrations have increased at Dan O'Connell Creek (upper catchment), and at the Hunter Road site in mid-catchment. Median and mean TP concentrations have also increased at the Hunter Road site over time, as indicated in Table 3-7.

The data from the 2018-2020 synoptic surveys were used to plot distributions of contaminant concentrations and fluxes at each stream monitoring site (Fig. 3-9). These plots indicate that TN and NNN concentrations and fluxes were elevated at the Mill Creek sites relative to the sites further up the catchment, then decrease downstream of Lake Hayes. TSS concentrations and fluxes also decreased downstream of Lake Hayes.

Table 3-5:   **Summary statistics derived from flow gauging results.** Site numbers are as shown in Figure 2-2. Values for Mill Creek at Lake Hayes include conditions during event sample collection.

Site no.	Site Name	Flow statistic (L/s)		
		25th percentile	Median	75th percentile
1	Dan O'Connell Creek at Coronet Station	47	59.5	76
2	Dan O'Connell Creek at Coronet Station 300m Upstream	12	19.5	22
3	Station Creek at Coronet Station	28	40	53
4	McMullan Creek at Malaghans Road	64	75.5	104
5	Mill Creek at Hunter Road	207	237	342
6	Mill Creek at Waterfall Park	377	425	580
	Mill Creek at Fish Trap	336	400	496
8	Mill Creek at Fish Trap – long term record	298	376.5	501.4
	Mill Creek at Lake Hayes (includes event samples)	859	1001	1165
7	Lake Hayes Spring at Lake Hayes	31	37	40
10	Hayes Creek at Lake Hayes Estate	467	533	619

Table 3-6:   **Median DRP concentrations at synoptic survey sites over time.** Site locations are shown in Figure 2-2. Change in concentration relative to 1997 is indicated by cell shades. Green: decrease, orange: increase, unshaded: no change.

Site name	DRP concentration per assessment period (mg/L)			
	1997	2018	2019	2020
Dan OC Ck 300 m u/s	0.004	0.002	0.003	0.006
Dan OC Ck at C. Station	0.007	0.002	0.003	0.007
Station Ck at Coronet	0.003	0.001	0.001	0.002
McMullan Ck at Malaghan	0.005	0.002	0.003	0.003
Mill Ck at Hunter Rd	0.004	0.003	0.003	0.006
Mill Ck at Fish Trap	0.004	0.002	0.002	0.004
Hayes Ck at L. Hayes	0.010	0.009	0.009	0.014

Table 3-7:   **Median TP concentrations at synoptic survey sites over time.** Cell shading as in Table 3.6.

Site	Median TP concentration per assessment period (mg/L)			
	1997	2018	2019	2020
Dan OC Ck 300 m u/s	0.036	0.028	0.025	0.020
Dan OC Ck at C. Station	0.064	0.022	0.019	0.038
Station Ck at Coronet	0.009	0.005	0.004	0.002
McMullan Ck at Malaghan	0.014	0.039	0.013	0.010
Mill Ck at Hunter Rd	0.030	0.034	0.016	0.032
Mill Ck at Fish Trap	0.026	0.024	0.018	0.018
Hayes Ck at L. Hayes	0.047	0.022	0.029	0.048
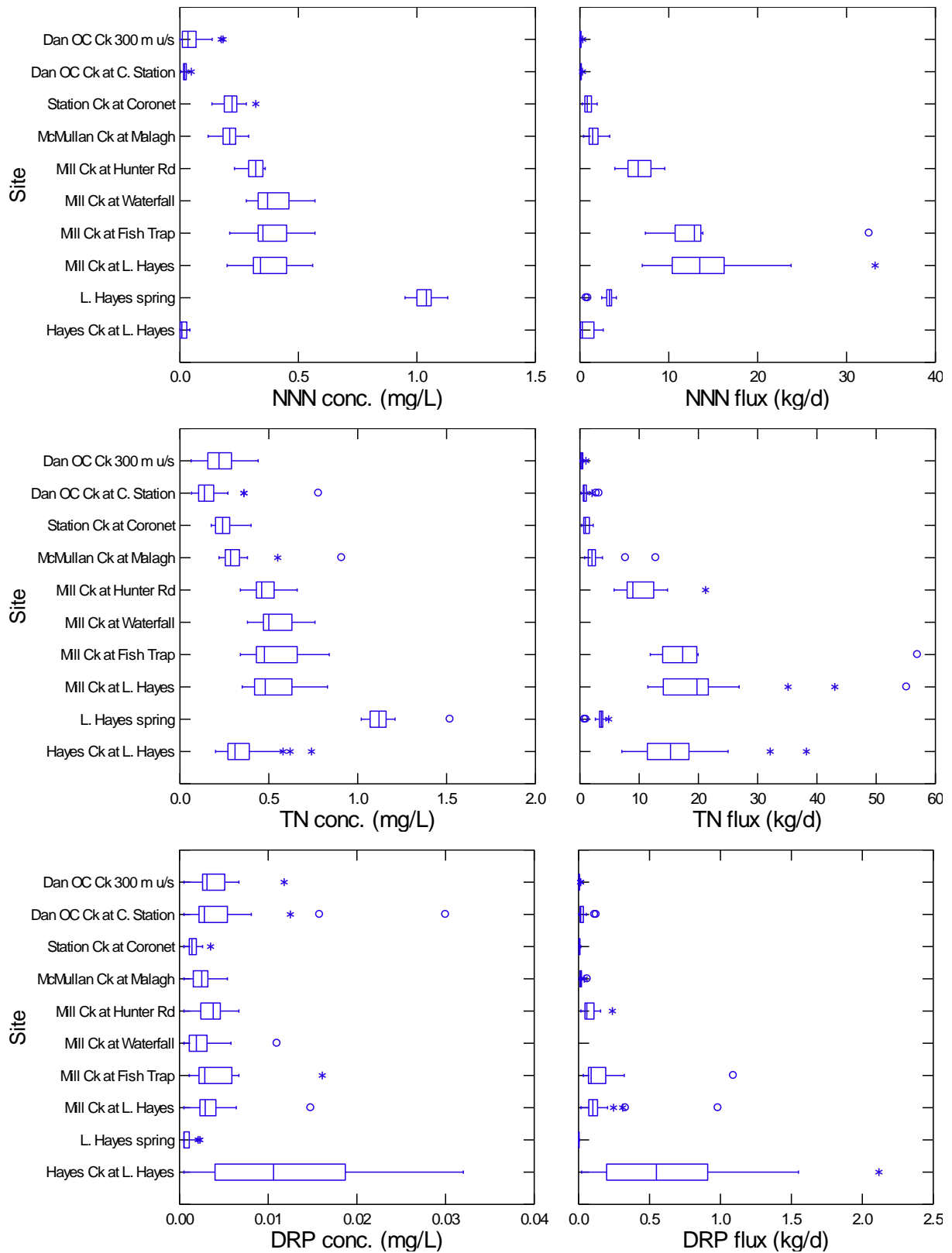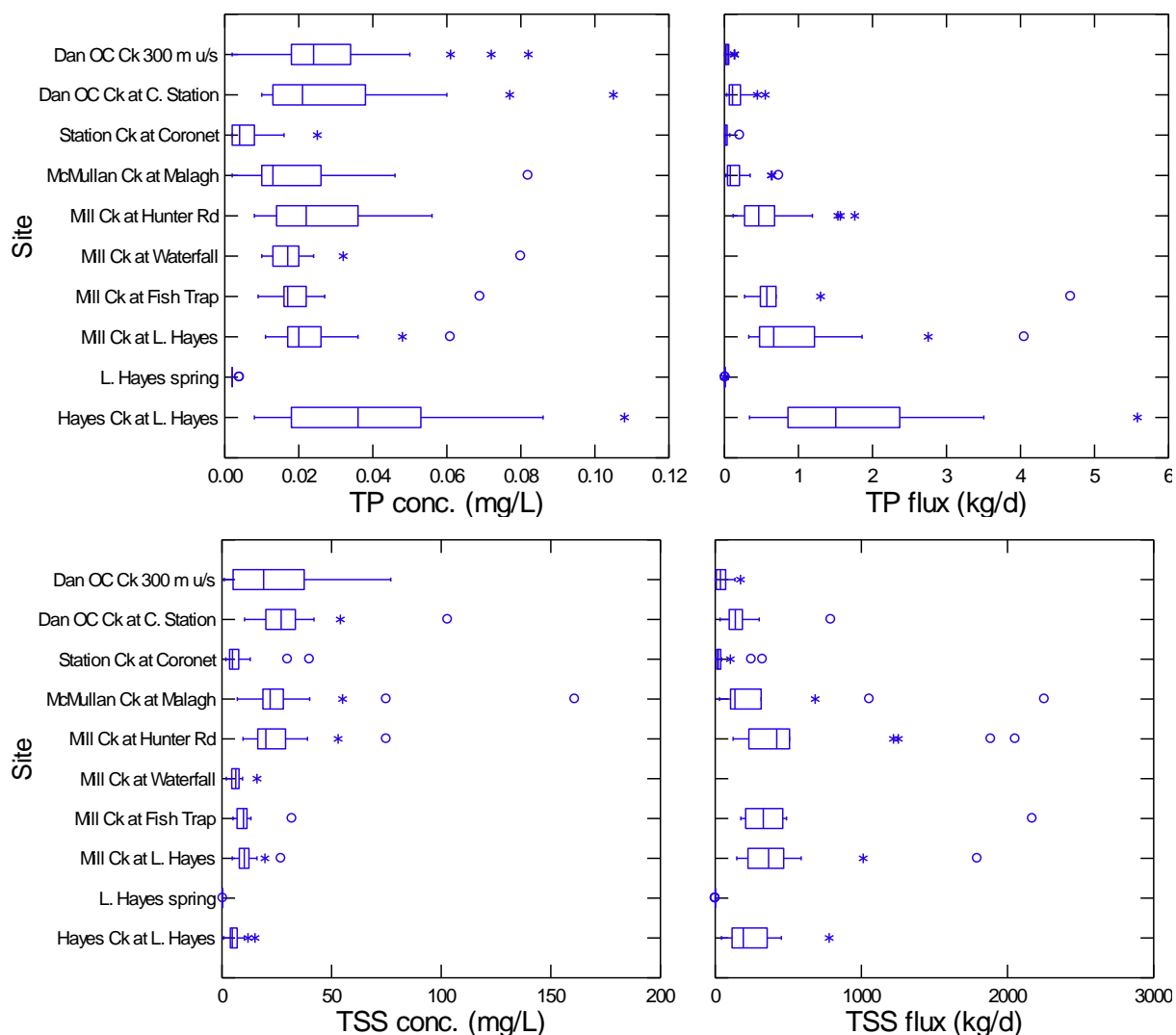
Figure 3-9: **Comparison of concentration and instantaneous load (flux) estimates for 10 sites in the Mill Creek/Hayes Creek catchment .** Flux estimates not included for Waterfall Park site due to poor alignment between gauging and grab sample collection times. Outlier removed from McMullan Creek TSS concentration and flux data for period 2018-2022. See Figure 3-6 for explanation of box plot components.

Synoptic data for the 2018-2020 period indicate:

- the concentrations and fluxes of NNN and TN increase in the reach downstream of the Hunter Road site;

- TN and NNN concentrations and flux are lower in Hayes Creek downstream of Lake Hayes;

- DRP and TP concentrations were relatively low throughout the catchment during the synoptic surveys; an increase of TP flux was evident downstream of the Hunter Road site;

- DRP and TP concentrations in the lake outflow (represented by the Hayes Creek sample site) were greater than any upstream site, suggesting that the lake was a net source of phosphorus in both dissolved and particulate forms;

- TSS concentrations were greatest in tributary and headwater streams, but the flux of particulate material increased downstream of the Hunter Road site;

- interpretation of the synoptic survey results requires care – these samples were generally obtained under average-flow conditions, whereas samples collected during event conditions generally represent higher than typical flows, as indicated in Figure 3-10; and

- samples collected to compare concentrations and the flux of contaminants at multiple sample points across a catchment should be collected within a suitably narrow time frame, or during similar flow conditions.

The approximate flow conditions at sites used for synoptic surveys in the period 2018-2020 are summarised in Figure 3.10 and Table 3-8. Approximately half of the samples collected during the synoptic surveys were collected when discharge at the Fish Trap site was less than the median flow and approximately 30% of samples were collected when flows at the Fish Trap site exceeded the 75th percentile.
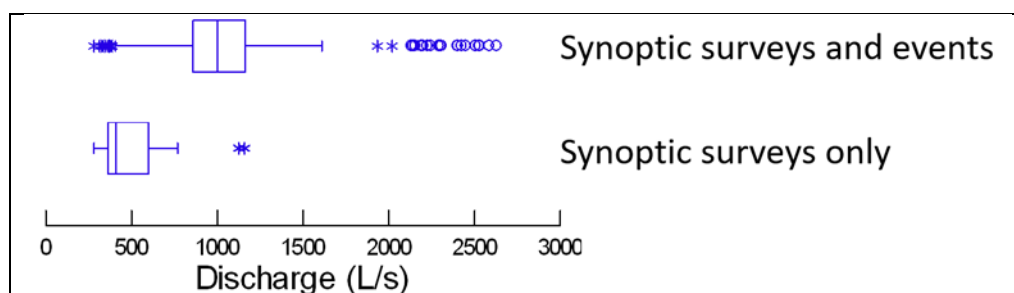
Figure 3-10:   Comparison of discharge conditions at Mill Creek at Fish Trap site at times of synoptic survey or event-related sample collection, 2018-2020.

Table 3-8:   Proportion of samples collected under general catchment discharge conditions, 2018-2020 period. Discharge conditions at each site determined according to flow in Mill Creek at Fish Trap site on day of collection. If different to number of synoptic samples, total number of samples collected during this period in parentheses.

Site name	No of synoptic samples in 2018-2020 period	Proportion of samples collected when discharge was less than…..		
		285 L/s (10th percentile)	376 L/s (Median)	501 L/s (75th percentile)
Dan OC Ck 300 m u/s	21			
Dan OC Ck at C. Station	21			
Station Ck at Coronet	21	5	45	68
McMullan Ck at Malaghan	21			
Mill Ck at Hunter Rd	21			
Mill Ck at Fish Trap	10 (~44)	0 (7)	50 (26)	70 (55)
Hayes Ck at L. Hayes	21 (~210	5 (1)	43 (5)	67 (7)

3.6   Instantaneous and modelled contaminant loads at Fish Trap site

Hourly and daily mass load estimates were derived from the LOADEST and rLOADEST software. Instantaneous flux estimates were also calculated using grab sample concentration data and flow at

the time of sampling. Instantaneous flux estimates were the product of discharge and concentration, adjusting units as required. Supplementary summary data are in Appendices E to I.

3.6.1 Total phosphorus – Fish Trap site

Time-series of grab sample and model-derived TP flux estimates at the Fish Trap site are shown in Figure 3-11. Annual mass load estimates for the period 1983 to 2021 are listed in Appendix G. The distributions of grab sample-based instantaneous TP loads and modelled TP loads for each month at the Fish Trap site are shown in Figure 3-12.
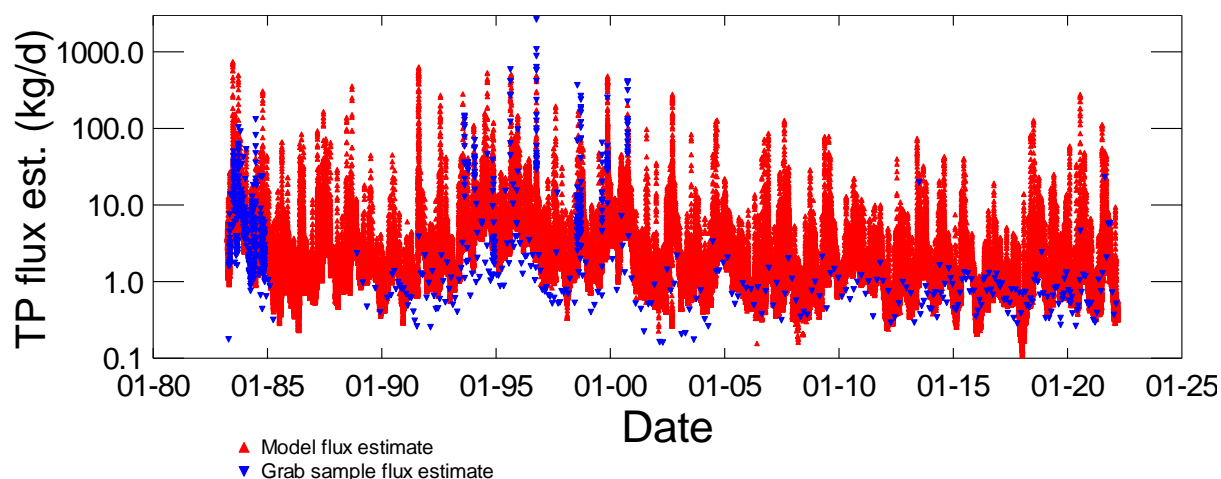
Figure 3-11: Comparison of instantaneous and modelled daily total phosphorus (TP) loads for the Fish Trap site. Note that the Y axis of the plot has $\log_{10}$ scale.
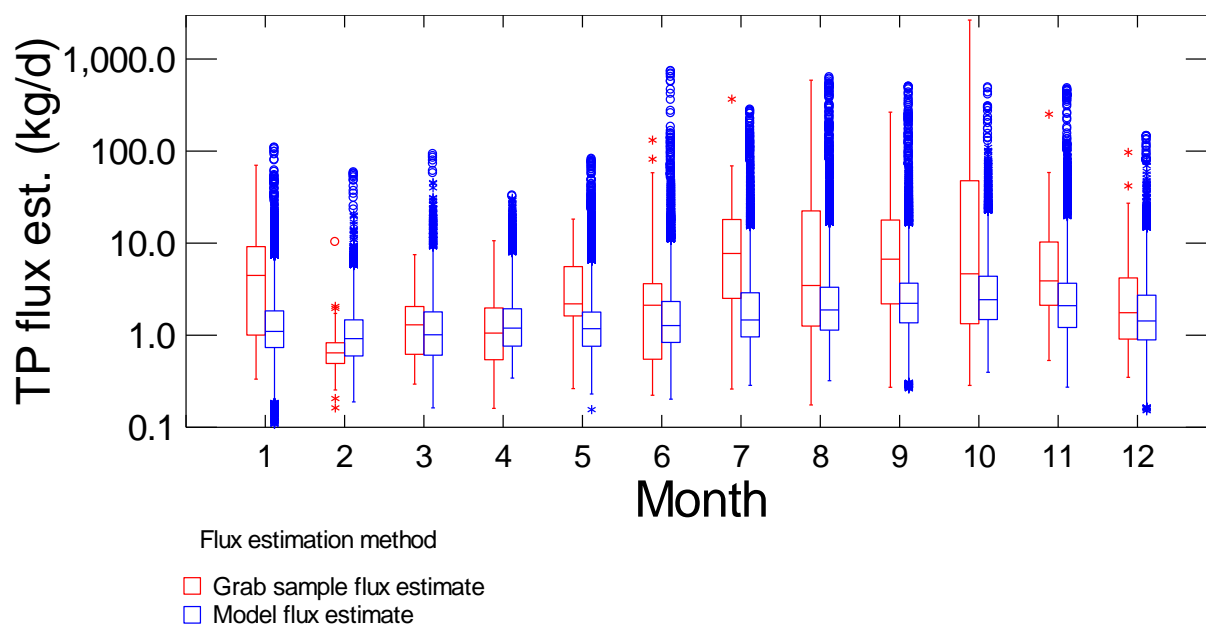
Figure 3-12: Comparison of grab sample-based instantaneous TP loads and modelled TP loads for the Fish Trap site. Note that the Y axis of the plot has $\log_{10}$ scale.

Figure 3-13 shows the monthly estimate of mean daily TP load from 1983 through 2021, along with an upper and lower 95th percent confidence interval. Figure 3-14 summarises annual TP loads over this period. Annual loads of similar magnitude were reported by Goeller *et al.* (2020).

Key features of these estimates include:

- During the eight-year period from 1993-2000, estimated annual TP loads were generally > 1 t/y. After 2002 and for the next 18 years, estimated annual TP loads were < 1 t/y.

- The temporal pattern in these estimates are consistent with the magnitude of runoff over the 38 complete years for which data were reviewed.
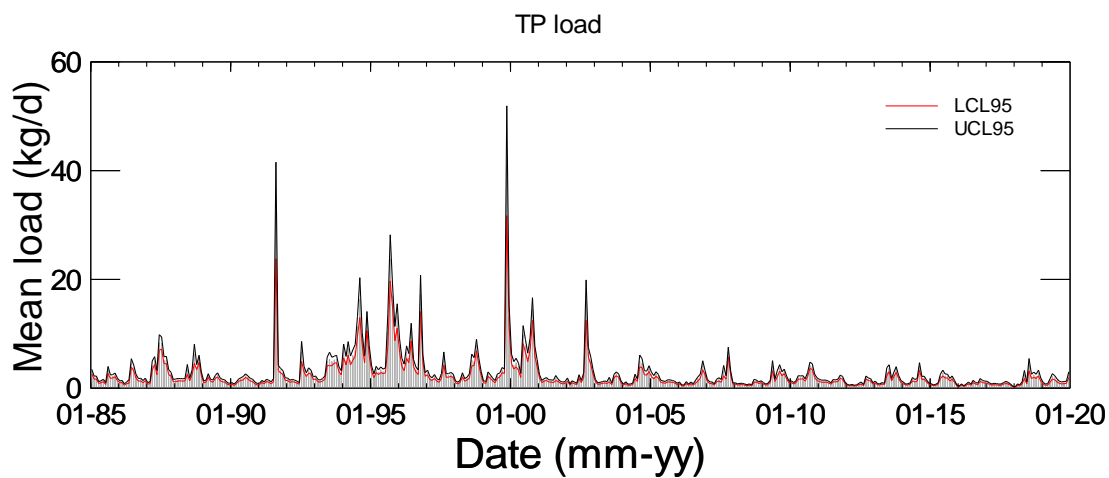
Figure 3-13:   Monthly estimates of mean daily TP load for the Fish Trap site. Modelled TP loads are shown with error bars representing a 95% CI around the mean.
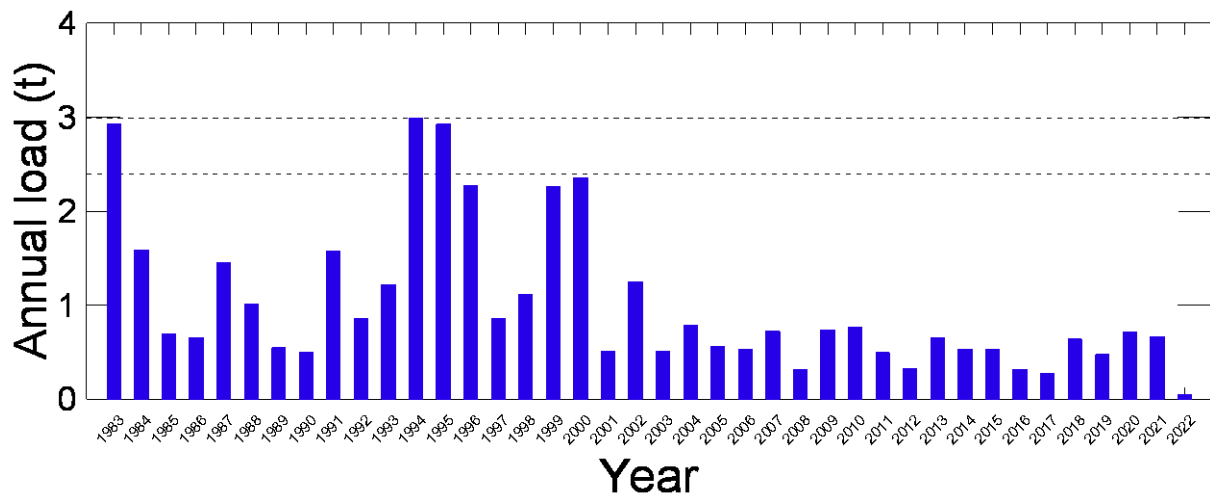
Figure 3-14:   Annual estimates of TP load for the Fish Trap site, showing 1994 estimate and Management Plan target value. The upper broken line is the 1994 annual TP load (3 t), and the lower line represents a 20% reduction of the 1994 annual total (2.4 t). The annual mass load estimate is incomplete for 2022.

Requirements of this report included:

- Indicating when a 20% reduction in TP load to Lake Hayes had been achieved, and

- Comparing contemporary TP loads with those measured in 1994.

Figure 3-14 indicates that a 20% reduction in the 1994 TP load has occurred since 1996, and that annual loads have been less than a third of the 1994 values consistently since 2002. In Table 3-9 we identify three periods that were used for comparison of loads over time. We did this because as Figure 3-7 indicates, annual discharge was considerably larger in 1994, 1995, 1996 and 2000 than more recently. To minimise bias because of unusual hydrological conditions in a key period selected for assessment and provide for assessment of more typical conditions, the periods chosen for assessment were:

- the 1994 calendar year (the baseline for the Management Plan)

- an additional assessment period (1996-1998 inclusive)

- a contemporary period against which values for the other two periods were compared – 2018-2020 inclusive.

The additional historical assessment period (the three calendar-year periods from 1996-1998 inclusive) was selected because the 1994 annual load was considerably larger than most annual loads estimated before and after that period. Data from the three-year period 1996-1998 provided a more typical estimate of annual average, but included two annual estimates that were considerably larger than contemporary values.

The estimated TP load for these three periods are compared in Table 3-9 as a change in annual mass measured in the period 2018-2020 relative to 1994 or 1996-1998, and as a proportion of the 1994 mass or the average load for the 1996-1998 period. The difference between the 1994 load and loads in all years (including contemporary estimates) is shown in Figure 3-14.

Table 3-9: Change in TP load – 1994 vs 2018-2020 and 1996-98 vs 2018-2020. Colours and shading indicate values being compared across time periods.

Assessment period	Annual load (t)	Average load (t)	Assessment period sum (t)
1994	2.99		
1996-1998		1.41	4.24
2018-2020		0.60	1.82
Difference (mass)	2.38 (decrease)	0.8 (decrease)	2.42 (decrease)
Difference (%)	79 (decrease)	56 (decrease)	43 (decrease)

The data summarised in Table 3-9 and Figure 3-14 indicate that the Management Plan target of 20% reduction in 1994 load has been met in all years since 1994 except three (1995, 1999 and 2002), and that since 2002 the annual TP load has been approximately 25% of the 1994 load. However, the annual load estimate appears sensitive to annual rainfall and resulting discharge, and from the information available, it is not possible to attribute the change in loads over time to specific management actions, changes in land use etc. For example, annual mass loads were generally

smaller and confidence intervals narrower for the period 2003 – 2016 and have increased slightly since 2016. These values are closely related to discharge values, which have also increased since 2016, with more high flow events (Figure 3-6).

The magnitude and variability of seasonal (monthly) TP loads for two 19-year periods 1984-2002 and 2003-2021 is summarised in Figure 3-15.
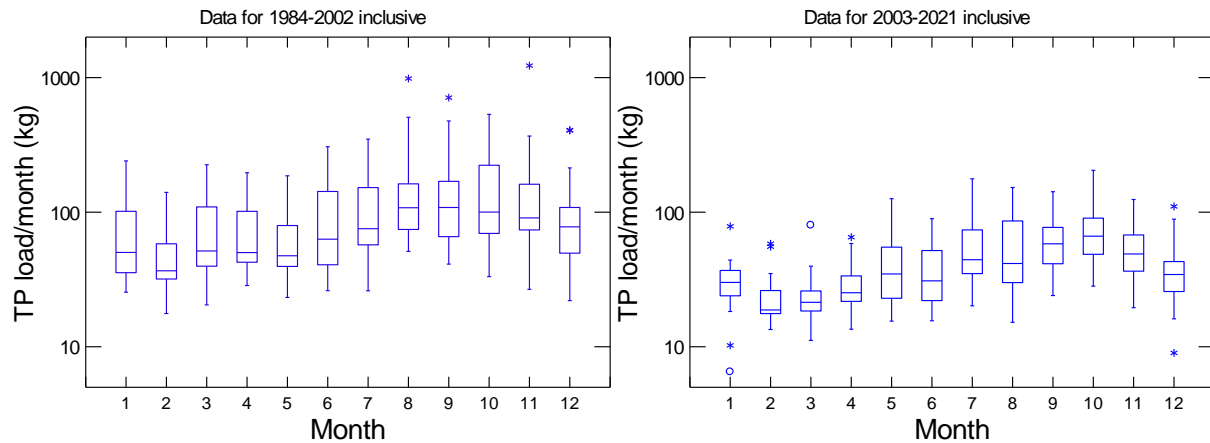
Figure 3-15:   Monthly estimates of TP load for the Fish Trap site for the 1984 to 2002 period and for the 2003 to 2021 period. See Figure 3-6 for explanation of box plot components.

Data summarised in Figure 3-15 confirms what was described in Figure 3-11; the TP load in the period prior to 2003 was considerably larger than post-2003, and a similar seasonal pattern exists for both periods (Figure 3-15).

3.6.2   Nitrate + nitrite N loads (NNN loads)

A time series of grab sample and model-derived NNN flux estimates is shown in Figure 3-16. Annual mass load estimates are listed in Appendix G. Both model-derived flux estimates, and those derived from instantaneous flux estimates as the product of concentration and discharge at the time of sampling show strong seasonality (Figure 3-16). Median NNN flux estimates approximately double from ca. 10 kg/d in late summer to ca. 20 kg/d in September annually.
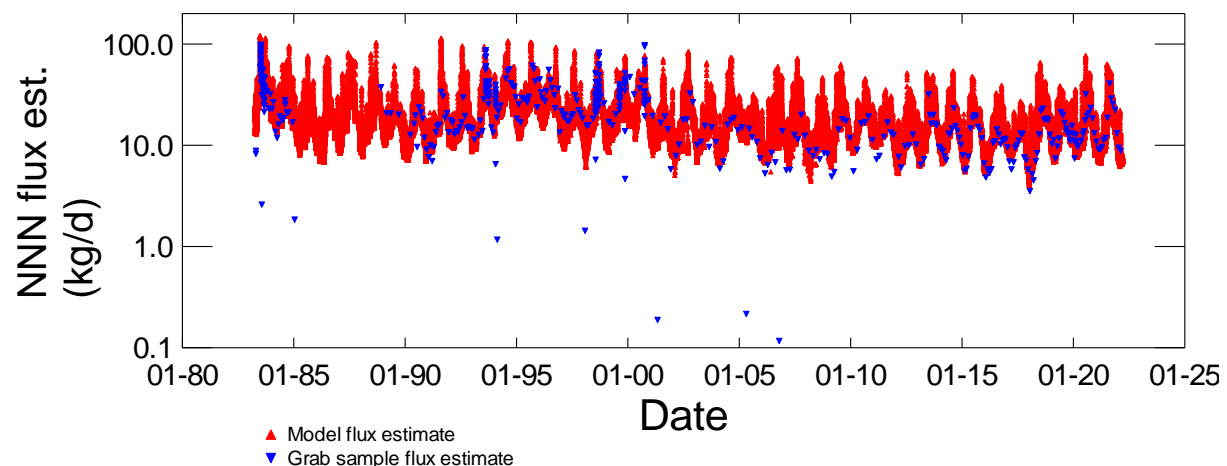
Figure 3-16:   Comparison of modelled NNN flux and grab sample NNN flux for the Fish Trap site. Note that the Y axis of the plot has $\log_{10}$ scale. The symbology is described in Appendix A.

Mean daily NNN loads at the Fish Trap site are summarised at monthly timestep for the period 1985 through 2020 in Figure 3-17 (top), and annual NNN loads are shown for the period 1989 to 2021 in Figure 3-17 (bottom). Both graphs include a confidence interval for measurements in the period represented.
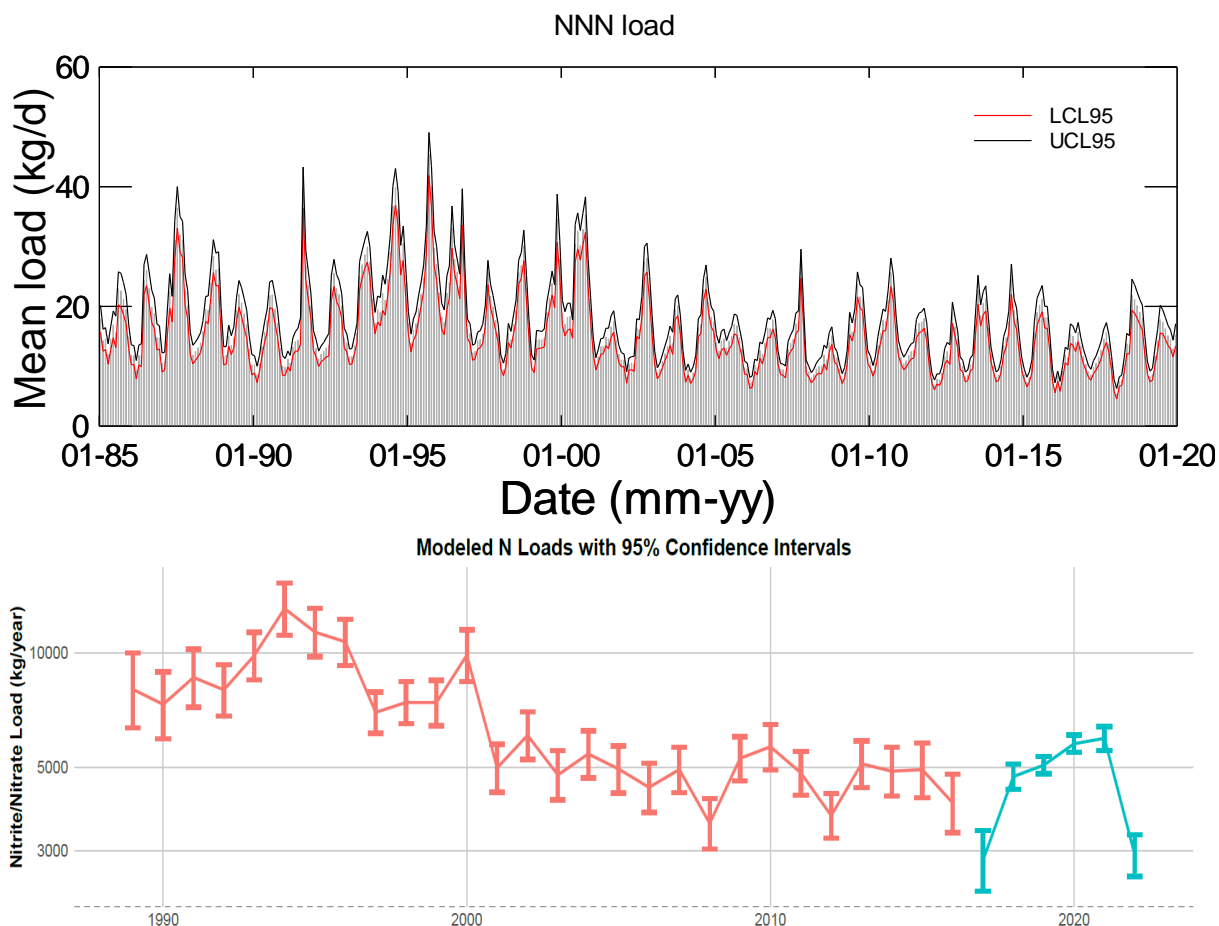
Figure 3-17: Modelled NNN loads at a monthly time-step (top panel) and an annual time-step (bottom panel). Modelled NNN loads are shown with error bars representing a 95% CI around the mean. Note that the Y axis has $\log_{10}$ scale. Annual value for 2022 is for part year only.

The change in NNN load between the same three assessment periods used for TP loads are shown in Table 3-10. The difference in NNN load 1994 and a contemporary period (2018-2020) was large, because of the high estimated NNN load in 1994.

Table 3-10: Change in NNN load – 1994 vs 2018-2020 and 1996-98 vs 2018-2020. Colours and shading indicate values being compared.

Assessment period	Annual load (t)	Average load (t)	Average load (t)	Assessment period sum (t)
1994	10.04			
1996-1998		7.24		21.71
2018-2020		5.14		15.41
Difference (mass)	4.86 (decrease)	2.10 (decrease)		6.30 (decrease)
Difference (%)	51.4 (decrease)	29 (decrease)		29 (decrease)

The magnitude and variability of seasonal (monthly) NNN loads for the two 19-year periods 1984-2002 and 2003-2021 is summarised in Figure 3-18, and statistics are provided in Appendix G and Appendix H. The seasonal pattern is similar in both assessment periods, but there is less variability in monthly load estimates in the recent period.
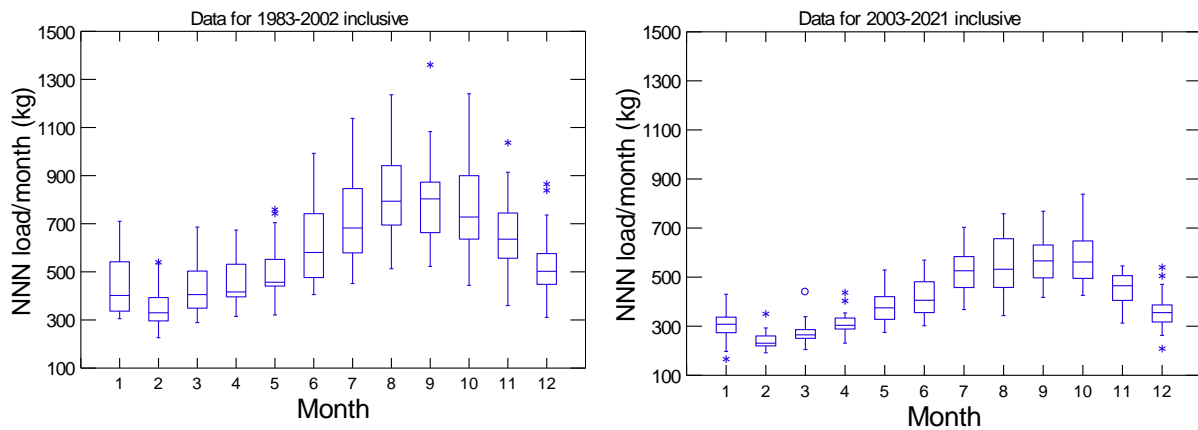
Figure 3-18: Monthly estimates of NNN load for the Fish Trap site for the 1983 to 2002 period and for the 2003 to 2021 period. See Figure 3-6 for explanation of box plot components.

Data summarised in Figure 3-18 confirms what was described in Figure 3-17; the NNN load in the period prior to 2003 was considerably larger than post-2003. There is a similar seasonal pattern between the two periods (Figure 3-18), but monthly NNN loads were generally smaller and less variable post-2002 than in the earlier period. This is even more noticeable in the late summer-early autumn perid than was the case for TP. As was seen for TP, NNN loads are clearly higher in the winter and spring, but the magnitude appears less variable and less dependent on the climate and runoff in that year.

3.6.3   Total suspended solids

A time series of grab sample and model-derived TSS flux estimates is shown in Appendix H, Figure H-3. It is worth noting that several grab samples collected in the period 1993-2002 represent conditions that have not been seen more recently. Annual TSS load estimates are listed in Appendix G. Model-derived estimates, and those derived from instantaneous flux estimates as the product of concentration and discharge at the time of sampling show moderate seasonality (Figure 3-19), with smallest loads in the late summer period, and maximum values observed in October annually.
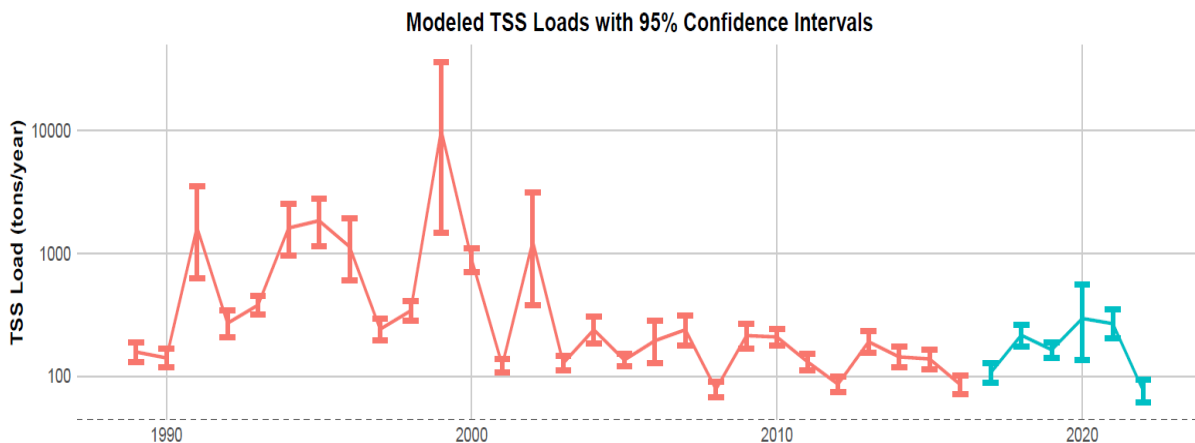
Figure 3-19: **Modelled TSS loads for the Fish Trap site.** Modelled TSS loads are shown with error bars representing a 95% CI around the mean. Note that the Y axis has a $\log_{10}$ scale.

The change in TSS load between the same three assessment periods used for TP and NNN are shown in Table 3-11. The difference in TSS load estimated in 1994 and a three-year historical period (1996-1998), and a contemporary period (2018-2020) was large, because the estimated TSS loads in the historical periods were relatively large, whereas the TSS loads estimated in the contemporary period were typical or representative of the lower and less variable loads observed since approximately 2001.

Table 3-11: **Change in TSS load – 1994 vs 2018-2020 and 1996-98 vs 2018-2020.** Colours and shading indicate values being compared. Loads derived from a regression modelling approach.

Assessment period	Annual load (t)	Average load (t)	Average load (t)	Assessment period sum (t)
1994	1543			
1996-1998		581		1745
2018-2020			683	682

Difference (mass)	860 (decrease)	354 (decrease)	1062 (decrease)
Difference (%)	56 (decrease)	60 (decrease)	61 (decrease)
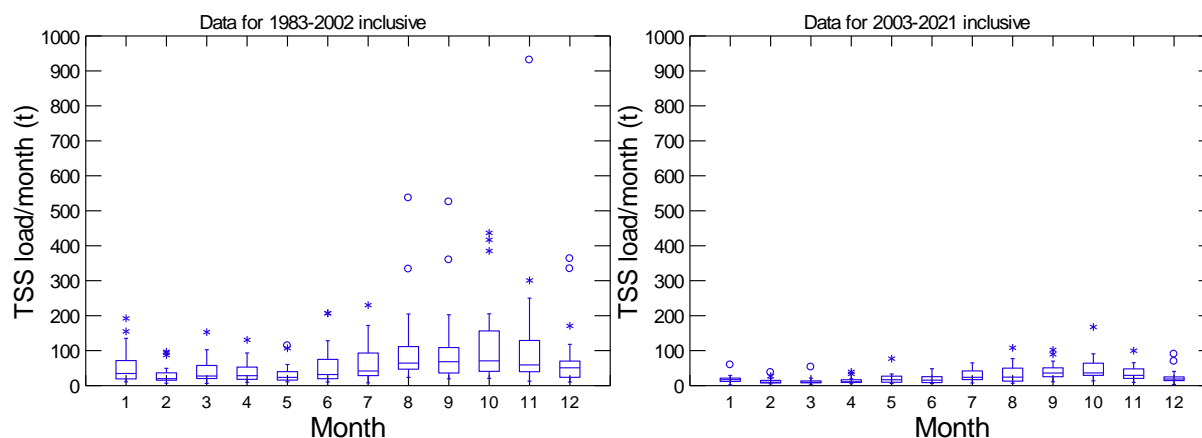
Figure 3-20: **Monthly estimates of TSS load for the Fish Trap site for the 1983 to 2002 period and for the 2003 to 2021 period.** See Figure 3-6 for explanation of box plot components.

Data summarised in Figure 3-20 confirms what was described in Figure 3-19; the TSS load in the period prior to 2003 was considerably larger than post-2003. There is a similar seasonal pattern between the two periods (Figure 3-20), but monthly TSS loads were generally smaller and less variable post-2002 than in the earlier period. Both periods of data indicate that the magnitude of the TSS load is much smaller in summer and autumn.

3.7 Instantaneous and modelled contaminant loads at Mill Creek at Lake Hayes site

Since 2018, event-related water samples have been collected at the "Mill Creek at Lake Hayes" site using an automatic sampler. These samples have been collected in addition to routine monthly grab samples. A total of approximately 150 samples have been collected during this four-year period and analysed for DRP, TP, NNN, TN, and TSS. A separate load estimation exercise was undertaken for this period using these data and the discharge data from the Mill Creek at Fish Trap site. Time series plots for LOADEST predicted loads and grab sample estimates are provided in Appendix I. Annual load estimates derived from LOADEST over the full four-year period are reported in Table 3-12. Seasonal loads and summary statistics from load estimates are also provided in Appendix I.

Table 3-12: Annual contaminant loads derived from LOADEST for the Mill Creek at Lake Hayes site.

Year	Load/year (kg)				Load/year (t)
	DRP	NNN	TN	TP	TSS
2018	29.88	5458.9	6126.5	642.1	396.8
2019	89.69	5207.7	8909.7	743.7	409.7
2020	146.01	5683.9	10171.4	1371.3	850.1
2021	62.64	5900.2	4128.0	913.4	480.0

The annual contaminant loads estimated at the Mill Creek at Lake Hayes site are similar to those estimated for the Fish Trap site (see Appendix G); the largest differences are for TSS. Comparison of these estimates should also consider the number of samples available to calibrate any model in either period, and the conditions under which these calibration data were collected.

3.8 Use of high frequency sensor data for load assessment

3.8.1 Nitrate-N load estimation

A TriOS hyperspectral nitrate-N sensor is deployed at the Mill Creek at Lake Hayes site. Stream discharge is measured at the Mill Creek at Fish Trap site, a few hundred metres upstream. In Figure 3-21, discharge and TriOS nitrate-N concentrations are plotted together, showing that spikes in the TriOS output coincide with some but not all discharge events in Mill Creek. The TriOS sensor measures "nitrate-N" only, the grab samples include nitrite- and nitrate-N forms; although nitrite-N is not reported separately, it is usually not present in surface waters in appreciable amounts. The TriOS sensor has several transient spikes, both in positive and negative direction. It is not obvious whether these spikes are related to sensor performance, or to discharge events. Figure 4-3, shown in Section 4, indicates a complex relationship between discharge and nitrate-N, both within events, and between events.
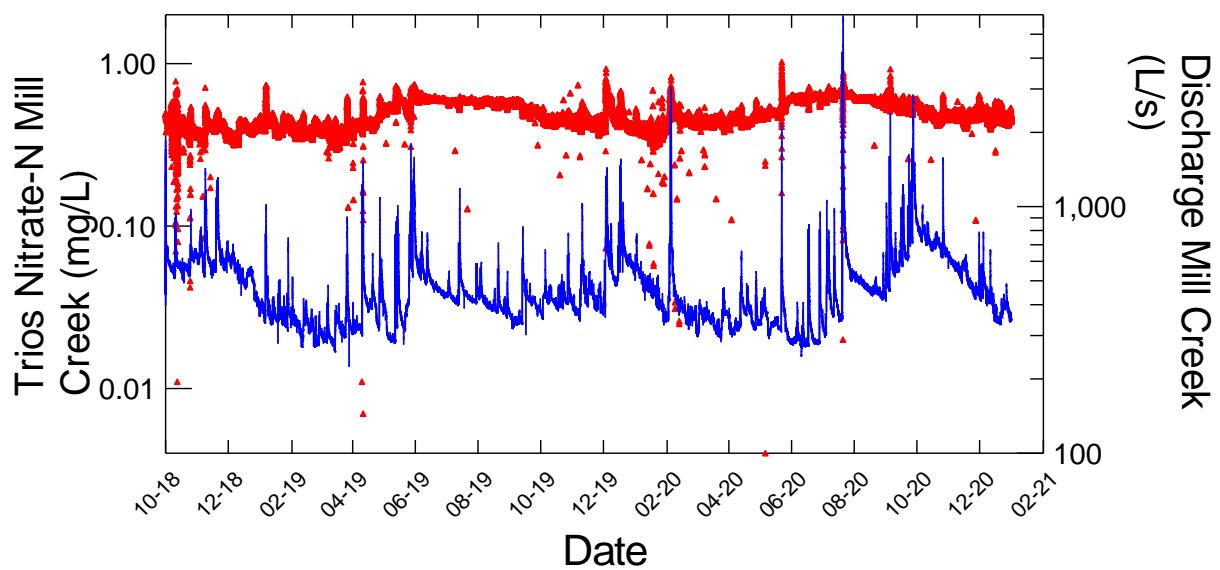
Figure 3-21:   Time-series of TriOS nitrate-N concentrations at Lake Hayes site (red), and discharge at Mill Creek at Fish Trap site (blue).

Estimates of nitrate-N load derived from the TriOS sensor (as a product of sensor concentration estimate and discharge), and grab samples (either as product of grab sample concentration and discharge at the time of sampling, or from the LOADEST model) are shown in Figure 3-22. There is good correlation between the grab sample estimates and the TriOS sensor estimates in nitrate-N flux, particularly during elevated discharge events. The relationship between the flux time series derived from the LOADEST model and the estimates from the TriOS sensor is also good, with the LOADEST estimates being consistently smaller than those from the TriOS measurements.

▲ Model flux estimate
▼ Trios flux estimate
● Grab sample flux estimate
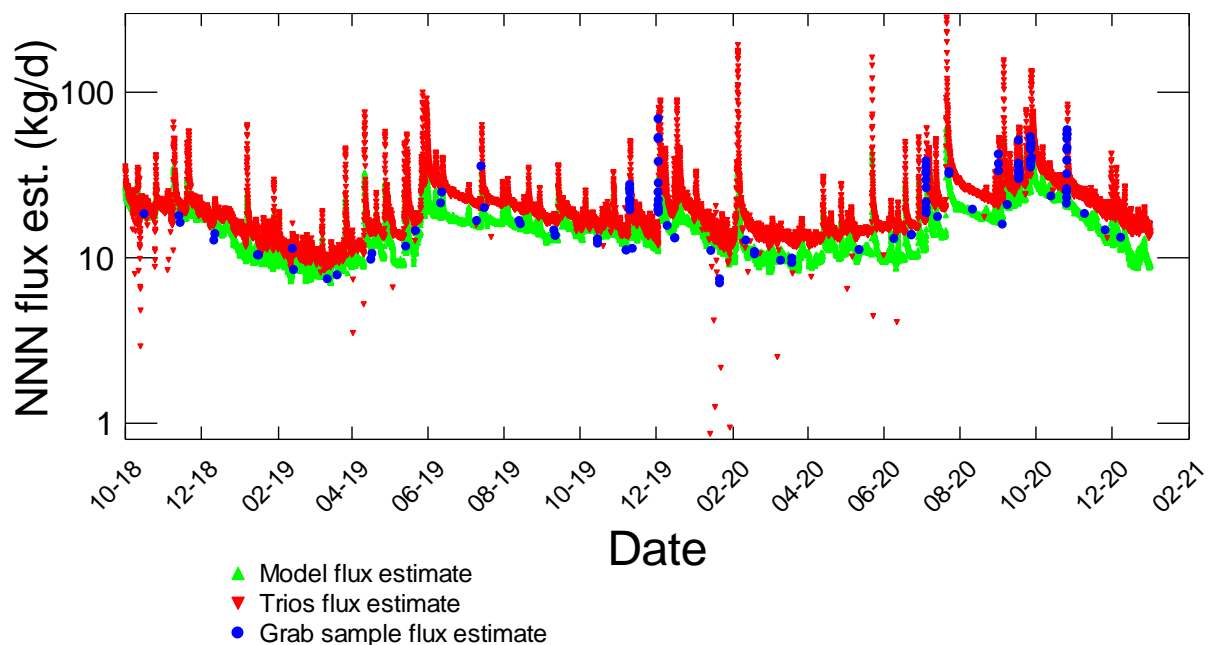
Figure 3-22:   Comparison of nitrate load estimates derived from TriOS sensor, and LOADEST model and grab sample nitrate-N estimates for the period between October 2018 and February 2021.

The LOADEST estimates are similar to the estimates from the TriOS sensor under baseflow conditions. However, the LOADEST does not predict overall nitrate loads (inclusive of high flow events) as well as the TriOS sensor or the grab samples (Figure 3-23). This is a consequence of two factors:

- the temporal resolution of this implementation of LOADEST modelling was limited by the timestep of calibration data – the model uses daily average discharge and concentration data as input which reduces the sensitivity of the model to short-duration or transient events.

- The LOADEST model was calibrated using the grab sample data from the Fish Trap site, where no event-based sampling occurred. Grab sample data were provided for seven specific flood events recorded at the Mill Creek at Lake Hayes site. On each occasion, up to 23 discrete samples were collected within a 24-hour period. The r version of LOADEST is limited to calculations based on data derived from daily timestep sampling, which limits the ability of the model to utilise high frequency calibration data.
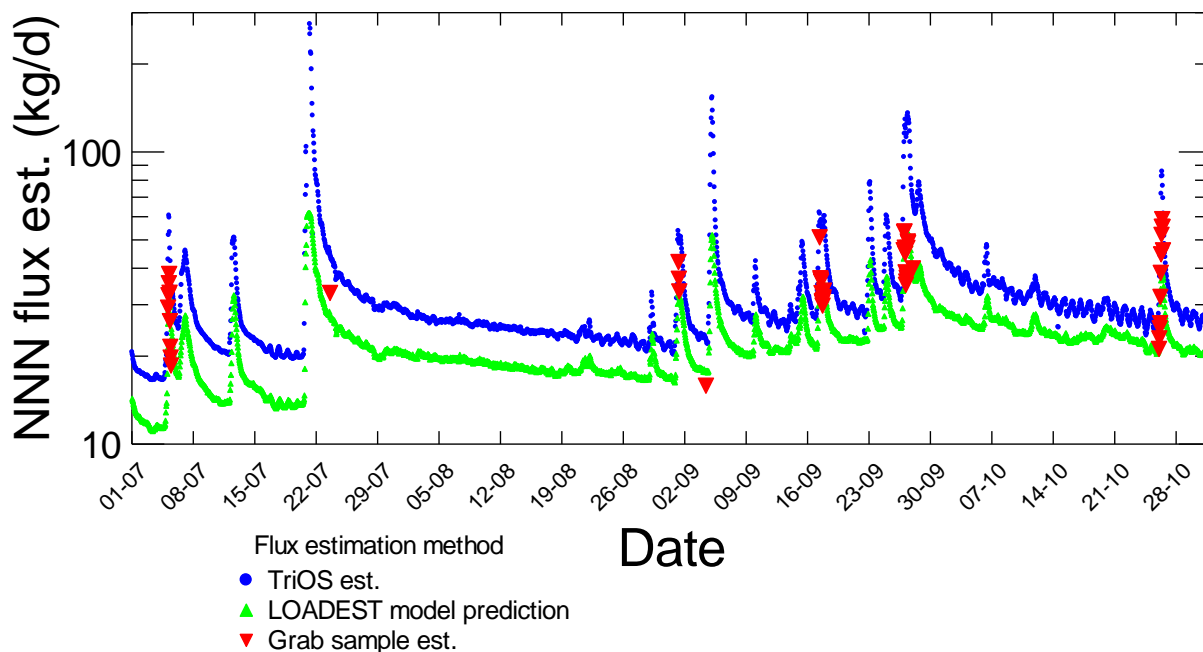
Figure 3-23: Comparison of nitrate load estimates derived from TriOS sensor, and LOADEST model and grab sample nitrate-N estimates, July-October 2020.

In streams where discharge is "flashy", the frequency of grab sampling significantly influences the estimate of contaminant load. In a previous assessment of the use of high frequency nitrate-N concentration data for contaminant load estimation (the Aparima River, Southland), it was demonstrated that in a larger river, the estimate of sample frequency had a smaller effect on the estimate of annual loads until nitrate-N measurements were acquired at less than approximately monthly frequency (Hudson and Baddock 2019). In the case of Mill Creek, the ability to calibrate a model using high frequency data has an obvious impact on the load estimates, as summarised in Table 3-13. The monthly estimates derived from the two methods differ by approximately 30% and 32% times over the two full years for which data were available (Figure 3-24). Differences of this magnitude are not unusual for modelling, particularly when relatively sparse data from grab samples are available for model calibration.
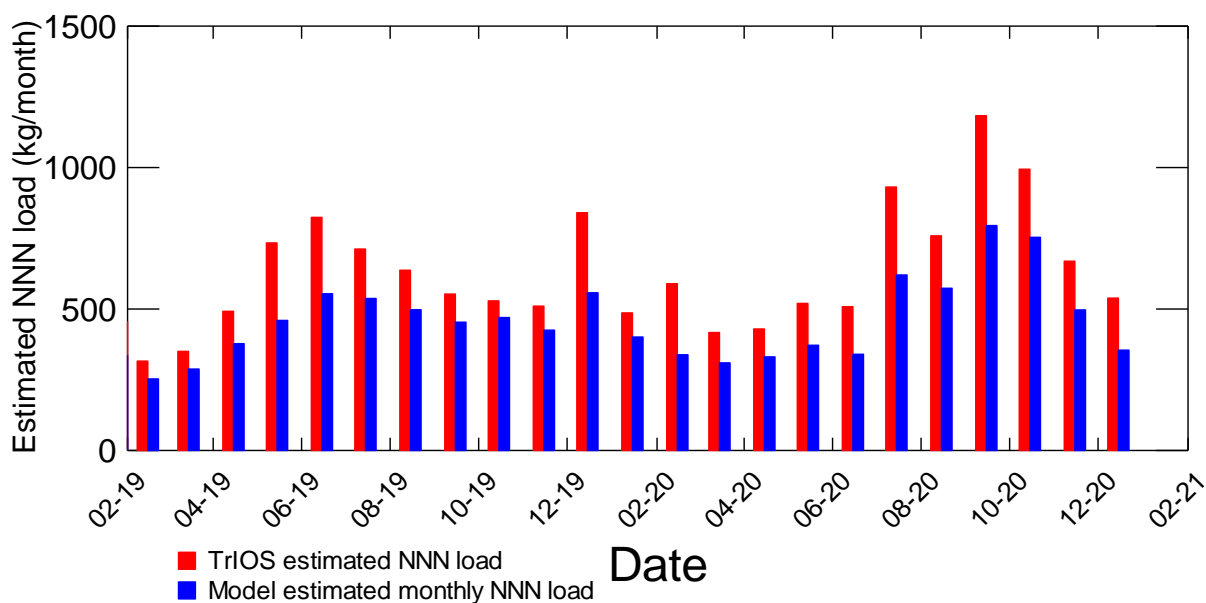
Figure 3-24: Monthly nitrate-N loads as determined from TriOS data and from LOADEST modelling for the period between February 2019 and January 2021.

Table 3-13: Comparison of annual load estimates derived from two approaches. , TriOS-nitrate = 15 minute frequency measurement, LOADEST – hourly estimates derived from grab samples.

Year	Annual load per estimation method (kg)	
	TriOS-nitrate	**LOADEST NNN**
2019	6951	5126
2020	8023	5841

3.8.2   Suspended sediment and total phosphorus load estimation

ExoSonde II instruments equipped with turbidity sensors were deployed at the Mill Creek at Lake Hayes and Mill Creek at Hunter Road sites. They recorded turbidity at 15-minute frequency coinciding with 15-minute discharge measurements made at the same sites. Monthly water quality grab samples were collected at both sites. Additionally, an automatic sampler was used to take flow-weighted samples at the Mill Creek at Lake Hayes site, which is very close to the Fish Trap site. Water quality samples were collected during seven separate discharge events. Samples collected during these events were analysed for lab turbidity, TSS and TP. The high frequency turbidity data and water quality data allowed us to investigate relationships between turbidity and both TSS and TP concentrations. These relationships were then used to convert the continuous turbidity record into continuous TSS and TP datasets for the Lake Hayes and Hunter Road sites. The flow data in turn were used to estimate loads of TSS and TP transport in Mill Creek from the estimated TSS and TP time series.

There are numerous examples in the literature of linear relationships between turbidity and sediment concentrations being used to create sediment concentration time series data. A very recent example is (Skarbøvik *et al.* 2023). They cite others (Marttila and Kløve 2012; Stutter *et al.* 2017; Wenng *et al.* 2021) stating the goodness-of-fit between turbidity and sediment varies from good to poor depending on other factors such as the presence of dissolved solids, organic matter,

soluble organic coloured compounds, high iron concentrations the some algae and other microorganisms, and on the size, shape and composition of particles.

The CLUES modelling estimated that much of the phosphorus load in the catchment is derived from soil erosion (see Section 3.2), but the phosphorus loads and concentrations in the catchment are low. Numerous catchment studies have also demonstrated that phosphorus is often mobilised in particulate form. "Total phosphorus" is a complex mixture of dissolved fractions (most common of which is dissolved reactive phosphate), as well as particulate-bound materials. This creates the possibility that TP may also be predicted from turbidity. Here we explore use of turbidity to estimate TP as well as TSS at the Mill Creek at Fish Trap/Lake Hayes and Hunter Road sites separately. In both assessments, the TSS and TP concentration measurements from each site were paired with the closest possible turbidity measurement from the relevant high frequency time series to develop the relationships with turbidity. Where two or more grab-samples were made during a 15-minute interval, the average concentration over the interval was used.

3.8.3 Mill Creek at Fish Trap and Mill Creek at Lake Hayes sites

The close proximity of these sites meant we were able to merge the water quality data from the Fish Trap and Lake Hayes sites to create a single water quality dataset that covered a greater range of flow conditions. The relationships between turbidity and each of TSS and TP in the combined water quality dataset were visually assessed by plotting the paired turbidity and concentration datasets (Figure 3-25). These relationships are essentially linear but with increasing divergence as the magnitude of the measured turbidity rises. We also explored other potential relationships, e.g., polynomial curves, and these did not improve the fit. This divergence is likely to be associated with the variability in the relationship between turbidity and discharge at higher flow rates (see Figure 3-26).

The discharge and turbidity time series are plotted together with TSS concentrations from grab samples in Figure 3-26; this figure shows the timing of the grab-samples and the high level of variability in the turbidity data. The grab samples taken during baseflow are from the Fish Trap water quality data while the spikes in turbidity during flow events are from the Lake Hayes water quality data. Note that not all flow events were sampled at Lake Hayes and the sampling does not cover the full range of flows at the site.

The continuous turbidity data span an approximately 3-4 $\log_{10}$ range of values. There are also several gaps in the data record, and one noticeable period (April to June 2019) where many elevated sonde turbidity values occur. As shown in Figure 3-27, the extremely elevated turbidity measured in the period April to June 2019 does not necessarily coincide with elevated flow conditions. These large turbidity values may also be of very limited duration, as shown in the inset to Figure 3-27. The inset also shows that that transient elevated turbidity values occurred in a period when discharge was in recession from around 3.9 to 3.4 m^3/s over the course of the day. It is possible that these very high turbidity values were the consequence of interference caused by detritus that became snared on the sensor or sonde body. The uncertainty in the data means that the TP and TSS load estimates made with these data should be treated with caution.
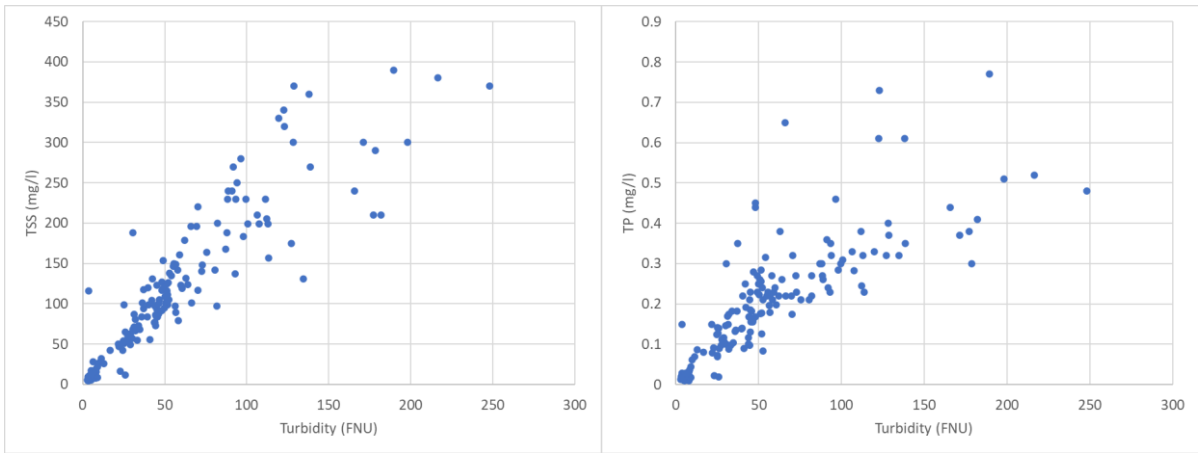
Figure 3-25: Comparison of turbidity from the ExoSonde sensor and TSS (left) and TP(right) for Mill Creek at Fish Trap/Lake Hayes. The concentration grab samples come from both the Fish Trap and Lake Hayes monitoring sites.
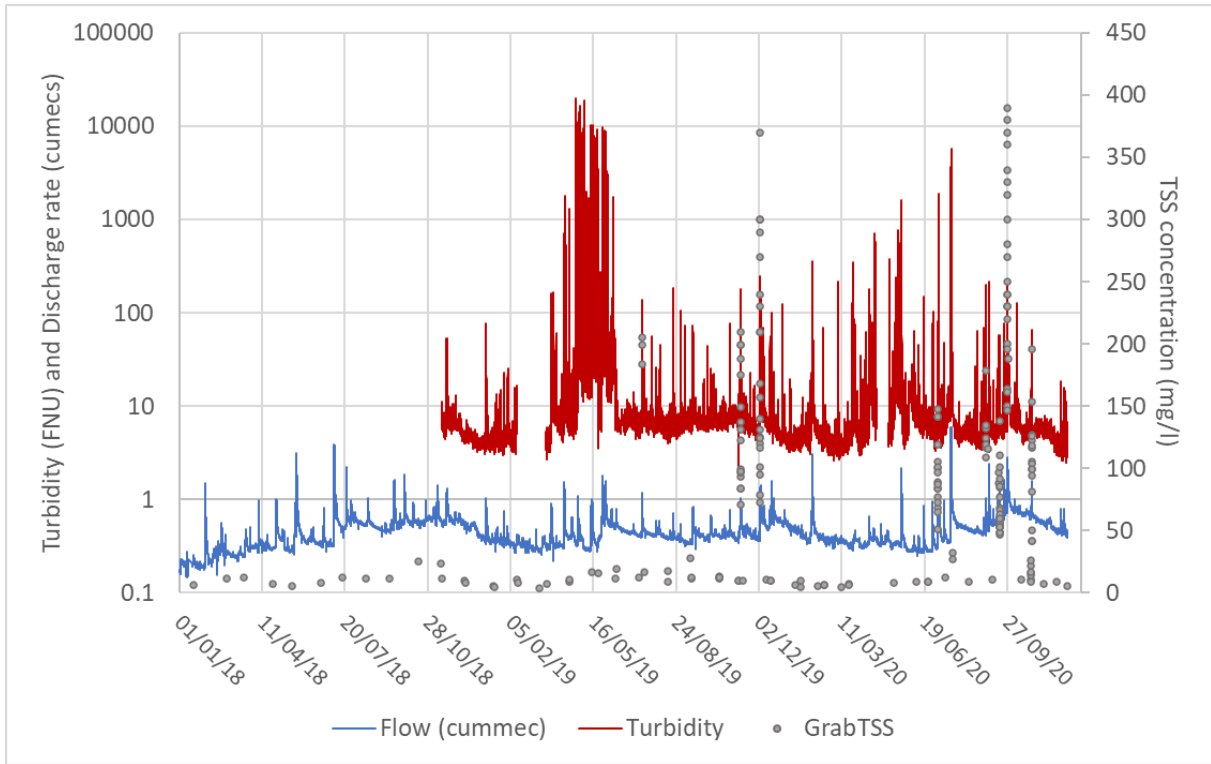
Figure 3-26: Continuous discharge and turbidity time series (from ExoSonde sensor), and grab sample TSS concentrations for Mill Creek at Fish Trap/Lake Hayes. Note left hand axis (turbidity and discharge) has $\log_{10}$ scale.

Estimation of contaminant losses
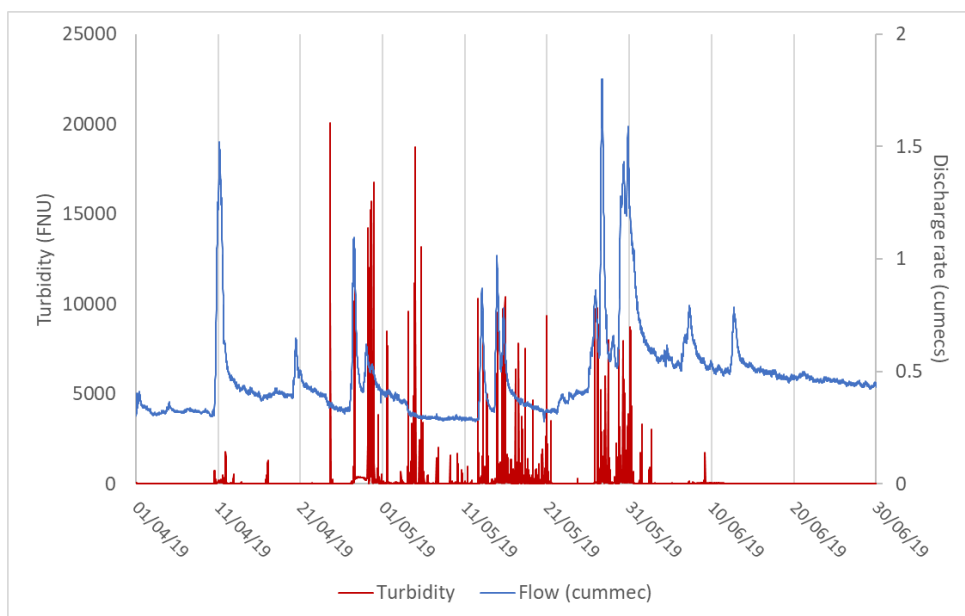
Figure 3-27: Continuous discharge and turbidity time series (from ExoSonde sensor) for 13 week period April-June 2019 for Mill Creek Creek at Fishtrap/Lake Hayes.

Regression models were developed between the sonde measured turbidity and the paired grab sample TSS and TP concentrations in order to estimate long-term TSS loads. In all, there were 183 pairs of data for both TSS and TP. For each of TSS and TP, the paired data were split into two groups, the first for calibration, and the second for testing. This was done by assigning every second pair to the test dataset so that the two sets cover the same period and have similar distributions in measured turbidity. The regression was done in Python using the SciPy[7] Least Squares Optimisation tool[8]. The resulting equations are:

$$TSS_{Conc.} = 1.82 \times turbidity + 12.37$$

$$TP_{Conc} = 0.003 \times turbidity + 0.034$$

Model fit was tested by applying the regression equation to the test data. The model performance for both the calibration and test data was comparable for both TSS and TP showed good fit (Table 3-14). However, the magnitude of the errors increases with turbidity, which suggests that these models are best suited to base-flow conditions.

Table 3-14: TSS and TP regression model performance for Mill Creek at Fish Trap/Lake Hayes.

Performance metric	TSS		TP	
	Calibration	Test	Calibration	Test
Coefficient of determination (R^2)	0.838	0.908	0.74	0.861
Nash-Sutcliff Efficiency (NSE)[9]	0.838	0.855	0.74	0.737

---

[7] https://scipy.org/ (date of last access 24 February 2023)
[8] https://docs.scipy.org/doc/scipy/reference/generated/scipy.optimize.least_squares.html (date of last access 24 February 2023)
[9] Nash, J.E. and Sutcliffe, J.V. (1970) River flow forecasting through conceptual models part I — A discussion of principles. *Journal of Hydrology*, 10(3): 282–290.

Performance metric	TSS		TP	
	Calibration	Test	Calibration	Test
Root mean square error (RMSE)	37.743	34.333	0.081	0.069
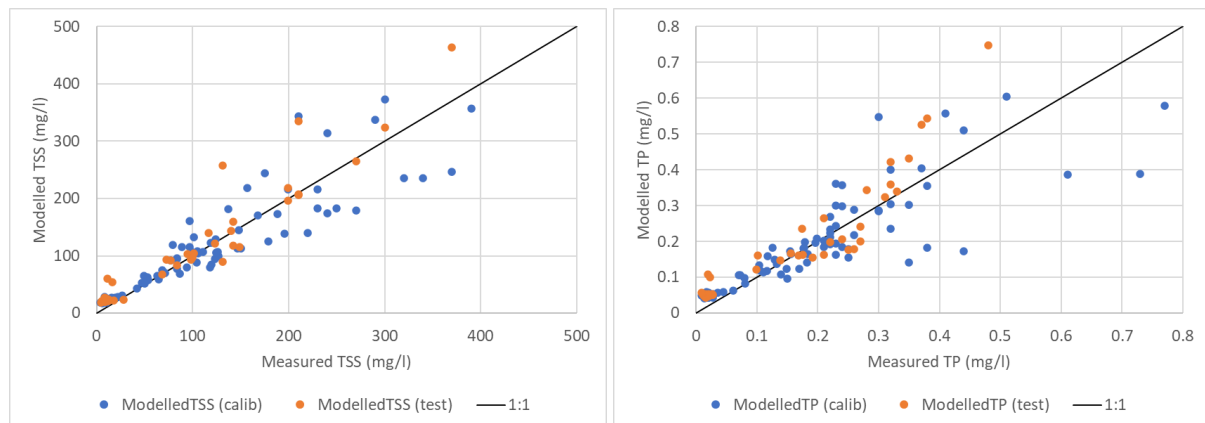
Figure 3-28:   Scatterplots of measured and modelled TSS (left) and TP (right) for the calibration and test datasets for Mill Creek at Fishtrap/Lake Hayes. The 1:1 lines are shown for reference.

The models were applied to all the ExoSonde turbidity measurements to obtain time series of estimated TSS and TP concentrations. This time series was used to derive an estimate of long-term average sediment and phosphorus loadings delivered to the lake. The loads are summarised by month and year over the monitoring period in Table 3-15. This was done by multiplying the estimated concentrations in mg/L by the discharge volume in litres estimated for each time step from the discharge time series. A simple approach was taken to estimate volumes whereby the volume was calculated as the product of the flow rate (converted to L/s) and the number of seconds in each time interval.

Although estimates of TSS and TP fluxes and loads were obtained for all dates when continuous turbidity data were available, these results should be treated with caution when apparently anomalous continuous sonde turbidity data exist, or when periods of continuous sonde turbidity data are missing. Where data do not fully represent a period, the estimates may be used with caution, e.g., to estimate loads over shorter periods (weekly or daily).

Table 3-15: **Estimated sediment yield per period, derived from a model utilising high-frequency turbidity estimates for Mill Creek at Fish Trap/Lake Hayes.** Results for periods of potentially questionable record are highlighted orange, periods where more than approximately 20% data are missing are shaded blue.

Time period	Proportion of theoretical data	TSS Load (t)	TP Load (kg)
Nov 2018	55%	27.5	343
Dec 2018	100%	30.0	498
Total 2018	13%	57.5	841
Jan 2019	97%	24.1	363
Feb 2019	41%	7.3	120
Mar 2019	40%	14.3	145
Apr 2019	100%	540.7	1206
May 2019	100%	1216.4	2325
Jun 2019	100%	73.2	545
Jul 2019	100%	37.5	447
Aug 2019	100%	30.5	399
Sep 2019	100%	29.0	378
Oct 2019	100%	32.5	420
Nov 2019	100%	34.4	421
Dec 2019	100%	72.8	668
Total 2019	**90%**	**2112.9**	**7438**
Jan 2020	100%	25.7	440
Feb 2020	100%	68.8	490
Mar 2020	100%	22.1	337
Apr 2020	71%	24.5	254
May 2020	82%	64.0	359
Jun 2020	100%	27.2	305
Jul 2020	100%	593.0	1457
Aug 2020	100%	27.8	450
Sep 2020	100%	116.5	844
Oct 2020	100%	50.6	715
Nov 2020	100%	30.6	494
Dec 2020	100%	35.7	413
Total 2020	**96%**	**1086.5**	**6559**

3.8.4 Mill Creek at Hunter Road

Fewer grab samples are available for the Hunter Road site than for the Lake Hayes site (20 pairs compared to 183 pairs); for this reason, we were unable to split the data into calibration and test datasets. All the water quality samples are monthly discrete samples taken for environmental reporting, rather than event based or flow-proportional samples. These samples were taken during low- to mid-flow conditions. No paired-high frequency turbidity data were available for five of the 20 water quality samples. In order to use these datapoints for modelling, we substituted the turbidity determined from the grab samples into the model inputs.

As was observed for the sonde turbidity and flow data at the Fish Trap site, there were sizable gaps in the high-frequency data record for the Hunter Road site. There were also periods where elevated or erratic turbidity were not related to flow; however, unlike the Fish Trap data, these periods were not as sustained and generally lasted for periods of approximately five days or less (e.g., between 6 and 11 May 2019, shown in Figure 3-29). The spikes in turbidity observed between 12 and 16 May occured during high flow periods and decrease as flow recedes.
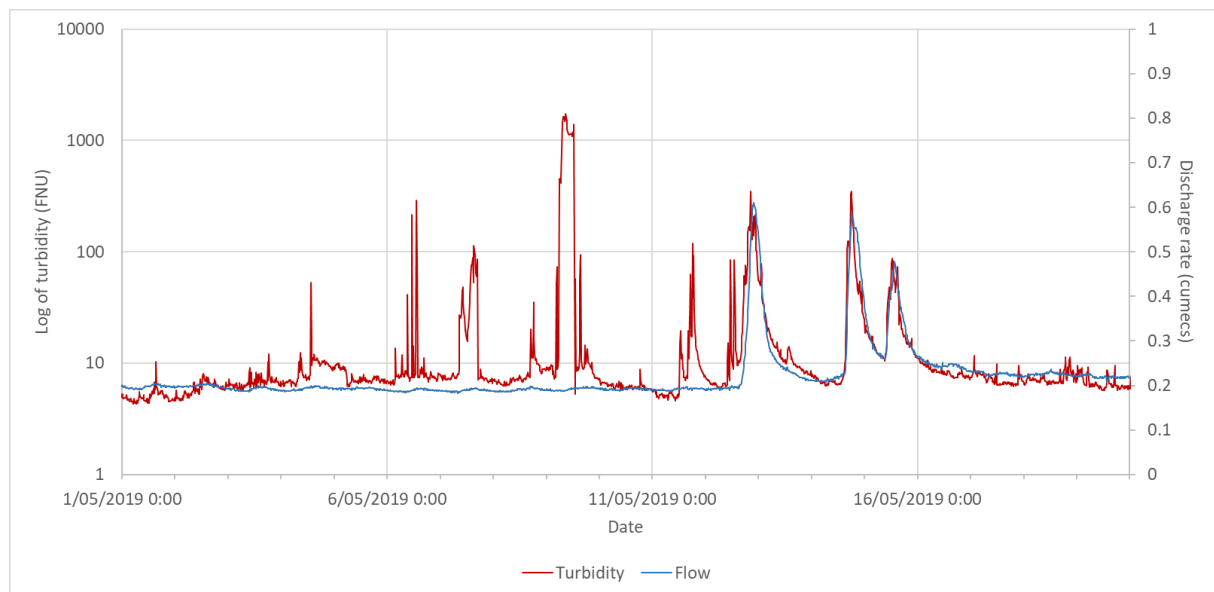
Figure 3-29: Turbidity and discharge at Mill Creek at Hunters Road showing spikes in turbidity during the first half of May 2019. At the beginning of the period, the turbidity does not track flow, however, there is good agreement between flow and turbidity from 12 May.

The limited data meant that we determined the regression equations using the inbuilt regression tools available in MS Excel (Figure 3-30) and the resulting equations are:

$$TSS_{Conc.} = 2.81 \times turbidity + 1.85$$

$$TP_{Conc} = 0.002 \times turbidity + 0.010$$

The model fit is given in Table 3-16 and plotted in Figure 3-31.
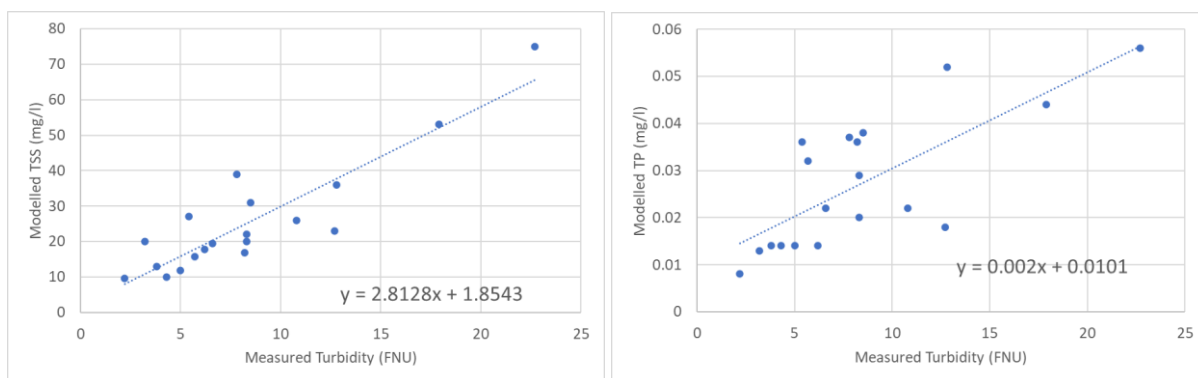
Figure 3-30: **Regression plots and equations for the relationship between turbidity and TSS (left) and TP (right) for Mill Creek at Hunter Road.**

Table 3-16: **TSS and TP regression model performance for Mill Creek at Hunter Road.**

Performance metric	TSS	TP
Coefficient of determination (R^2)	0.80	0.55
Nash-Sutcliff Efficiency (NSE)[10]	0.80	0.55
Root mean square error (RMSE)	6.98	0.009
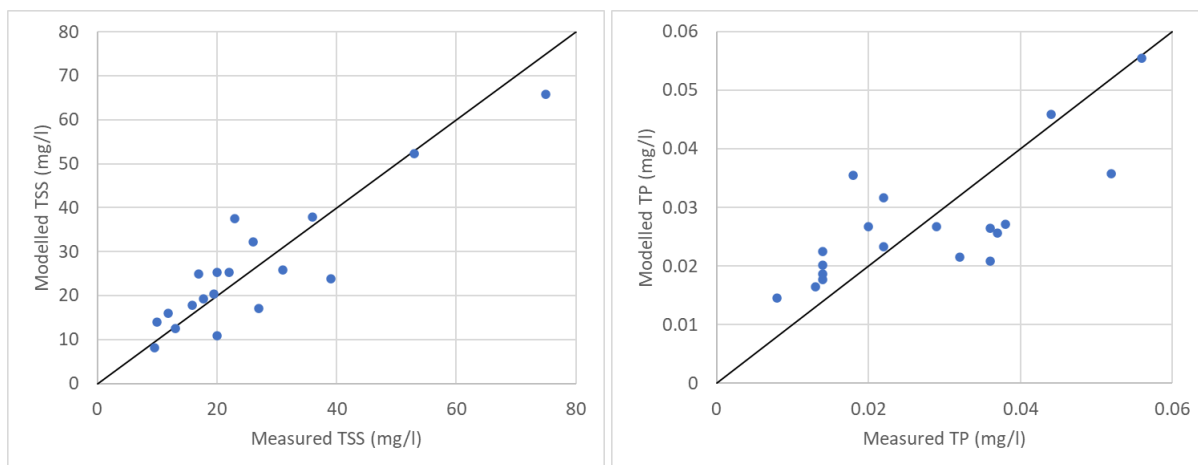
Figure 3-31: **Scatterplots of measured and modelled TSS (left) and TP (right) for Mill Creek at Hunter Road.** The one-to-one lines are shown for reference.

We used the same method described for the Fish Trap/Lake Hayes data to estimate sediment and phosphorus loads in Mill Creek at the site. The predicted monthly and annual loads are summarised in Table 3-17.

---

[10] Ibid.

Table 3-17:   Estimated sediment yield per period, derived from a model utilising high-frequency turbidity estimates for Mill Creek at Hunter Road. Results for periods of potentially questionable record are highlighted blue.

Time period	Proportion of theoretical data	TSS Load (t)	TP Load (kg)
Sep 2018	41%	0.95	3.57
Oct 2018	100%	2.74	10.34
Nov 2018	98%	3.50	12.27
Dec 2018	100%	3.00	11.09
Total 2018	**28%**	**10.19**	**37.28**
Jan 2019	93%	1.83	7.30
Feb 2019	41%	0.49	2.11
Mar 2019	40%	0.50	2.16
Apr 2019	100%	1.33	5.59
May 2019	100%	1.88	7.41
Jun 2019	100%	2.22	8.69
Jul 2019	100%	1.97	7.92
Aug 2019	100%	1.61	6.73
Sep 2019	100%	1.28	5.53
Oct 2019	100%	1.45	6.15
Nov 2019	100%	1.69	6.95
Dec 2019	100%	3.79	13.02
Total 2019	**90%**	**20.03**	**79.56**
Jan 2020	100%	2.37	9.17
Feb 2020	100%	2.02	7.56
Mar 2020	100%	1.33	5.75
Apr 2020	100%	1.06	4.71
May 2020	100%	1.04	4.62
Jun 2020	100%	1.08	4.77
Jul 2020	100%	2.50	8.35
Aug 2020	100%	1.82	7.47
Sep 2020	100%	3.66	12.27
Oct 2020	44%	2.04	6.83
Total 2020	**79%**	**18.92**	**71.48**

4 Discussion

4.1 Catchment land use

Review of available data indicated that land cover in the Lake Hayes catchment has not changed substantially over the last 25-years. The extent of urban area is approximately four times greater than in 1996, but it only comprises 5% of the catchment area.

The lower reaches of Mill Creek were identified by Caruso (2000) as the dominant source of contaminants of concern (phosphorus, nitrogen and sediment). The lower reaches of the basin are largely covered in grassland. CLUES modelling substantiates this view, indicating relatively low TN loads in the upper catchment, which increase steadily from the Hunter Road site through to the inflow to Lake Hayes. The overall pattern is similar for TP loads.

The upper catchment (represented by the four tributary catchments) contributes a relatively small proportion of the total TN and TP load annually – approximately 10% of TN and 15% of the TP load. The relative contribution of various reaches of the catchment to the total lake TN and TP inflow load is summarised in Figure 4-1. More than approximately two-thirds of the total TP and TN load entering the lake is estimated to enter Mill Creek downstream of the Hunter Road site. This relative contribution is similar to that estimated by Caruso (2000), and was similar to that identified by Goeller *et al.* (2020), who recommended that efforts to mitigate sediment contaminant loads (which would also reduce TP loads) should target the lower catchment.
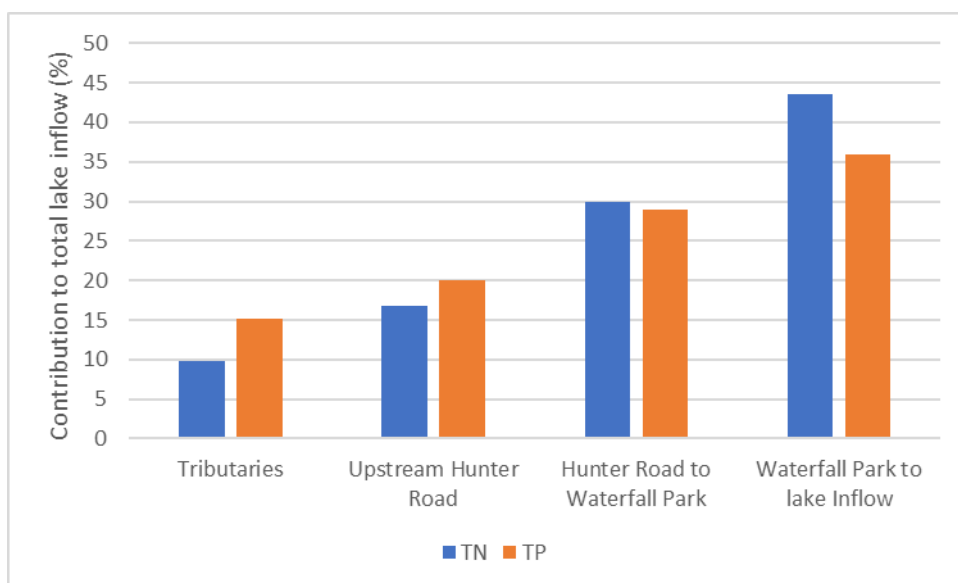
Figure 4-1: **Relative contribution of reaches in the Mill Creek catchment to total lake TN and TP load (%).** Values derived from CLUES (Table 3-4).

4.2 Synoptic surveys

The synoptic surveys undertaken in 2018-2020 have provided a valuable recent benchmark of catchment-wide physio-chemical water quality information. Although more data are available for the recent ca. 18-month period than the earlier (1997) period, the relative contributions of tributary sub-catchments were similar to those derived from earlier surveys, and the characteristics of the area remains largely unchanged. Approximately 50% of samples were collected under below-median

flow conditions, and therefore provide an indication of baseflow concentrations and loads at various locations along the Mill Creek catchment.

Comparison of recent sample results with those of a 1997 survey indicates that DRP concentrations have increased in Dan O'Connell Creek in the upper catchment, and in the mid catchment (Hunter Road) and in the inflow to Lake Hayes. Trends in TP concentrations in the mid- and lower catchment were similar, and the concentration in McMullan Creek was considerably larger than the 1997 estimate in 2018. These trends should be used cautiously – they do not account for flow (flow at the time of sampling are not available for the 1997 survey data).

4.3   Instantaneous and modelled loads

Several methods were used to estimate contaminant loads. The Fish Trap site has an extensive water quality and hydrological record, which allows estimate of stream contaminant loads for selected water quality variables over an approximately 40-year period. The long-term record of annual load estimates indicates that for all water quality variables considered in this study, the annual load estimates have decreased since approximately 2002. This decrease is closely related to the decrease in annual discharge that has been quantified since 2000.

The Management Plan target for the Lake Hayes inflow was established in 1994, during a period of well-above rainfall and discharge. As rainfall and runoff decreased markedly in the 2000-2002 period, stream TP loads also decreased. As a result, the 20% reduction in annual TP load relative to the 1994 base year TP load has been achieved since 1996, and the annual load has been less than 1 t/y since approximately 2002. The 1994 annual load was almost 3 t/y. The average load estimated for the period 2018-2020 was 0.6 t/y – this represents a decrease of approximately 79% relative to the 1994 annual load. The TP load has a seasonal pattern (Figure 3-12); for example, the seasonal range in 2018 was 6.5 kg in the month of January to 82.5 kg inv the month of November.

The contemporary NNN load at the Fish Trap site has also decreased relative to the load estimated for the Management Plan base year (1994). The annual load decreased by approximately 50% from 10 t/y to 5.14 t/y (the average over the period 2018-2020). As with TP, the NNN load at the Fish Trap site also has a distinct seasonal pattern (Figure 3-18); for example, the monthly load in 2018 varied from a minimum of 207 kg in February to 677 kg in July.

Comparison of the LOADEST NNN estimates with those derived from the TriOS sensor was possible for a 28-month period. Monthly estimates derived from the two techniques are summarised in Table 4-1 (annual load estimates derived from these two techniques are in Table 3-13). As was noted previously, the LOADEST technique under-estimates the "direct" estimate derived from a simple calculation – the product of the TriOS estimate of NNN concentrate and Mill Creek discharge at the time of measurement. The annual load estimates based on TriOS data were approximately 26% larger than those derived from LOADEST. The magnitude of the relative difference between the two estimates is consistent with observations in earlier work (Hudson and Baddock 2019).

Table 4-1: **Comparison of the LOADEST NNN estimates with those derived from the TriOS sensor, Mill Creek at Lake Hayes site.** LOADEST estimates are also presented as a proportion of TriOS estimates.

Month	Nitrate-N load/month (kg)		LOADEST estimate as proportion of TriOS estimate
	Trios	LOADEST	
Sep-2018	719.7	622.2	86%
Oct-2018	664.5	636.1	96%
Nov-2018	709.3	612.9	86%
Dec-2018	550.8	477.4	87%
Jan-2019	456.3	337.0	74%
Feb-2019	315.7	252.8	80%
Mar-2019	350.1	287.7	82%
Apr-2019	491.8	377.4	77%
May-2019	733.4	459.4	63%
Jun-2019	823.9	553.8	67%
Jul-2019	711.9	537.2	75%
Aug-2019	636.9	497.2	78%
Sep-2019	552.8	453.3	82%
Oct-2019	528.5	469.7	89%
Nov-2019	509.9	425.1	83%
Dec-2019	840.3	557.1	66%
Jan-2020	486.0	400.8	82%
Feb-2020	589.3	338.2	57%
Mar-2020	416.7	309.4	74%
Apr-2020	429.4	330.6	77%
May-2020	519.7	371.7	72%
Jun-2020	508.1	339.9	67%
Jul-2020	931.2	620.3	67%
Aug-2020	758.5	573.2	76%
Sep-2020	1183.3	795.0	67%
Oct-2020	994.0	753.3	76%
Nov-2020	668.8	496.8	74%
Dec-2020	538.4	354.6	66%

Examination of the two model outputs indicated that the TriOS data were able to follow the hydrograph more closely, because the data were acquired at much finer temporal scale. Even though grab sample data collected using an automatic sampler was able to collect data at two to five minute intervals, this sampling intensity was limited to the number of bottles available (typically 24); the TriOS sensor was set to acquire data at 15 minute intervals, and data were acquired at this frequency for a period longer than two years, with very limited data gaps. The TriOS sensor offers additional benefits for water quality assessments in sensitive water bodies or tributaries to sensitive lakes. The high frequency of data collection allows the effect of diurnal processes such as primary

production to be estimated. When using LOADEST to estimate nitrate-N loads in small streams, the model (as well as multivariate regression models) was unable to replicate the loss of nitrate-N during low flow periods. This was presumably due to denitrification and utilisation of nitrate-N in primary production (Hudson and Baddock 2019; Hudson et al. 2019b; Hudson et al. 2019c). Diurnal variation in nitrate-N has been observed in larger rivers in New Zealand. For example, Burkitt et al. (2017) recorded daily cycles in nitrate-N concentrations that varied seasonally, and in response to the source of the nitrate-N. The discharge of treated wastewater to the river was linked with some of the variation observed. The good correlation between the LOADEST load estimates and those derived from the TriOS sensor suggests that the TriOS sensor could be deployed tactically. The TriOS sensor could be used to collect concentration data over several events, which could subsequently be used to calibrate other models. This would allow other models to perform better, and allow the TriOS sensor to be deployed for shorter periods, to collect data for specific hydrological events, or during seasons when data may be sparse.

In Figure 4-2 we compare NNN concentration values derived from grab samples, the TriOS sensor, and estimates back-calculated from the hourly load estimate generated as an optional output by LOADEST. The latter values should be regarded as approximate because they are influenced by multiple sources of bias – the dependent variable is a transform of the original data. Nevertheless, the figure indicates the good fit between the grab samples and the TriOS concentration estimates, and a reasonable approximation of a nitrate-N timeseries derived from relatively few concentration grab samples.
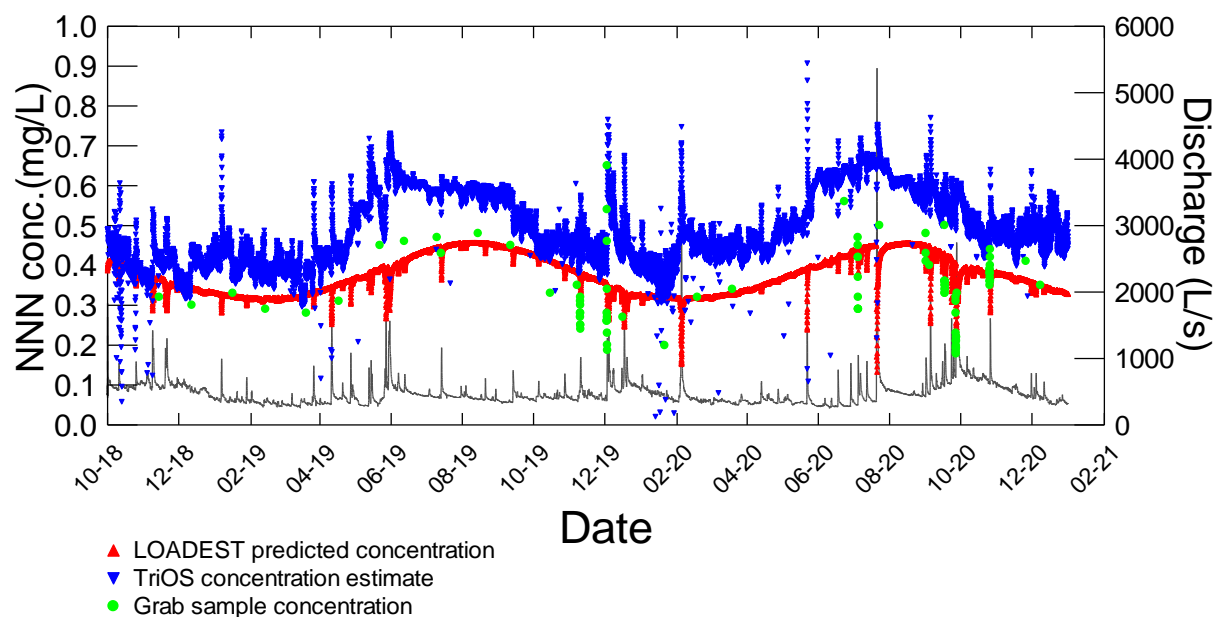
Figure 4-2:   **Comparison of NNN concentrations derived from LOADEST model, TriOS sensor and grab samples.** Values from LOADEST model are approximate, back-calculated from hourly predicted load and discharge.

High frequency data may also be used to better understand the sources of key contaminants, as well as the timing of delivery of the nitrate-N contaminant load. Lloyd et al. (2016) demonstrated how measurements of key water quality variables at frequencies of 15-30 minutes provide insights into the catchment processes controlling hydrological response and hydrochemical transport of nutrient loads from land to stream and within the stream itself, both in dissolved and particulate forms. Using two years of high resolution information it was possible to differentiate the mechanisms which

transport nitrate-N, TP and fine-grained sediment to the stream. An example of the level of detail that is available from high frequency monitoring data is provided in Figure 4-3. The data point labels indicate the hour in which the sample or measurement was made – the TriOS device was set to take four readings per hour, and the autosampler collected samplers every 30 mins. Detailed analysis of these data may provide insights into the factors that drive nitrate mobilisation, or the areas of the catchment from which the nitrate may originate.
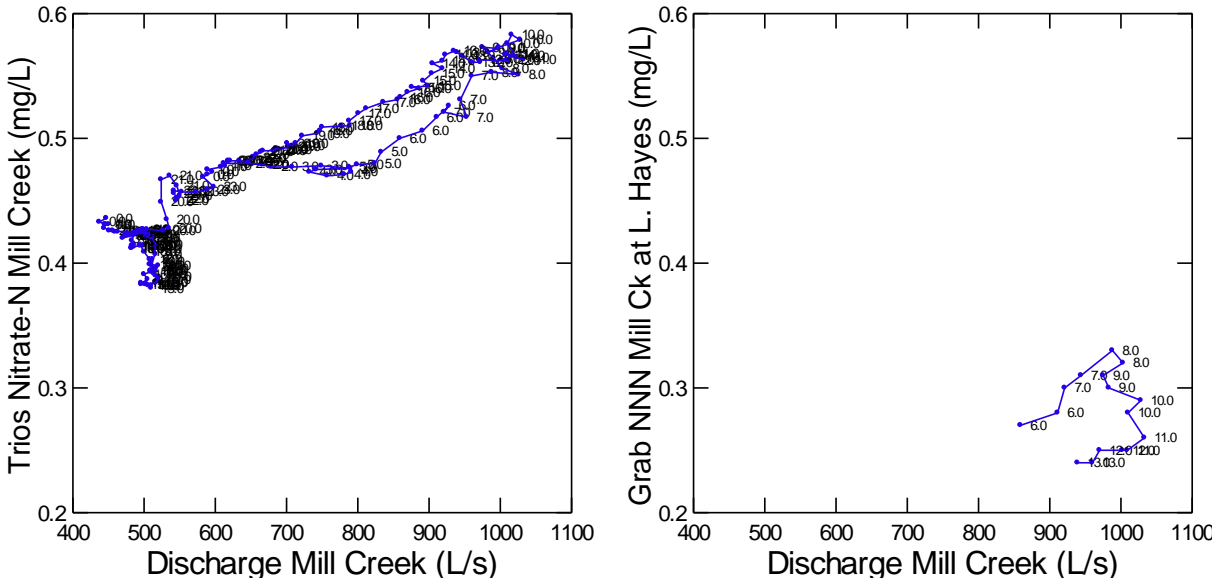
Figure 4-3: **Relatonship between TriOS nitrate-N estimates and nitrate-N grab sample concentrations collected during one event, and stream discharge at the Mill Creek at Lake Hayes site.**

To conclude this section, we set out several recommendations for water quality monitoring and load estimation in near future. Our first recommendation concerns the monitoring site on Mill Creek at Hunter Road. This site is important for evaluating the importance of the upper catchment as a contaminant source for Lake Hayes. The monitoring equipment setup at the Hunter Road site should be considered carefully. Currently the monitoring site furthest downstream on Mill Creek provides detailed data for model calibration and load estimation – event-related gab samples, routing low flow samples, as well as data from two sophisticated in-situ sensors. It would be useful to collect similar data at the Hunter Road site; contaminant loads estimated at the two sites can then be compared directly. Having information of similar quality and rigour for both sites will enable mitigation actions to be directed to areas of the catchment where they will be most effective.

The water quality variables that are currently being measured are current fit for purpose as they provide information about dissolved and particulate forms of nitrogen and phosphorus, as well as sediment. A standard suite of variables is now analysed, which ensures that the data are suitable for load estimation and catchment modelling.

Catchment modelling is an area that ORC may wish to explore further. Water quality and hydrology are controlled by many discrete but inter-related catchment processes that may operate synergistically or antagonistically at times. Catchment processes are further complicated by larger scale drivers such as climate variability and climate change. Catchment models may be used to provide understanding of basic processes occurring in a catchment, or be used to explore the likely outcomes of policy of management actions. In the case of a catchment-surface and groundwater drainage system that is coupled to a lake, models may be used to determine areas of a catchment

where contaminants are being generated and which subsequently impact adversely on the lake. In this study, CLUES was used to indicate the relative proportion of contaminants generated in various parts of the catchment. CLUES is a national scale model, but may be used to assess contaminant yields and losses at national and reach (REC) scale. Although CLUES is a static budget model (it produces estimates of annual loads or yields), it is under constant development to meet stakeholder needs and and keep pace with advances in software and operating systems. CLUES may be used to assess the likely outcomes of mitigation actions ("what effect would restoring native forest have on catchment and stream contaminant yields?", "in which part of the catchment should we implement mitigation actions first?"), possible policy or regulatory outcomes ("would restricting stock access to all lands in this catchment steeper than 15° have a measurable impact on sediment yields?") etc. One of the significant benefits of CLUES is ease of use, and the rapid delivery of immediately useful information.

If a more sophisticated tool is required to provide the information required, several proprietary and open-source model options are available. SWAT (Arnold *et al.* 2012; Gassman *et al.* 2014) and HYPE (Lindström *et al.* 2010) are some options. These models require more data as input, more parameters may need to be calibrated, and they are relatively expensive to establish and operate, but they are far more sophisticated, and may operate at temporal and spatial scales that are not achievable for simpler models such as CLUES. The more complex models may be coupled tightly or loosely to other models to account for groundwater processes, or may be linked to lake ecosystem models to predict the likely ecological effects from continuing land management practices, or those proposed in order to further improve lake water quality.

Models may be set up and run in-house or developed as turnkey solutions by others. A decision to develop a model may reveal that few key data exist and may give new insights into the factors that are really important when planning to achieve water quality outcomes.

5   Summary

ORC has collected a useful dataset, including high-frequency data, that allows the mass loads of key contaminants generated in the Lake Hayes catchment to be estimated. The use of high frequency data for monitoring to obtain new insights into the source, magnitude and dynamics of contaminants generated in catchments for more effective management purposes is increasing (e.g., Duvert *et al.* 2011; Li *et al.* 2019; Tada and Tanakamaru 2021). The approach followed by ORC is pragmatic: there is a clear strategy to obtain additional data to support and build on the current physico-chemical grab sampling approach. This ensures that historical data remain useful, and the future monitoring will enable the council to improve the amount, quality and timeliness of information derived from monitoring. These data also provide impetus in terms of assessing and extracting additional information from modelling applications.

In this report, we have estimated loads of key contaminants (nitrogen, phosphorus and suspended sediment) entering Lake Hayes for periods of record for different monitoring sites in the lake catchment. The most extensive record is for the Mill Creek at Fish Trap site (continuous discharge, and water quality data derived from flow-related event sampling, as well as routine grab samples).

More recently, water quality data have been collected nearer the inflow to the lake (Mill Creek at Lake Hayes site); data for this site are primarily from routine monthly monitoring and event-related samples. Additional data have been collected using a turbidity sensor, and a nitrate sensor which have provided surrogate measurements of suspended sediment and nitrate-N concentrations at 15 minute frequency.

An additional site was established by ORC at Hunter Road, to better estimate the proportion of contaminant loads entering the upper Mill Creek catchment. A continuous turbidity sensor was established at this site as well.

In addition, ORC collected a set of catchment-wide water quality samples as part of a series of synoptic surveys. Samples were collected at locations previously sampled in 1997, and these data were used to compare water quality over time, and to assess the "typical" water quality at the synoptic surveys under the flow conditions that prevailed at the time of sampling.

We were able to relate the proxy measurement turbidity (a measure of water cloudiness) to total suspended sediment concentrations and TP concentration. These relationships were used to created continuous records of TSS and TP. These were then used together with the continuous flow record to determine TSS and TP loads. The certainty of load estimations derived from the turbidity proxy were strongly dependent on the number of data available to calibrate a statistical relationship between the proxy measurement and measured TSS or TP.

We were also able to relate nitrate concentrations estimated by a TriOS water quality sensor to nitrate-N concentrations measured in grab samples at a laboratory. The load estimates derived from the TriOS sensor data better represented the peaks in contaminant load during rainfall and high-flow events.

Stream contaminant loads were estimated as follows:

- By relating measured concentration samples to discharge estimates, and using calibrated models to predict stream flow concentrations, and contaminant loads at daily, monthly and annual intervals.

- Calibrated statistical models were developed in Microsoft Excel using the "Solver" regression-fitting technique, in Python using an open-source regression modelling library (the Least Squares Optimisation tool).

- Using the LOADEST software modelling tool developed by the USGS. The modelling tool selected the "best" model for the purpose using in-built processes based on several statistical criteria.

5.1   Long term contaminant load estimates

Key results derived from the Mill Creek at Fish Trap site include a 20% reduction in the 1994 TP load since 1996, and annual loads that are less than a third of the 1994 values consistently since 2002. The annual TP load was 2.99 t in 1994, and the annual average load over the three-year period 2018-202 was 0.6 t (a 79% decrease). The decrease in TP load estimated over time is primarily related to rainfall and runoff. The period 1994-2000 was characterised by having five of the seven largest annual discharge estimates measured between 1984 and 2021.

When the estimated TP load data were separated into pre-2003 and post 2003 groups, seasonal patterns in the magnitude of TP load were similar between the two periods, but were considerably lower in all months during the post-2003 period. When estimated over the two periods, the median TP load/month decreased approximately 50%, from approximately 73 kg TP/month in 1984-2002, to approximately 36 kg TP/month in the period 2003-2021. During 2020, the estimated TP load varied from approximately 20 t TP in May to a maximum of 177 t TP in August.

For NNN, annual loads decreased from more than 10 t/year in 1994 to an average of approximately 5 t/year over the period 2018-202 (a decrease of 51%).

The long-term estimated NNN load at the Fish Trap site has a strong seasonal pattern, with a minimum in February and a maximum in spring. For the post-2002 period the maximum monthly load occurred in September. In 2020, the minimum estimated monthly load (280 kg NNN) occurred in June, and the maximum estimated load was observed in September (738 kg NNN).

Predicted TSS loads were more variable in the pre-2002 period that the other contaminants, and the magnitude of the estimated load was sensitive to the estimation technique. Using the LOADEST estimations, pre-2002 annual load estimates ranged from 230 t/y (1990) through to 2,100 t/y (1994 and 1995). Post 2002, seasonal loads have been generally lower and more consistent, ranging from 932 t in 2002 to a low of 120 t/y in 2017. A strong seasonal pattern was evident in both periods, but with considerably fewer very high estimates of TSS load in the latter period.

It should be noted that relatively few event-related samples exist for the Fish Trap site, and these results are concentrated in the early period of record (particularly 1983 and 1984). A substantial set of flow-related grab sample-based data exist for the Mill Creek at Lake Hayes site, which provide a good foundation for development of regression relationships and load estimation.

Using grab sample data for the Mill Creek site to calibrate the LOADEST model suite, annual contaminant loads were estimated as listed in Table 5-1.

Table 5-1: Annual contaminant loads for the Mill Creek at Lake Hayes site.

Year	Load/year (kg)				Load/year (t)
	DRP	NNN	TN	TP	TSS
2018	29.88	5458.9	6126.5	642.1	396.8
2019	89.69	5207.7	8909.7	743.7	409.7
2020	146.01	5683.9	10171.4	1371.3	850.1
2021	62.64	5900.2	4128.0	913.4	480.0

5.2 Use of surrogate measurements to estimate contaminant loads.

Nitrate-N estimates were obtained for the Mill Creek at Lake Hayes site as the product of concentration derived from the TriOS sensor and discharge; annual loads derived from these estimates are compared with those derived from LOADEST modelling in Table 5-2. Within the limitations imposed on the LOADEST method by available calibration data, there is some concordance between these estimates and those obtained at monthly timestep (Figure 3-16).

Table 5-2: Comparison of annual load estimates derived from two approaches. , TriOS-nitrate = 15 minute frequency measurement, LOADEST – hourly estimates derived from grab samples.

Year	Annual load per estimation method (kg)	
	TriOS-nitrate	LOADEST NNN
2019	6951	5126
2020	8023	5841

Several approaches were explored to estimate TSS and TP loads at the Millcreek at Hunter Road and Mill Creek at Lake Hayes sites using turbidity as a surrogate metric. Regression equations were derived, and model fit was evaluated using several performance metrics. Monthly and annual loads were derived for both water quality variables at both sites. The reliability of these estimates was influenced by several factors, including:

- The completeness of the surrogate measurement record (proportion of theoretical total amount of data),

- The amount of extraneous record (turbidity values that were possibly spurious, influenced by interference with the optical method of measurement)

- The number of grab sample data currently available for calibration of regression models developed for the Hunter Road site

- The nature of grab sample data available for the Hunter Road site – these data are all collected at monthly frequency, rather than in flow-proportional manner.

Recognising these factors, the techniques indicate that usable contaminant loads may be estimated using surrogate measurements. The accuracy of measurement could be improved by modifying

calibration sample collection procedures, and ensuring that a greater proportion of sensor data are of known quality.

5.3   Synoptic survey results

We were able to compare the DRP and TP concentrations and fluxes measured at seven sites in the Lake Hayes catchment at two time periods: 1997 and the three-year period 2018-2020. Concentrations of TP increased at three sites since 1997 McMullan Ck at Malaghan Road, Mill Creek at Hunter Road, and at the inflow to Lake Hayes. Median DRP concentrations increased at the latter two sites and at the "Dan O'Connell Ck 300 m u/s" site over this period.

The synoptic survey data collected from 2018-2020 surveys represent both base and event sized flows, and they indicate some consistent spatial variation in the magnitude of instantaneous load for several water quality variables:

- Relatively small contaminant loads were evident at all sites upstream of the Mill Creek at Hunter Road site.

- Of the tributary sites TSS and TP loads were largest for the Dan O'Connell Ck at Coronet Station site, indicating that the phosphorus load from this catchment was probably particulate bound.

- A step-change in both concentration and flux on TN and NNN was evident at the Hunter Road site, suggesting that nitrogen was entering Mill Creek in runoff or groundwater from adjacent land, or from unmonitored tributaries.

- A similar step change was evident for TP and DRP, which was accompanied by a significant step change in median TSS flux. These results indicate that the TSS entering Mill Creek upstream of Hunter Road are likely to contribute the bulk of the TP load as well.

- The DRP and TP flux increases slightly downstream of Hunter Road, suggesting that the bulk of phosphorus load enters Mill Creek upstream of Hunter Road.

Most nitrogen enters Mill Creek in the reach downstream of Hunter Road (as indicated by flux estimates). Although it is not clear from these data whether the NNN load is groundwater dominated or not. The NNN flux from Lake Hayes Spring is the considerably smaller than that at the sampling sites downstream of the Hunter Road site. This suggests that the bulk of the nitrogen load is derived from surface runoff or shallow groundwater that discharges to Mill Creek, and not to the deeper groundwater system that discharges to the lake from the spring.

5.4   Seasonal variation in contaminant loads

The load estimation process has demonstrated consistent seasonal patterns, with smaller loads in late summer/autumn, and the bulk of the load transported in late winter/spring period. The bulk of the contaminant load is therefore transported during high-flow conditions (either during rain events or during snowmelt). From the data available, it is not possible to differentiate between rainfall or snowmelt events.

5.5   Land use and catchment modelling

Land use in the Lake Hayes catchment has remained relatively constant since 1996. The dominant land cover classes may be considered pasture (ca. 55%), tussock (ca. 18%) and native and exotic forest (ca. 23%). Collectively, these cover classes currently comprise ca. 95% of the catchment, with urban land cover comprising 5% of the Lake Hayes catchment (an increase from 66 to 242 hectares, 1996-2018).

The spatial variation in N and P loads predicted by CLUES were consistent with the spatial variation indicated by the synoptic survey results. The bulk of the TP load that eventually reaches Lake Hayes enters Mill Creek upstream of the Hunter Road site (56%), an additional 25% in the reach between Hunter Road and Waterfall Park, and the remaining 19% in the reach between Waterfall Park and the lake.

CLUES results indicated that a smaller proportion of the TN load enters Mill Creek upstream of the Hunter Road site (39%), with the balance entering upstream of Waterfall Park (40%) and the lake inflow (31%).

5.6   Mitigation actions

The assessment of land cover, catchment modelling and load estimation indicates that the bulk of N, P and sediment load enters Mill Creek in the reach downstream of Hunter Road. The bulk of the contaminant loads enter the stream under elevated flow conditions. Land cover types contributing both N and P are dominated by pasture, and soil P comprises approximately one third of the total P load at each of the Hunter Road, Waterfall Park and lake inflow reaches.

Mitigation of what are almost exclusively diffuse source loads of N, P and sediment will require careful assessment, including identification of contaminant source areas, identification of routes whereby these contaminants are delivered to Mill Creek, and then, selection of the mitigation tools most likely to deliver the water quality improvements in a cost-effective manner. Conventional mitigation tools include riparian buffers[11], restored (Rutherford and Nguyen 2001; Matheson *et al.* 2002; Rutherford and Nguyen 2004) and constructed wetlands (Tanner and Sukias 2011; Bunce *et al.* 2018)[12], woodchip denitrification filters (Goeller *et al.* 2016; Pluer *et al.* 2016; Christianson *et al.* 2017; Hudson *et al.* 2019a; Hudson *et al.* 2019c), phosphorus sorbing/binding and chelating materials, and flocculating agents. The lake is sensitive to P loading, but reducing other contaminants is likely to deliver broader water quality benefits. With the exception of denitrification filters and P sorbing materials, other mitigation actions are all likely to reduce the input of the three broad categories of contaminant (N, P and sediment) to some extent.

Goeller *et al.* (2020) recently reviewed mitigation options for the Lake Hayes catchment. These included maintaining and restoring existing wetlands and riparian buffers, constructing sediment traps along the main stem of Mill Creek to capture total suspended solids and total phosphorus, and which may also buffer storm- and snowmelt flows. A constructed wetland was identified as desirable, but limited space near to the lake inflow may be an impediment. More widespread actions included livestock exclusion (particularly in the upper catchment), and channel restoration in the lower catchment to slow movement of water and reduce bank erosion. Riparian conditions could be improved by re-establishing riparian vegetation and making use of riparian buffer elements such as grass filter strips, mixed vegetation buffers and shrubs and trees. These plantings would

---

[11] https://niwa.co.nz/freshwater/management-tools/riparian-buffer-design-guide
[12] https://niwa.co.nz/freshwater/management-tools/restoration-tools/constructed-wetland-guidelines

generally intercept sediment and particulate-bound nutrients, as well as soluble nutrients transported in shallow groundwater.

Achieving a cost-effective water quality outcome will likely require a mix of mitigation actions. We recommend reviewing the actions proposed by Goeller *et al.* (2020). The nutrient load estimates derived from this report should be considered together with the outcomes from work that has focussed on the lake and lake processes (Schallenberg and Schallenberg 2017; Gibbs 2018) to identify contaminant removal targets, mitigation actions and to prioritise these activities.

References

Aqualinc (2014) Contaminant Load Calculator. Prepared for Environment Southland, Envirolink Project 1476- ESRC266: 21.

Arnold, J.G., Kiniry, J.R., Srinivansan, R., Williams, J.R., Haney, E.B., Neitsch, S.L. (2012) Soil and Water Assessment Tool: Input/Output Documentation, Version 2012, Texas Water Resources Institute, TR-439. https://swat.tamu.edu/docs/

Aulenbach, B.T., Burns, D.A., Shanley, J.B., Yanai, R.D., Bae, K., Wild, A.D., Yang, Y., Yi, D. (2016) Approaches to stream solute load estimation for solutes with varying dynamics from five diverse small watersheds. *Ecosphere*, 7(6): e01298. 10.1002/ecs2.1298

Bunce, J.T., Ndam, E., Ofiteru, I.D., Moore, A., Graham, D.W. (2018) A Review of Phosphorus Removal Technologies and Their Applicability to Small-Scale Domestic Wastewater Treatment Systems. *Frontiers in Environmental Science*, 6(8). 10.3389/fenvs.2018.00008

Burkitt, L.L., Jordan, P., Singh, R., Elwan, A. (2017) High resolution monitoring of nitrate in agricultural catchments - a case study on the Manawatu River, New Zealand. Envirolink report prepared for Horizons Regional Council.

Caruso, B.S. (2000) Spatial and temporal variability of stream phosphorus in a New Zealand high-country agricultural catchment. *New Zealand Journal of Agricultural Research*, 43(2): 235-249. 10.1080/00288233.2000.9513424

Caruso, B.S. (2001) Risk-based targeting of diffuse contaminant sources at variable spatial scales in a New Zealand high country catchment. *Journal of Environmental Management*, 63(3): 249-268. https://doi.org/10.1006/jema.2001.0476

Christianson, L.E., Lepine, C., Sibrell, P.L., Penn, C., Summerfelt, S.T. (2017) Denitrifying woodchip bioreactor and phosphorus filter pairing to minimize pollution swapping. *Water Research*, 121: 129-139. https://doi.org/10.1016/j.watres.2017.05.026

Duvert, C., Gratiot, N., Némery, J., Burgos, A., Navratil, O. (2011) Sub-daily variability of suspended sediment fluxes in small mountainous catchments &ndash implications for community-based river monitoring. *Hydrol. Earth Syst. Sci.*, 15(3): 703-713. 10.5194/hess-15-703-2011

Elliot, A.H., Alexander, R.B., Schwarz, G.E., Shankar, U., Sukias, J.P.S., McBride, G.B. (2005) Estimation of nutrient sources and transport for New Zealand using the hybrid mechanistic-statistical model SPARROW. http://pubs.er.usgs.gov/thumbnails/outside_thumb.jpg

Elliott, A.H., Alexander, R.B., Schwartz, G.E., Shankar, U., Sukias, J.P.S., McBride, G.B. (2005) Estimation of nutrient sources and transport for New Zealand using the hybrid mechanistic-statistical model SPARROW. *Journal of Hydrology (NZ)*, 44(1): 1-27.

Elliott, A.H., Semadeni-Davies, A.F., Shankar, U., Zeldis, J.R., Wheeler, D.M., Plew, D.R., Rys, G.J., Harris, S.R. (2016) A national-scale GIS-based system for modelling impacts of land use on water quality. *Environmental Modelling & Software*, 86: 131-144. http://dx.doi.org/10.1016/j.envsoft.2016.09.011

Gao, J., White, M.J., Bieger, K., Arnold, J.G. (2021) Design and development of a Python-based interface for processing massive data with the LOAD ESTimator (LOADEST). *Environmental Modelling & Software*, 135: 104897. https://doi.org/10.1016/j.envsoft.2020.104897

Gassman, P.W., Sadeghi, A.M., Srinivasan, R. (2014) Applications of the SWAT Model Special Section: Overview and Insights. *Journal of Environmental Quality*, 43(1): 1-8. https://doi.org/10.2134/jeq2013.11.0466

Gibbs, M. (2018) Lake Hayes Water Quality Remediation Options. NIWA client report prepared for Otago Regional Council, 2018042HN2: 62.

Gibbs, M.M., Hickey, C.W. (2018) Flocculent and sediment capping for phosphorus management. In: D.P. Hamilton, K. Collier, C. Howard-Williams & J. Quinn (Eds). *Lake Restoration Handbook: A New Zealand Perspective.* . Springer.

Goeller, B.C., Febria, C.M.,Harding, J.S., McIntosh, A.R. (2016) Thinking beyond the Bioreactor Box: Incorporating Stream Ecology into Edge-of-Field Nitrate Management. *Journal of Environmental Quality*, 45(3): 866-872. 10.2134/jeq2015.06.0325

Goeller, B.C., Sukias, J., Hughes, A. (2020) Scoping of diffuse pollution mitigation options for Mill Creek. NIWA client report prepared for Friends of Lake Hayes Society, Inc., Otago Regional Council, Queenstown Lakes District Council, Department of Conservation, 2020009HN: 71.

Goldsmith, M., Hanan, D. (2019) Lake Hayes Remediation, Options Overview Report. GHC Consulting Limited Consultancy Report, 2019/1: 55.

Hicks, M., Semadeni-Davies, A., Haddadchi, A., Shankar, U., Plew, D. (2018) Updated sediment load estimator for New Zealand, NIWA client report prepared for Ministry for the Environment, report: 2018341CH.

Hirsch, R.M., Moyer, D.L., Archfield, S.A. (2010) Weighted Regressions on Time, Discharge, and Season (WRTDS), with an Application to Chesapeake Bay River Inputs. *J Am Water Resour Assoc*, 46(5): 857-880. 10.1111/j.1752-1688.2010.00482.x

Hudson, N., Baddock, E. (2019) Review of high frequency water quality data. Advice regarding collection, management and use of nitrate-nitrogen data. NIWA client report prepared for Environment Southland, Otago Regional Council and Environment Canterbury as deliverable for MBIE-funded projects ELF18203 and FWWQ1909., 2019135HN: 184.

Hudson, N., Baddock, E., McKergow, L., Heubeck, S., Tanner, C., Scandrett, J., Burger, D., Wright-Stow, A., Depree, C. (2019a) Efficacy of a nitrate-N woodchip filter: three years of field trials. 32nd Annual FLRC Workshop. *Nutrient Loss Mitigations for Compliance in Agriculture*, Palmerston North, 12th, 13th and 14th February 2019.

Hudson, N., Baddock, E., McKergow, L., Sukias, J., Heubeck, S., Montemezzani, V., Olsen, G. (2019b) Applications of continuous nitrate-N analysers in New Zealand for improved nutrient estimation. *Hydrology Society Workshop*, Blenheim, April 2019.

Hudson, N., Heubeck, S., Baddock, E. (2019c) Woodchip denitrification filter- performance evaluation: Third year of operation. NIWA client report 2019086HN prepared for DairyNZ., 2019086HN: 151.

Larned, S., Booker, D., Dudley, B., Moores, J., Monaghan, R.; Baillie, B.; Schallenberg, M., Moriarty, E., Zeldis, J., Short, K. (2018) Land-use impacts on freshwater and marine environments in New Zealand. *NIWA Client Report*, 2018127CH: 291.

Li, Y., Yen, H., Daren Harmel, R., Lei, Q., Zhou, J., Hu, W., Li, W., Lian, H., Zhu, A.X., Zhai, L., Wang, H., Qiu, W., Luo, J., Wu, S., Liu, H., Li, X. (2019) Effects of sampling strategies and estimation algorithms on total nitrogen load determination in a small agricultural headwater watershed. *Journal of Hydrology*, 579: 124114. https://doi.org/10.1016/j.jhydrol.2019.124114

Lindström, G., Pers, C., Rosberg, J., Strömqvist, J., Arheimer, B. (2010) Development and testing of the HYPE (Hydrological Predictions for the Environment) water quality model for different spatial scales. *Hydrology Research*, 41(3-4): 295-319. 10.2166/nh.2010.007

Littlewood, I.G. (1997) Estimating contaminant loads in rivers: a review, Report No. 117: 87.

Lloyd, C.E.M., Freer, J.E., Johnes, P.J., Collins, A.L. (2016) Using hysteresis analysis of high-resolution water quality monitoring data, including uncertainty, to infer controls on nutrient and sediment transfer in catchments. *Science of The Total Environment*, 543(Part A): 388-404. https://doi.org/10.1016/j.scitotenv.2015.11.028

Marttila, H., Kløve, B. (2012) Use of Turbidity Measurements to Estimate Suspended Solids and Nutrient Loads from Peatland Forestry Drainage. *Journal of Irrigation and Drainage Engineering*, 138(12): 1088-1096. doi:10.1061/(ASCE)IR.1943-4774.0000509

Matheson, F.E., Nguyen, M.L., Cooper, A.B., Burt, T.P., Bull, D.C. (2002) Fate of N-15-nitrate in unplanted, planted and harvested riparian wetland soil microcosms. *Ecological Engineering*, 19(4): 249-264. 10.1016/s0925-8574(02)00093-9

McBride, C., Muraoka, K., Allan, M. (2019) Lake water quality modelling to assess management options for Lake Hayes. Client report prepared for Otago Regional Council by Environmental Research Institute , The University of Waikato, ERI Report No. 124: 72.

Meals, D.W., Richards, R.P., Dressing, S.A. (2013) Pollutant load estimation for water quality monitoring projects. Tech Notes 8, Developed for U.S. Environmental Protection Agency by

Tetra Tech, Inc., Fairfax, VA: 21. https://www.epa.gov/polluted-runoff-nonpoint-source-pollution/nonpoint-source-monitoringtechnical-notes.

Nash, J.E., Sutcliffe, J.V. (1970) River flow forecasting through conceptual models part I — A discussion of principles. *Journal of Hydrology*, 10(3): 282–290.

New Zealand Government (2020a) National Policy Statement for Freshwater Management: 70.

New Zealand Government (2020b) Resource Management (National Environmental Standards for Freshwater) Regulations: 62.

New Zealand Government (2023) National Policy Statement for Freshwater Management 2020, as amended February 2023. https://environment.govt.nz/acts-and-regulations/national-policy-statements/national-policy-statement-freshwater-management/

ORC and QLDC (1995) Lake Hayes management strategy, un-numbered: 60.

Pluer, W.T., Geohring, L.D., Steenhuis, T.S., Walter, M.T. (2016) Controls Influencing the Treatment of Excess Agricultural Nitrate with Denitrifying Bioreactors. *Journal of Environmental Quality*, 45(3): 772-778. 10.2134/jeq2015.06.0271

Quilbé, R., Rousseau, A.N., Duchemin, M., Poulin, A., Gangbazo, G., Villeneuve, J.-P. (2006) Selecting a calculation method to estimate sediment and nutrient loads in streams: Application to the Beaurivage River (Québec, Canada). *Journal of Hydrology*, 326(1): 295-310. https://doi.org/10.1016/j.jhydrol.2005.11.008

Rosen, M.R., Reeves, R.R., Green, S., Clothier, B., Ironside, N. (2004) Prediction of groundwater nitrate contamination after closure of an unlined sheep feedlot. *Vadose Zone Journal*, 3(3): 990-1006.

Runkel, R.L., Crawford, C.G., Cohn, T.A. (2004) Load Estimator (LOADEST): A FORTRAN Program for Estimating Constituent Loads in Streams and Rivers (updated 2013): 69. https://water.usgs.gov/software/loadest/doc/

Rutherford, J.C., Nguyen, M.L. (2001) *Flow paths and denitrification in riparian wetlands*.

Rutherford, J.C., Nguyen, M.L. (2004) Nitrate removal in riparian wetlands: Interactions between surface flow and soils. *Journal of Environmental Quality*, 33(3): 1133-1143. <Go to ISI>://WOS:000221509200041

Schallenberg, M., Schallenberg, L. (2017) Lake Hayes Restoration and Monitoring Plan. , Un-numbered: 55.

Schwarz, G.E., Hoos, A.B., Alexander, R.B., Smith, R.A. (2006) *The SPARROW Surface Water-Quality Model – Theory, Application, and User Documentation. *. USGS, Reston, Virginia.

Semadeni-Davies, A., Jones-Todd, C., Srinivasan, M.S., Muirhead, R., Elliott, A., Shankar, U., Tanner, C. (2020) CLUES model calibration and its implications for estimating contaminant attenuation. *Agricultural Water Management*: 105853. https://doi.org/10.1016/j.agwat.2019.105853

Semadeni-Davies, A.F., Jones-Todd, C.M., Srinivasan, M.S., Muirhead, R.W., Elliott, A.H., Shankar, U., Tanner, C.C. (2019) CLUES model calibration: residual analysis to investigate potential sources of model error. *New Zealand Journal of Agricultural Research*: 1-24. 10.1080/00288233.2019.1697708

Skarbøvik, E., Gyritia Madsen van't Veen, S., Lannergård, E.E., Wenng, H., Stutter, M., Bieroza, M., Atcheson, K., Jordan, P., Fölster, J., Mellander, P.-E., Kronvang, B., Marttila, H., Kaste, Ø., Lepistö, A., Kämäri, M. (2023) Comparing in situ turbidity sensor measurements as a proxy for suspended sediments in North-Western European streams. *CATENA*, 225: 107006. https://doi.org/10.1016/j.catena.2023.107006

Snelder, T., Biggs, B. (2002) Multiscale river environment classification for water resources management. *Journal of the American Water Resources Association*, 38(5): 1225 - 1239.

Snelder, T., Biggs, B., Weatherhead, M. (2010) New Zealand River Environment Classification User Guide. March 2004 (Updated June 2010), ME Number 499.

Snelder, T.H., McDowell, R.W., Fraser, C.E. (2016) Estimation of Catchment Nutrient Loads in New Zealand Using Monthly Water Quality Monitoring Data. *JAWRA Journal of the American Water Resources Association*, 53(1): 158-178. 10.1111/1752-1688.12492

Stutter, M., Dawson, J.J.C., Glendell, M., Napier, F., Potts, J.M., Sample, J., Vinten, A., Watson, H. (2017) Evaluating the use of in-situ turbidity measurements to quantify fluvial sediment and phosphorus concentrations and fluxes in agricultural streams. *Science of the Total Environment*, 607-608: 391-402. https://doi.org/10.1016/j.scitotenv.2017.07.013

Tada, A., Tanakamaru, H. (2021) Unbiased Estimates and Confidence Intervals for Riverine Loads. *Water Resources Research*, 57(3): e2020WR028170. https://doi.org/10.1029/2020WR028170

Tanner, C.C., Sukias, J.P.S. (2011) Multiyear Nutrient Removal Performance of Three Constructed Wetlands Intercepting Tile Drain Flows from Grazed Pastures. *Journal of Environmental Quality*, 40(2): 620-633. 10.2134/jeq2009.0470

Wenng, H., Barneveld, R., Bechmann, M., Marttila, H., Krogstad, T., Skarbøvik, E. (2021) Sediment transport dynamics in small agricultural catchments in a cold climate: A case study from Norway. *Agriculture, Ecosystems & Environment*, 317: 107484. https://doi.org/10.1016/j.agee.2021.107484

Wheeler, D., Shepherd, M., Freeman, M., Selbie, D. (2014) OVERSEER® nutrient budgets: selecting appropriate timescales for inputting farm management and climate information. In: L.D. Currie & C.L. Christensen (Eds). *Nutrient Management for the Farm, Catchment and Community, Occasional Report No. 27*. Fertilizer and Lime Research Centre, Massey University, Palmerston North, New Zealand. http://flrc.massey.ac.nz/publications.html

Appendix A   Overview of load calculation methods

Many methods exist for estimating stream contaminant loads (e.g., for a review of methods, limitations and recommendations undertaken for regional councils, see Aqualinc 2014). A widely used technique is the rating curve method, which is based on extrapolating contaminant concentration measurements over the entire period of interest by developing a relationship between contaminant concentration and stream discharge at the time of sampling. The relationship between contaminant concentration and discharge is typically log-log in nature, i.e., a linear relationship exists between the log of the contaminant concentration and the log of discharge is linear, giving rise to relationships of the form:

$$c = aQ^b$$

Where a and b are regression coefficients estimated for the specific site, and which c and Q are concentration and discharge respectively.

If both flow and concentration data are available at a sufficiently high frequency (relative to the variation in flow and concentration during the period of estimation), then good load estimates can be calculated. When such data are spaced regularly in time, the load may be calculated with little error as the sum of the products of flow and concentration, multiplied by the data time interval and a constant to account for the units used:

$$Load = \text{K}\Delta\text{t} \sum(c_i \times Q_i)$$

where K is a constant

Δt is the data time interval

c_i is the sample contaminant concentration

Q_i is discharge at the time of sample collection

If the high-frequency data are spaced irregularly in time (improving definition of flow and concentration during periods of high flows when variability may be greatest), load may be calculated with less error as the sum of the products of individual time intervals, concentration and flow:

$$Load = \text{K} \sum(\Delta\text{t}_i \; c_i \times Q_i)$$

where Δt_i is a short time interval over which c_i and Q_i apply.

Many mass load calculation techniques have been developed to estimate stream loads (e.g., Littlewood 1997; Runkel *et al.* 2004; Quilbé *et al.* 2006; Hirsch *et al.* 2010; Meals *et al.* 2013; Aulenbach *et al.* 2016; Snelder *et al.* 2016; Li *et al.* 2019). Snelder et al., (2016) reviewed multiple methods for calculation of stream loads, including three commonly used and recommended methods:

i.   The Beale ratio method, which adjusts for bias arising from covariance between unit loads and discharge.

ii.   The "L7" and "L5" models, which are based on a rating-table approach, which relate the log of concentration to three explanatory variables – discharge, time and season, using seven fitted parameters (the models are described in Table A-1).

The L5 and L7 models are implemented in the LOAD ESTimator (LOADEST) tool (Runkel *et al.* 2004; Gao *et al.* 2021)[13], [14] together with other models of varying complexity.

Table A-1:   Standard models provided in the LOADEST model suite. From Table 7 of Runkel et al (2004). lnQ = ln(streamflow) - centre of ln(streamflow); dtime = decimal time - centre of decimal time; per = user-defined period etc. For full details refer to Runkel et al. (2004)..

Specified value	Regression model
0	automatically select best model from models 1-9.
1	$a_0 + a_1 \ln Q$
2	$a_0 + a_1 \ln Q + a_2 \ln Q^2$
3	$a_0 + a_1 \ln Q + a_2 dtime$
4	$a_0 + a_1 \ln Q + a_2 \sin(2\pi dtime) + a_3 \cos(2\pi dtime)$
5	$a_0 + a_1 \ln Q + a_2 \ln Q^2 + a_3 dtime$
6	$a_0 + a_1 \ln Q + a_2 \ln Q^2 + a_3 \sin(2\pi dtime) + a_4 \cos(2\pi dtime)$
7	$a_0 + a_1 \ln Q + a_2 \sin(2\pi dtime) + a_3 \cos(2\pi dtime) + a_4 dtime$
8	$a_0 + a_1 \ln Q + a_2 \ln Q^2 + a_3 \sin(2\pi dtime) + a_4 \cos(2\pi dtime) + a_5 dtime$
9	$a_0 + a_1 \ln Q + a_2 \ln Q^2 + a_3 \sin(2\pi dtime) + a_4 \cos(2\pi dtime) + a_5 dtime + a_6 dtime^2$
10	$a_0 + a_1 per + a_2 \ln Q + a_3 \ln Q\ per$
11	$a_0 + a_1 per + a_2 \ln Q + a_3 \ln Q\ per + a_4 \ln Q^2 + a_5 \ln Q^2\ per$
99	user defined

---

[13] https://github.com/USGS-R/rloadest - LOADEST implemented in the R modelling framework.
[14] In the Aqualinc (2014) report, NZ researchers mentioned use of LOADEST, which was incorrectly named "LowDesk".

Appendix B   Symbology used in Systat box and whisker plots
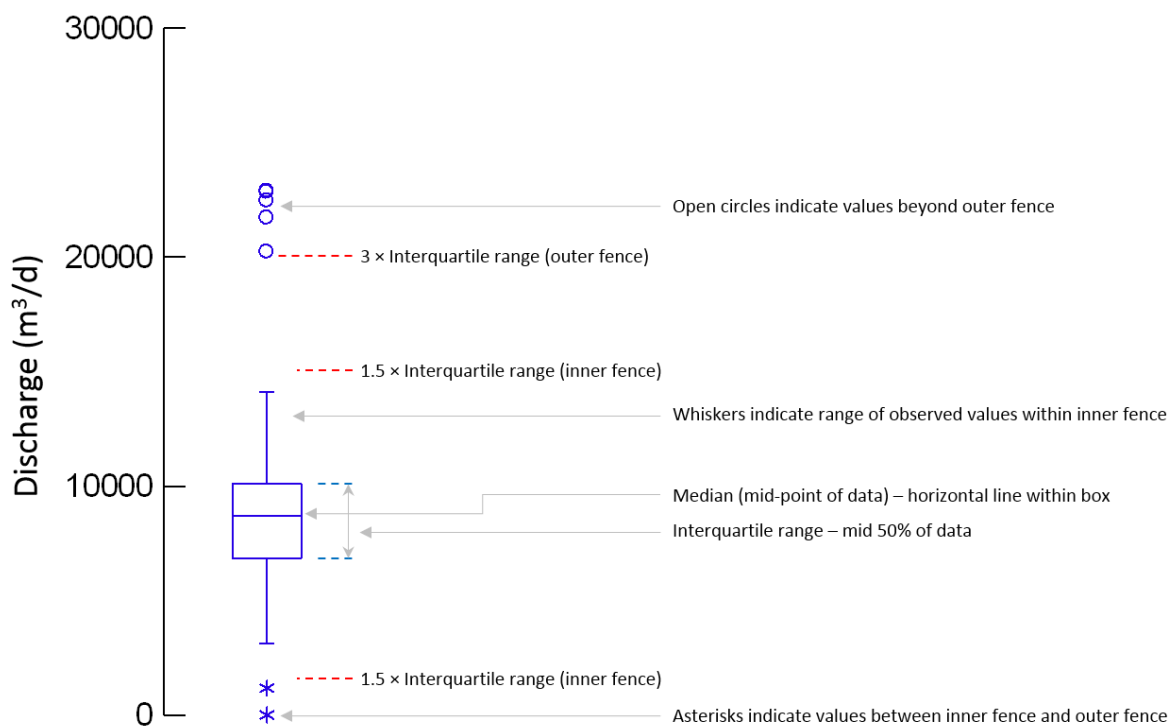
Appendix C   Summary statistics - discharge
Discharge - Mill Creek at Fish Trap,

Full period	Daily mean flow (L/s)
N of Cases	341640
Minimum	124.6
Maximum	5964.9
Arithmetic Mean	432.0
Standard Deviation	231.0
CLEVELAND percentiles	
1.000%	200.8
5.000%	228.7
10.000%	252.8
20.000%	285.6
25.000%	298.0
30.000%	311.6
40.000%	340.6
50.000%	376.5
60.000%	418.4
70.000%	468.6
75.000%	501.4
80.000%	538.5
90.000%	659.4
95.000%	796.5
99.000%	1197.3
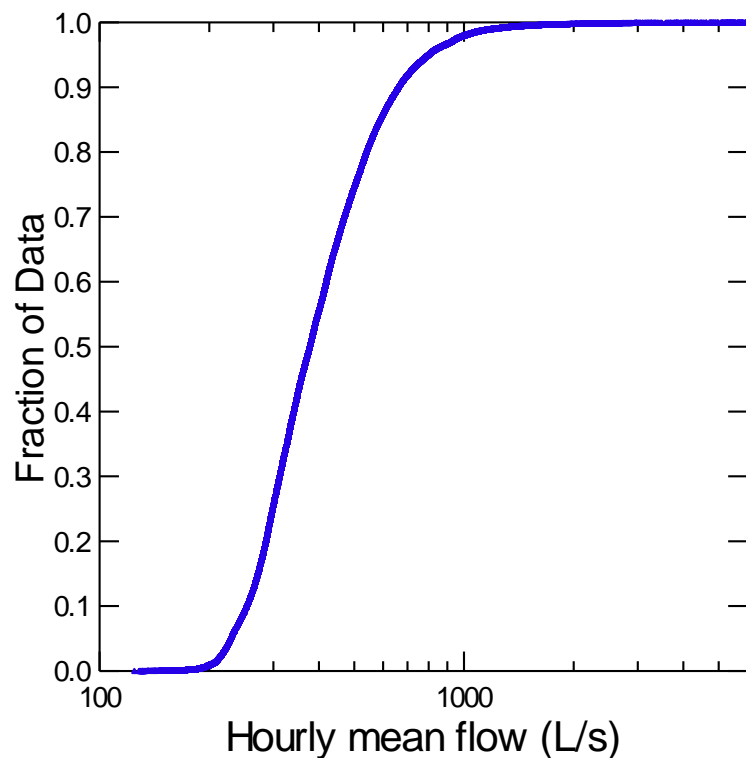
Data for the following results were selected according to
SELECT YYYY =1994

	Hourly mean flow (L/s)
N of Cases	8760
Minimum	342.3
Maximum	5419.5
Arithmetic Mean	705.1
Standard Deviation	249.2
Method = CLEVELAND	
1.000%	400.0
5.000%	503.3
10.000%	521.6
20.000%	556.3
25.000%	574.6

	Hourly mean flow (L/s)
30.000%	598.0
40.000%	631.5
50.000%	663.2
60.000%	690.8
70.000%	742.5
75.000%	773.0
80.000%	803.2
90.000%	895.5
95.000%	1008.2
99.000%	1583.6

▼ Descriptive Statistics

Data for the following results were selected according to
SELECT YYYY=1990 OR YYYY= 1991 OR YYYY=1992 OR YYYY=1993

	Hourly mean flow (L/s)
N of Cases	35064
Minimum	163.0
Maximum	5803.3
Arithmetic Mean	380.3
Standard Deviation	216.8
Method = CLEVELAND	
1.000%	209.0
5.000%	227.1
10.000%	239.7
20.000%	265.7
25.000%	277.7
30.000%	288.0
40.000%	309.1
50.000%	331.2
60.000%	365.1
70.000%	423.8
75.000%	448.3
80.000%	469.2
90.000%	537.2
95.000%	599.3
99.000%	988.0

Data for the following results were selected according to
SELECT PERIOD$ <>""

Mann-Whitney U Test for 52608 Cases

The categorical values encountered during processing are

Variables	Levels				
Year (6 levels)	1996.0	1997.0	1998.0	2018.0	2019.0
	2020.0				
Month (12 levels)	1.0	2.0	3.0	4.0	5.0
	6.0	7.0	8.0	9.0	10.0
	11.0	12.0			
PERIOD$ (2 levels)	One	Two			

Dependent Variable	Hourly mean flow (L/s)
Grouping Variable	PERIOD$

Group	Count	Rank Sum
One	26304	729033038.0
Two	26304	654794098.0

```
Mann-Whitney U Test Statistic :  383069678.0
p-Value                       :  0.0
Chi-Square Approximation      :  454.2
df                            :  1
```

Kruskal-Wallis Test Statistic: 454.2
The p-value is 0.0 assuming chi-square distribution with 1 df.

Dwass-Steel-Chritchlow-Fligner Test for All Pairwise Comparisons

Group(i)	Group(j)	Statistic	p-Value
One	Two	-30.1	0.0

Results for PERIOD$ = One

Data for the following results were selected according to
SELECT PERIOD$ <>""

Statistic	Hourly mean flow (L/s)	
	Period One	Period Two
N of Cases	26304	263024
Minimum	175.4	146.6
Maximum	5621.8	5932.5
Arithmetic Mean	491.8	461.2
Standard Deviation	215.2	233.6
CLEVELAND percentiles		
1.000%	252.6	192.7
5.000%	288.9	255.8
10.000%	299.3	288.8
20.000%	322.1	323.6

Statistic	Hourly mean flow (L/s)	
	Period One	Period Two
25.000%	343.6	338.2
30.000%	365.2	351.4
40.000%	412.3	382.4
50.000%	454.8	414.72
60.000%	493.6	453.5
70.000%	539.1	503.2
75.000%	569.8	535.9
80.000%	614.6	564.4
90.000%	725.6	646.5
95.000%	845.6	762.2
99.000%	1121.4	1265.5
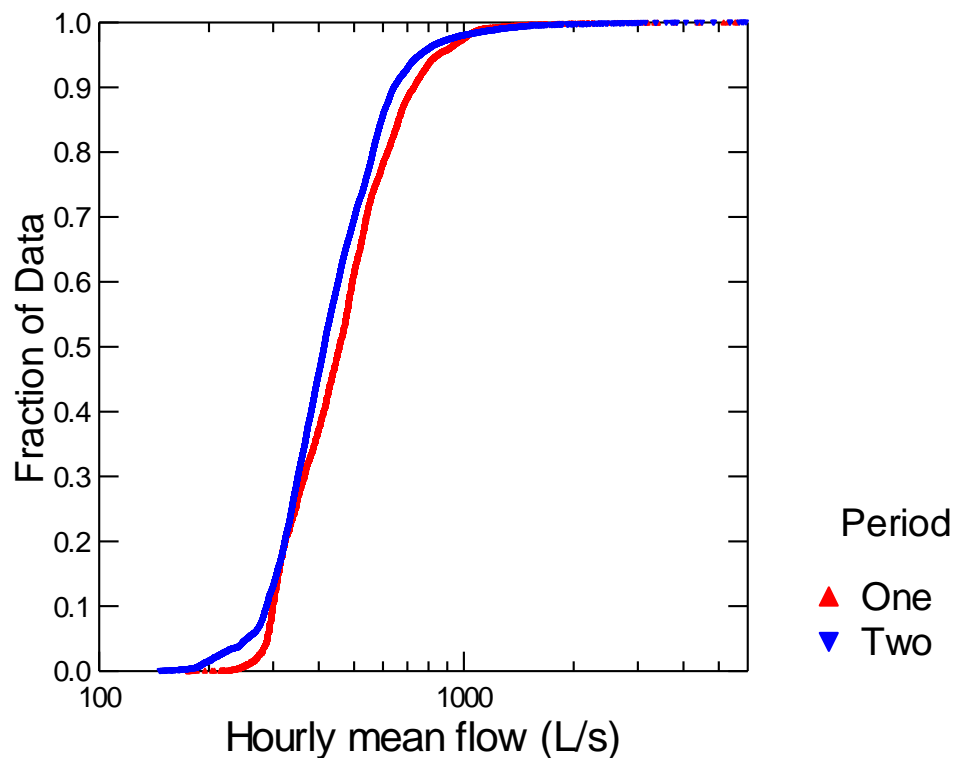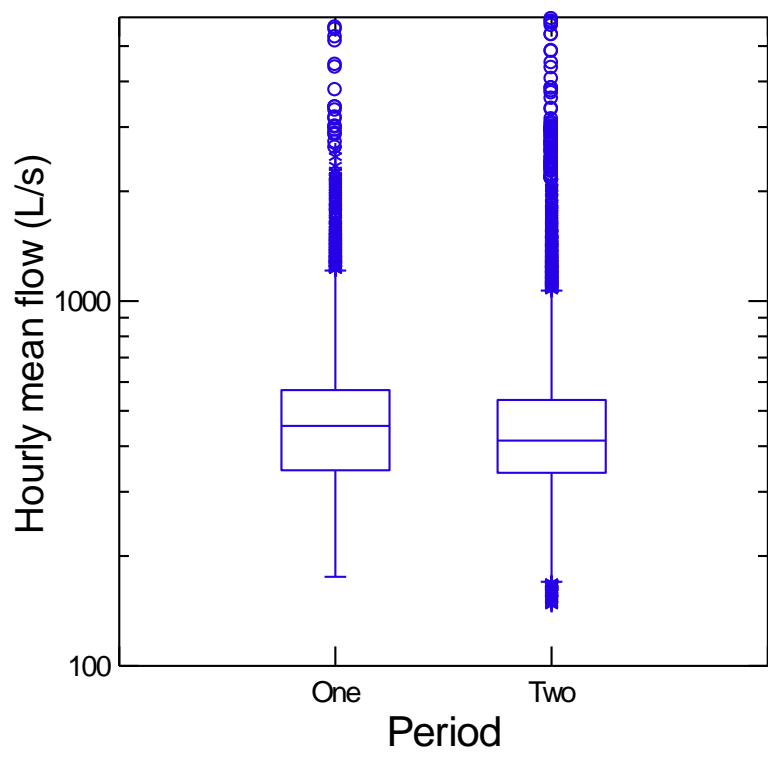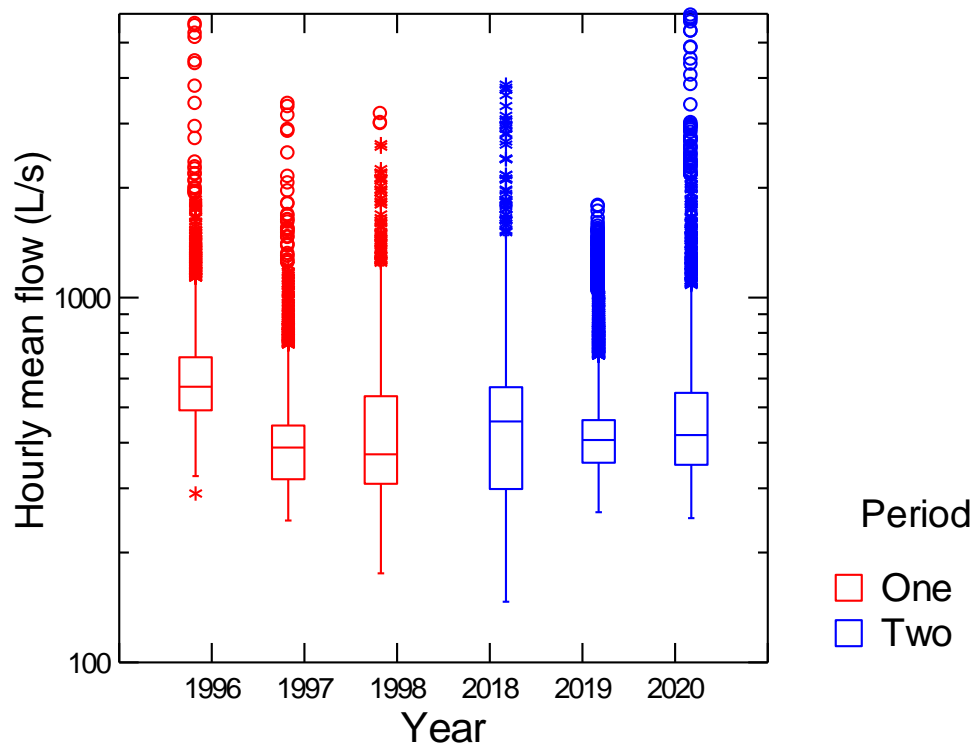
Appendix D   Information relevant to synoptic surveys

Number of sample results for synoptic surveys per year

Site name	Number of sample results per assessment period - DRP			
	1997	2018	2019	2020
Dan OC Ck 300 m u/s	7	4	12	5
Dan OC Ck at C. Station	6	4	12	5
Hayes Ck at L. Hayes	6	4	12	5
McMullan Ck at Malagh	7	4	12	5
Mill Ck at Fish Trap	14	12	16	16
Mill Ck at Hunter Rd	14	4	12	5
Station Ck at Coronet	6	4	12	5

Site name	Number of sample results per assessment period -TP			
	1997	2018	2019	2020
Dan OC Ck 300 m u/s	7	4	12	5
Dan OC Ck at C. Station	6	4	12	5
Hayes Ck at L. Hayes	6	4	12	5
McMullan Ck at Malagh	7	4	12	5
Mill Ck at Fish Trap	15	12	16	16
Mill Ck at Hunter Rd	14	4	12	5
Station Ck at Coronet	6	4	12	5
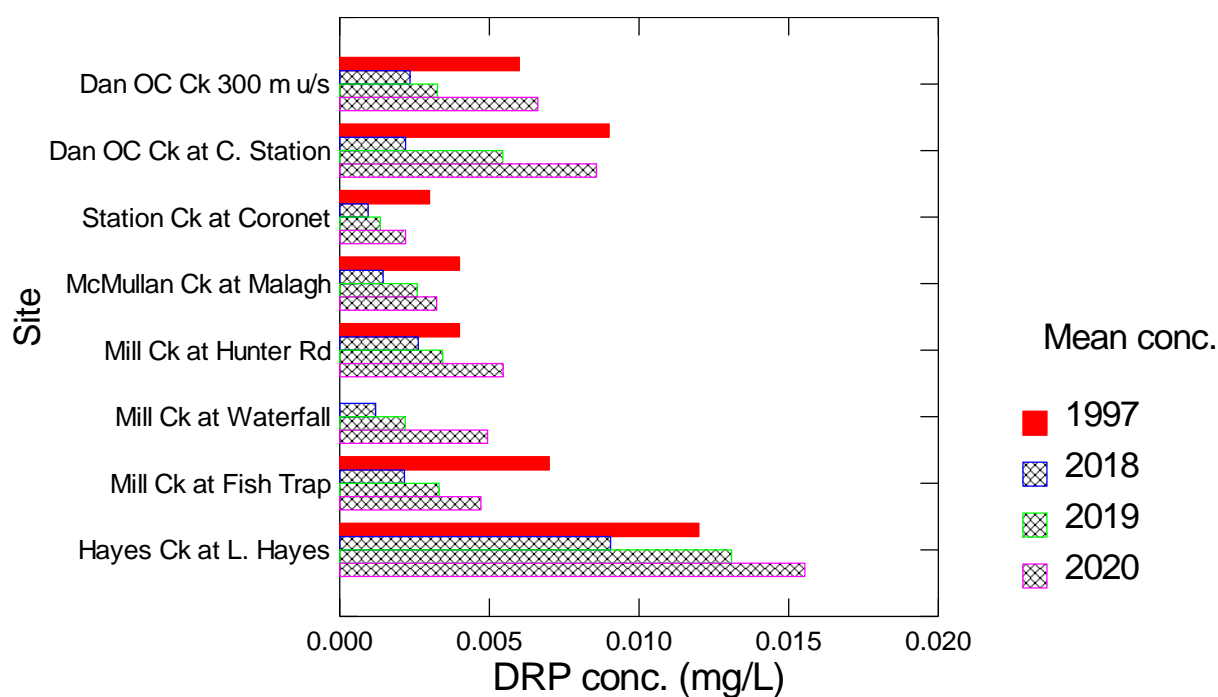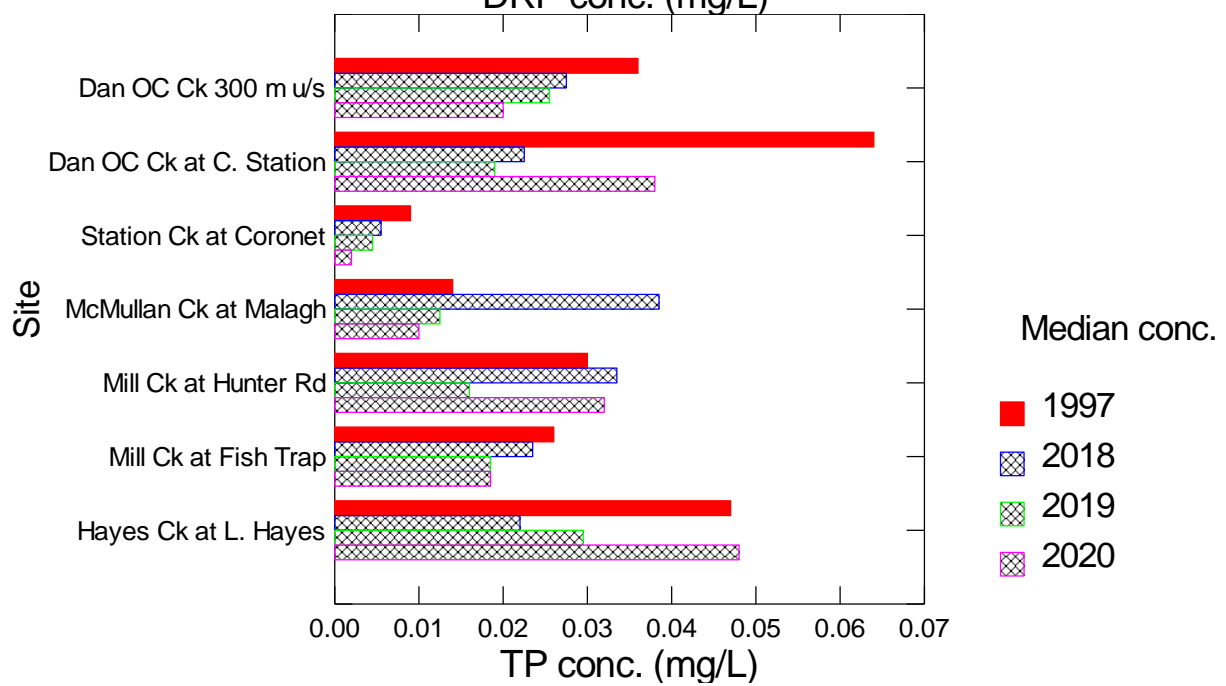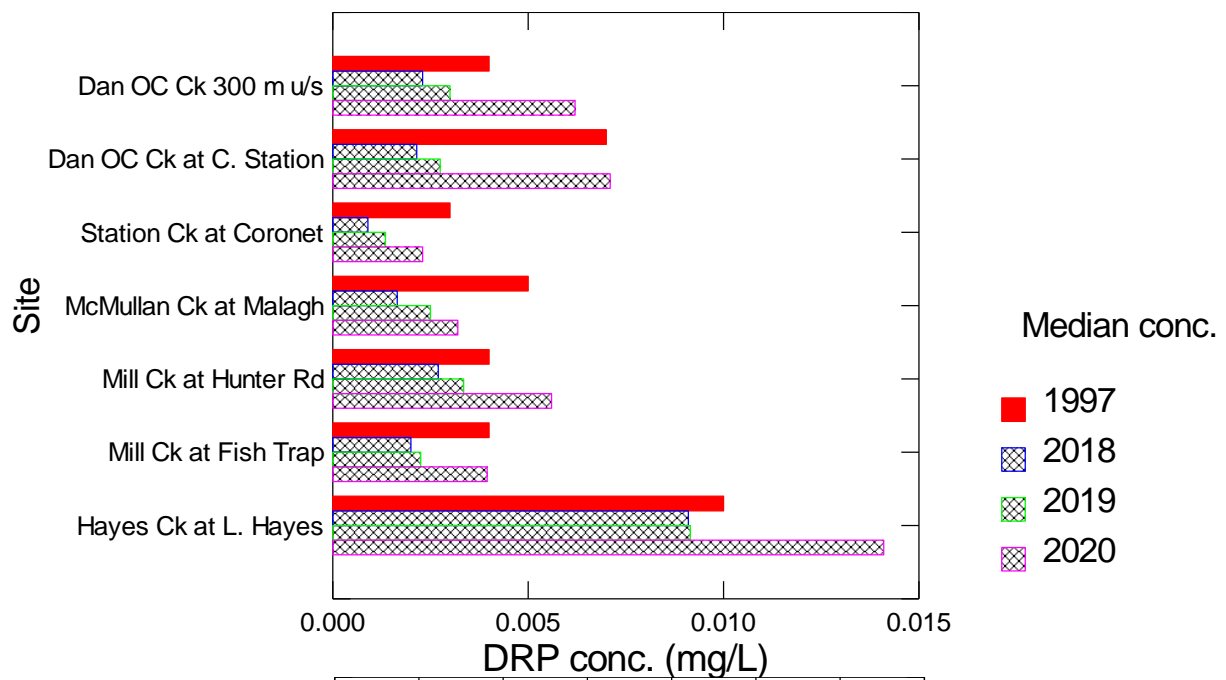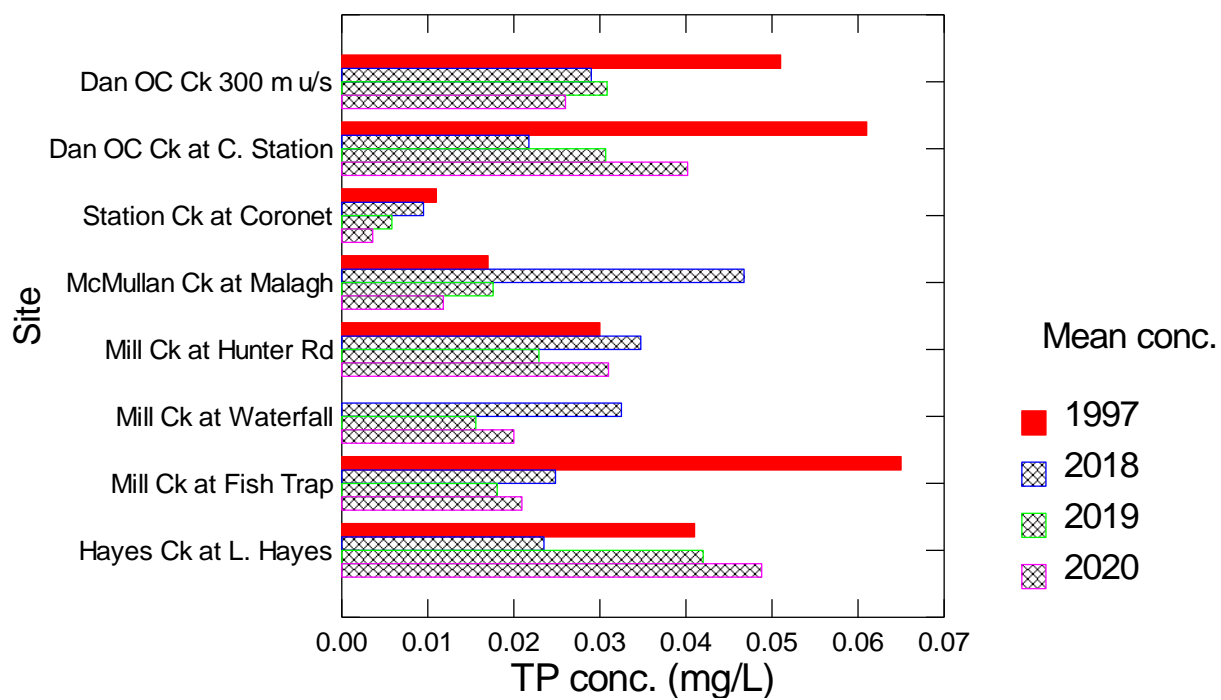
Appendix E Summary statistics for water quality data (2018-2020)

Site(rows) by Month(columns) – Number of results per month													
	1	**2**	**3**	**4**	**5**	**6**	**7**	**8**	**9**	**10**	**11**	**12**	**Total**
Dan OC Ck 300 m u/s	2	2	2	1	1	2	2	1	2	2	2	2	21
Dan OC Ck at C. Station	2	2	2	1	1	2	2	1	2	2	2	2	21
Station Ck at Coronet	2	2	2	1	1	2	2	1	2	2	2	2	21
McMullan Ck at Malagh	2	2	2	1	1	2	2	1	2	2	2	2	21
Mill Ck at Hunter Rd	2	2	2	1	1	2	2	1	2	2	2	2	21
Mill Ck at Waterfall	2	2	2	1	1	2	2	1	2	2	2	2	21
Mill Ck at Fish Trap	4	4	4	2	3	4	4	3	4	4	4	4	44
Mill Ck at L. Hayes	4	4	4	2	2	3	44	2	70	26	28	28	217
L. Hayes spring	2	2	2	1	1	2	2	1	2	2	2	2	21
Hayes Ck at L. Hayes	2	2	2	1	1	2	2	1	2	2	2	2	21
Total	**24**	**24**	**24**	**12**	**13**	**23**	**64**	**13**	**90**	**46**	**48**	**48**	**429**

Results for SITE_NAME$ = Dan O'C Ck at C. Station

	NNN conc. (mg/L)	TN conc. (mg/L)	DRP conc. (mg/L)	TP conc. (mg/L)	Turbidity (NTU)	TSS conc. (mg/L)	Discharge (L/s)
N of Cases	20	20	20	20	20	18	20
Minimum	0.004	0.065	0.001	0.010	1.440	10.300	34.000
Maximum	0.048	0.780	0.030	0.105	21.000	103.000	98.000
Median	0.020	0.139	0.003	0.021	4.350	25.000	59.500
Arithmetic Mean	0.021	0.190	0.006	0.032	6.517	30.483	61.800
Standard Deviation	0.009	0.163	0.007	0.026	5.193	21.042	19.311
Percentiles							
10.000%	0.012	0.072	0.002	0.011	2.500	14.700	37.000
25.000%	0.014	0.095	0.002	0.013	3.350	20.000	47.500
40.000%	0.019	0.134	0.003	0.019	4.000	21.700	52.500
60.000%	0.025	0.153	0.003	0.026	5.000	27.000	65.000
75.000%	0.026	0.191	0.006	0.048	8.050	31.000	78.000
90.000%	0.030	0.360	0.014	0.069	15.400	50.400	90.000

Results for SITE_NAME$ = Dan O'C Ck 300 m u/s

	NNN conc. (mg/L)	TN conc. (mg/L)	DRP conc. (mg/L)	TP conc. (mg/L)	Turbidity (NTU)	TSS conc. (mg/L)	Discharge (L/s)
N of Cases	22	22	22	22	22	20	22
Minimum	0.001	0.063	0.001	0.002	0.630	1.000	1.000
Maximum	0.182	0.440	0.012	0.082	14.100	77.000	60.000
Median	0.034	0.215	0.003	0.022	6.200	22.000	20.000
Arithmetic Mean	0.049	0.218	0.004	0.029	6.379	25.440	19.136
Standard Deviation	0.053	0.100	0.002	0.021	4.413	22.075	11.890
Percentiles							
10.000%	0.001	0.079	0.002	0.009	1.260	2.350	2.000
25.000%	0.010	0.155	0.003	0.015	1.840	5.100	14.000
40.000%	0.026	0.181	0.003	0.020	4.500	16.450	18.300
60.000%	0.045	0.240	0.004	0.026	6.640	27.500	20.700
75.000%	0.068	0.290	0.005	0.034	10.500	38.500	22.000
90.000%	0.147	0.343	0.007	0.064	12.760	57.500	27.000

Results for SITE_NAME$ = Hayes Ck at L. Hayes

	NNN conc. (mg/L)	TN conc. (mg/L)	DRP conc. (mg/L)	TP conc. (mg/L)	Turbidity (NTU)	TSS conc. (mg/L)	Discharge (L/s)
N of Cases	21	21	21	21	21	19	19
Minimum	0.001	0.200	0.001	0.008	0.460	0.800	304.000
Maximum	0.042	0.740	0.032	0.108	3.900	15.100	845.000
Median	0.008	0.310	0.011	0.036	1.130	4.700	513.000
Arithmetic Mean	0.013	0.369	0.013	0.040	1.475	5.763	541.211
Standard Deviation	0.014	0.144	0.011	0.026	0.983	3.592	126.453
Percentiles							
10.000%	0.001	0.232	0.001	0.015	0.564	1.920	404.200
25.000%	0.001	0.270	0.004	0.018	0.835	3.775	469.750
40.000%	0.003	0.299	0.007	0.028	1.029	4.220	502.600
60.000%	0.010	0.353	0.014	0.046	1.318	5.620	533.900
75.000%	0.029	0.402	0.020	0.054	1.752	7.325	613.750
90.000%	0.035	0.596	0.031	0.076	3.280	11.220	724.400

Results for SITE_NAME$ = Station Ck at Coronet

	NNN conc. (mg/L)	TN conc. (mg/L)	DRP conc. (mg/L)	TP conc. (mg/L)	Turbidity (NTU)	TSS conc. (mg/L)	Discharge (L/s)
N of Cases	21	21	21	21	21	19	18
Minimum	0.135	0.176	0.001	0.002	0.110	1.800	18.000
Maximum	0.320	0.400	0.004	0.025	6.800	40.000	96.000
Median	0.220	0.240	0.001	0.004	0.960	4.800	41.000
Arithmetic Mean	0.220	0.246	0.001	0.006	1.515	8.568	48.611
Standard Deviation	0.043	0.054	0.001	0.006	1.540	9.926	25.252
Percentiles							
10.000%	0.164	0.189	0.001	0.002	0.344	2.140	22.600
25.000%	0.186	0.200	0.001	0.002	0.725	3.500	32.000
40.000%	0.219	0.229	0.001	0.002	0.864	3.950	38.700
60.000%	0.231	0.251	0.002	0.005	1.203	6.570	44.200
75.000%	0.242	0.285	0.002	0.008	1.647	7.825	53.000
90.000%	0.262	0.300	0.002	0.014	3.400	23.160	93.700

Results for SITE_NAME$ = McMullan Ck at Malagh

	NNN conc. (mg/L)	TN conc. (mg/L)	DRP conc. (mg/L)	TP conc. (mg/L)	Turbidity (NTU)	TSS conc. (mg/L)	Discharge (L/s)
N of Cases	21	21	21	21	21	19	21
Minimum	0.119	0.220	0.001	0.002	1.560	7.000	37.000
Maximum	0.290	0.910	0.005	0.082	23.000	420.000	188.000
Median	0.200	0.280	0.003	0.013	3.400	22.000	76.000
Arithmetic Mean	0.203	0.328	0.003	0.022	5.355	54.437	91.048
Standard Deviation	0.045	0.152	0.001	0.019	6.071	94.997	42.036
Percentiles							
10.000%	0.137	0.230	0.001	0.006	1.756	13.200	46.600
25.000%	0.178	0.250	0.002	0.010	2.150	19.000	65.500
40.000%	0.185	0.269	0.002	0.012	2.980	22.000	73.400
60.000%	0.220	0.310	0.003	0.018	4.040	24.800	82.200
75.000%	0.232	0.333	0.003	0.029	5.000	37.000	110.500
90.000%	0.264	0.448	0.004	0.045	13.700	126.600	162.400

Results for SITE_NAME$ = Mill Ck at Fish Trap

	NNN conc. (mg/L)	TN conc. (mg/L)	DRP conc. (mg/L)	TP conc. (mg/L)	Turbidity (NTU)	TSS conc. (mg/L)	Discharge (L/s)
N of Cases	44	43	43	44	44	44	42
Minimum	0.173	0.330	0.001	0.009	0.870	4.200	242.000
Maximum	0.570	0.840	0.016	0.069	18.100	32.000	785.000
Median	0.350	0.490	0.002	0.019	4.100	9.850	400.000
Arithmetic Mean	0.371	0.530	0.004	0.021	4.624	11.127	422.762
Standard Deviation	0.096	0.124	0.003	0.010	2.994	6.102	120.828
Percentiles							
10.000%	0.265	0.388	0.002	0.011	2.290	5.680	279.500
25.000%	0.300	0.430	0.002	0.016	2.700	6.950	336.000
40.000%	0.341	0.470	0.002	0.018	3.440	8.810	382.000
60.000%	0.380	0.542	0.003	0.020	4.390	10.890	426.800
75.000%	0.460	0.647	0.005	0.025	5.250	12.150	496.000
90.000%	0.490	0.666	0.006	0.029	7.420	18.240	556.300

Results for SITE_NAME$ = Mill Ck at Hunter Rd.

	NNN conc. (mg/L)	TN conc. (mg/L)	DRP conc. (mg/L)	TP conc. (mg/L)	Turbidity (NTU)	TSS conc. (mg/L)	Discharge (L/s)
N of Cases	21	21	21	21	21	19	19
Minimum	0.230	0.340	0.001	0.008	0.620	9.600	142.000
Maximum	0.360	0.660	0.007	0.056	12.100	75.000	412.000
Median	0.320	0.460	0.004	0.022	5.500	20.000	226.000
Arithmetic Mean	0.315	0.474	0.004	0.027	5.496	25.600	251.579
Standard Deviation	0.040	0.075	0.002	0.013	2.754	16.176	77.204
Percentiles							
10.000%	0.246	0.384	0.002	0.014	2.800	10.760	163.400
25.000%	0.290	0.430	0.002	0.014	3.750	16.075	204.500
40.000%	0.310	0.449	0.003	0.020	4.300	19.550	222.200
60.000%	0.332	0.470	0.004	0.030	5.810	22.900	242.600
75.000%	0.350	0.532	0.005	0.036	6.275	30.000	304.500
90.000%	0.360	0.568	0.007	0.047	9.620	47.400	384.000

Results for SITE_NAME$ = Mill Ck at Waterfall

	NNN conc. (mg/L)	TN conc. (mg/L)	DRP conc. (mg/L)	TP conc. (mg/L)	Turbidity (NTU)	TSS conc. (mg/L)	Discharge (L/s)
N of Cases	21	21	21	21	21	19	0
Minimum	0.280	0.380	0.001	0.010	0.920	2.000	.
Maximum	0.570	0.760	0.011	0.080	32.000	16.000	.
Median	0.370	0.500	0.002	0.017	2.900	6.300	.
Arithmetic Mean	0.393	0.546	0.003	0.020	4.480	6.432	.
Standard Deviation	0.084	0.114	0.002	0.015	6.453	3.146	.
Percentiles							
10.000%	0.296	0.436	0.001	0.011	1.696	3.040	.
25.000%	0.328	0.468	0.001	0.013	2.075	4.375	.
40.000%	0.350	0.479	0.002	0.014	2.400	5.260	.
60.000%	0.386	0.536	0.003	0.018	3.420	7.200	.
75.000%	0.465	0.635	0.003	0.020	4.150	7.900	.
90.000%	0.502	0.734	0.005	0.027	5.600	9.240	.

Results for SITE_NAME$ = L. Hayes spring

	NNN conc. (mg/L)	TN conc. (mg/L)	DRP conc. (mg/L)	TP conc. (mg/L)	Turbidity (NTU)	TSS conc. (mg/L)	Discharge (L/s)
N of Cases	21	21	21	21	21	19	21
Minimum	0.950	1.020	0.001	0.002	0.060	0.250	8.000
Maximum	1.130	1.520	0.002	0.004	0.300	0.450	44.000
Median	1.040	1.120	0.001	0.002	0.110	0.250	37.000
Arithmetic Mean	1.030	1.129	0.001	0.002	0.129	0.261	34.952
Standard Deviation	0.046	0.105	0.001	0.001	0.067	0.046	9.739
Percentiles							
10.000%	0.960	1.036	0.001	0.002	0.070	0.250	20.200
25.000%	0.998	1.065	0.001	0.002	0.080	0.250	32.500
40.000%	1.030	1.099	0.001	0.002	0.099	0.250	37.000
60.000%	1.040	1.130	0.001	0.002	0.120	0.250	39.000
75.000%	1.060	1.160	0.001	0.002	0.140	0.250	40.250
90.000%	1.080	1.198	0.002	0.003	0.248	0.250	43.400

Results for SITE_NAME$ = Mill Ck at L. Hayes

	NNN conc. (mg/L)	TN conc. (mg/L)	DRP conc. (mg/L)	TP conc. (mg/L)	Turbidity (NTU)	TSS conc. (mg/L)	Discharge (L/s)
N of Cases	215	201	201	215	209	213	200
Minimum	0.177	0.350	0.001	0.010	1.980	4.200	281.000
Maximum	0.670	2.200	0.050	0.770	260.000	390.000	2,630.000
Median	0.350	1.020	0.013	0.200	51.000	107.000	1,001.500
Arithmetic Mean	0.347	1.052	0.018	0.203	59.747	122.401	1,104.635
Standard Deviation	0.090	0.344	0.013	0.138	45.588	86.708	496.362
Percentiles							
10.000%	0.220	0.556	0.003	0.021	4.000	10.980	618.000
25.000%	0.280	0.868	0.010	0.098	25.750	59.250	859.000
40.000%	0.330	0.960	0.012	0.169	44.100	94.700	970.000
60.000%	0.370	1.110	0.019	0.230	56.000	126.000	1,029.500
75.000%	0.410	1.260	0.024	0.277	95.000	187.250	1,165.000
90.000%	0.460	1.468	0.037	0.350	116.200	230.000	2,076.500

Appendix F Instantaneous load (flux) – grab samples, 2017-2021

"MGS" = mg/s

	NNN mg/s	TN mg/s	DRP mg/s	TP mg/s	SS mg/s
N of Cases	20	20	20	20	18
Minimum	0.140	2.470	0.018	0.360	391.400
Maximum	3.360	37.440	1.440	6.391	9,167.000
Median	1.235	8.688	0.174	1.333	1,552.500
Arithmetic Mean	1.356	11.597	0.343	2.025	1,989.022
Standard Deviation	0.744	9.374	0.389	1.731	1,950.738
Percentiles					
10.000%	0.536	3.558	0.090	0.467	539.280
25.000%	0.934	5.801	0.123	0.768	960.000
40.000%	1.103	7.308	0.141	1.238	1,458.800
60.000%	1.378	10.110	0.225	1.710	1,669.080
75.000%	1.850	13.193	0.430	2.784	2,156.000
90.000%	2.226	27.900	0.974	5.101	3,217.800
	NNN mg/s	**TN mg/s**	**DRP mg/s**	**TP mg/s**	**SS mg/s**
N of Cases	21	22	22	22	20
Minimum	0.007	0.168	0.006	0.020	2.000
Maximum	3.640	11.880	0.252	1.586	2,160.000
Median	0.858	4.243	0.051	0.461	438.500
Arithmetic Mean	1.059	4.209	0.070	0.587	620.040
Standard Deviation	1.028	2.889	0.061	0.535	659.862
Percentiles					
10.000%	0.016	0.366	0.007	0.026	4.950
25.000%	0.155	1.921	0.034	0.187	82.600
40.000%	0.561	3.534	0.046	0.309	261.450
60.000%	1.309	5.334	0.059	0.590	567.500
75.000%	1.617	5.950	0.084	0.780	877.000
90.000%	2.395	7.010	0.165	1.566	1,782.000
	NNN mg/s	**TN mg/s**	**DRP mg/s**	**TP mg/s**	**SS mg/s**
N of Cases	19	19	19	19	17
Minimum	0.152	82.080	0.245	3.920	495.200
Maximum	30.420	442.520	24.505	64.584	9,029.800
Median	3.229	177.080	6.355	17.416	2,226.300
Arithmetic Mean	8.977	194.758	7.811	20.925	2,910.488
Standard Deviation	10.486	93.274	7.032	14.898	2,113.477
Percentiles					
10.000%	0.241	105.792	0.520	5.719	1,153.600
25.000%	0.707	131.085	2.013	9.303	1,333.850
40.000%	1.678	163.758	3.692	12.300	2,068.290
60.000%	7.301	185.891	8.517	24.817	2,615.290
75.000%	19.725	213.495	10.605	27.839	4,123.500
90.000%	25.261	338.904	17.714	37.529	5,227.520
	NNN mg/s	**TN mg/s**	**DRP mg/s**	**TP mg/s**	**SS mg/s**
N of Cases	18	18	18	18	16
Minimum	3.096	3.492	0.011	0.036	37.800
Maximum	22.560	26.040	0.186	2.400	3,760.000
Median	9.630	10.625	0.053	0.126	242.000
Arithmetic Mean	10.902	12.088	0.067	0.366	658.544
Standard Deviation	6.301	6.821	0.048	0.568	1,087.336

	NNN mg/s	TN mg/s	DRP mg/s	TP mg/s	SS mg/s
Percentiles					
10.000%	3.521	4.312	0.014	0.050	43.320
25.000%	6.460	7.488	0.038	0.070	110.600
40.000%	8.280	9.360	0.046	0.090	186.450
60.000%	10.206	10.944	0.062	0.224	295.220
75.000%	15.040	18.630	0.112	0.424	437.650
90.000%	21.309	22.896	0.130	0.843	2,711.970

	NNN mg/s	TN mg/s	DRP mg/s	TP mg/s	SS mg/s
N of Cases	21	21	21	21	19
Minimum	4.847	9.460	0.032	0.260	343.000
Maximum	38.880	148.330	0.713	8.528	78,960.000
Median	16.720	23.780	0.184	0.924	1,628.000
Arithmetic Mean	18.554	32.788	0.230	2.407	7,874.089
Standard Deviation	8.764	31.545	0.178	2.833	18,260.219
Percentiles					
10.000%	8.392	13.258	0.079	0.356	697.500
25.000%	12.148	16.563	0.118	0.488	1,224.025
40.000%	16.222	20.418	0.163	0.854	1,492.850
60.000%	18.122	25.114	0.201	1.376	2,029.800
75.000%	24.966	34.680	0.245	2.976	3,640.000
90.000%	30.035	62.160	0.536	7.630	20,539.200

	NNN mg/s	TN mg/s	DRP mg/s	TP mg/s	SS mg/s
N of Cases	42	41	41	42	42
Minimum	41.866	81.510	0.385	3.024	1,159.200
Maximum	376.800	659.400	12.639	54.165	25,120.000
Median	148.125	207.270	1.014	7.744	4,189.500
Arithmetic Mean	159.672	232.080	1.685	9.643	5,143.117
Standard Deviation	67.580	105.216	1.984	8.357	4,297.682
Percentiles					
10.000%	83.658	128.742	0.576	3.863	1,953.770
25.000%	119.350	161.695	0.798	5.681	2,444.000
40.000%	132.378	197.592	0.948	7.024	3,293.710
60.000%	155.367	228.633	1.092	8.371	5,120.320
75.000%	206.040	292.023	2.169	11.600	5,767.200
90.000%	246.178	353.778	3.234	14.423	8,677.060

	NNN mg/s	TN mg/s	DRP mg/s	TP mg/s	SS mg/s
N of Cases	19	19	19	19	17
Minimum	45.440	66.740	0.186	1.384	1,420.000
Maximum	110.600	245.520	2.760	20.384	23,775.000
Median	75.900	103.500	0.678	5.368	4,876.000
Arithmetic Mean	77.715	119.612	0.941	7.304	7,334.053
Standard Deviation	18.608	43.337	0.656	5.838	6,889.851
Percentiles					
10.000%	58.132	78.956	0.299	2.324	1,853.840
25.000%	62.425	91.610	0.521	3.143	2,662.525
40.000%	65.740	97.692	0.635	4.265	4,647.400
60.000%	80.486	117.376	0.864	6.253	4,977.800
75.000%	93.645	146.410	1.351	7.843	7,942.500
90.000%	104.036	170.132	1.795	17.978	20,370.400

	NNN mg/s	TN mg/s	DRP mg/s	TP mg/s	SS mg/s
N of Cases	21	21	20	21	19

	NNN mg/s	TN mg/s	DRP mg/s	TP mg/s	SS mg/s
Minimum	8.240	9.120	0.005	0.016	2.000
Maximum	47.520	56.240	0.078	0.156	18.000
Median	38.480	41.810	0.021	0.076	9.500
Arithmetic Mean	35.960	39.261	0.031	0.077	9.237
Standard Deviation	10.120	11.083	0.022	0.032	3.281
Percentiles					
10.000%	21.170	22.904	0.014	0.040	4.500
25.000%	34.852	38.087	0.018	0.065	8.438
40.000%	37.072	40.314	0.020	0.074	9.250
60.000%	39.992	42.226	0.022	0.080	9.750
75.000%	41.360	44.828	0.045	0.086	10.625
90.000%	44.908	48.976	0.071	0.112	11.000

	NNN mg/s	TN mg/s	DRP mg/s	TP mg/s	SS mg/s
N of Cases	200	200	200	200	198
Minimum	81.192	132.840	0.194	3.817	1,706.100
Maximum	755.950	4,852.000	72.803	1,851.850	937,950.000
Median	368.410	1,084.605	15.824	223.585	120,123.000
Arithmetic Mean	364.229	1,262.722	21.340	280.486	173,459.704
Standard Deviation	133.645	857.869	16.777	285.817	184,589.792
Percentiles					
10.000%	217.025	340.425	1.517	14.471	9,999.800
25.000%	253.700	785.095	9.780	116.329	68,229.000
40.000%	347.130	987.500	12.119	171.820	101,521.900
60.000%	385.660	1,189.065	20.121	249.795	148,449.000
75.000%	438.015	1,387.665	33.085	322.345	191,400.000
90.000%	549.900	2,490.025	48.216	621.090	411,750.000

Appendix G   Annual mass load estimates, Fish Trap site

Year	Annual load (t)			
	NNN	TP	TSS	
			Regression model	LOADEST
1983	9.56	2.93	2446.1	1330.3
1984	8.77	1.59	1440.9	728.8
1985	6.29	0.70	664.8	304.1
1986	6.03	0.66	596.1	286.0
1987	8.13	1.45	1234.4	734.6
1988	6.94	1.01	871.1	536.0
1989	5.71	0.55	517.1	250.4
1990	5.46	0.50	473.3	232.9
1991	6.50	1.57	1332.7	864.8
1992	6.20	0.86	812.1	498.0
1993	7.39	1.22	1153.6	770.3
1994	10.04	2.99	2714.8	2101.0
1995	9.25	2.93	2790.3	2159.5
1996	8.85	2.27	2192.5	1630.7
1997	6.18	0.86	892.8	565.7
1998	6.68	1.12	1172.2	801.9
1999	6.91	2.26	2390.6	1700.6
2000	8.98	2.36	2477.1	1832.6
2001	4.96	0.51	584.5	311.9
2002	6.03	1.25	1410.4	932.2
2003	4.95	0.51	632.2	331.2
2004	5.55	0.79	959.8	553.1
2005	5.13	0.56	716.4	354.2
2006	4.54	0.53	710.6	357.6
2007	5.20	0.72	961.0	498.6
2008	3.97	0.31	457.9	176.7
2009	5.55	0.74	1026.7	471.3
2010	5.91	0.76	1138.0	491.1
2011	5.03	0.49	804.7	288.7
2012	4.13	0.33	559.3	180.1
2013	5.36	0.66	1083.6	383.6
2014	5.12	0.53	927.5	290.8
2015	5.13	0.52	938.3	272.2
2016	4.23	0.31	616.7	148.1
2017	4.06	0.28	575.7	119.9
2018	5.23	0.64	1306.4	310.4
2019	4.92	0.47	1046.7	211.5
2020	5.26	0.71	1595.0	309.6
2021	5.38	0.67	1585.2	283.2

Estimation of contaminant losses

Appendix H   Monthly load estimates, Fish Trap site

Table H-1:   Monthly estimate of TP load. Derived from LOADEST model using Fish Trap data. * = incomplete year.

Year	Load per month (kg)												Annual Total (kg)
	Jan.	Feb.	June	Mar.	Apr.	May	Aug.	July	Sep.	Oct.	Nov.	Dec.	
2001	67.0	34.2	46.2	50.1	41.2	39.3	37.2	56.4	42.9	33.2	27.9	32.6	508.1
2002	48.4	18.8	35.7	29.1	23.3	63.0	38.1	74.1	476.4	203.4	149.4	92.4	1251.9
2003	42.5	23.2	28.2	30.6	35.0	30.9	47.7	23.9	66.3	81.5	67.5	35.3	512.7
2004	19.8	27.7	19.5	19.5	24.2	63.9	44.3	152.5	135.9	86.8	82.8	110.4	787.4
2005	78.4	55.4	80.0	65.1	39.4	34.5	32.6	41.2	39.3	38.1	33.3	23.6	560.9
2006	30.1	14.0	15.5	30.0	19.2	29.1	20.8	36.3	50.4	67.6	124.2	88.7	525.8
2007	44.0	27.4	30.7	20.7	43.1	47.4	40.9	97.0	58.8	204.6	83.4	25.4	723.5
2008	26.4	18.8	23.3	23.1	20.8	15.6	20.8	15.2	39.6	40.3	29.4	36.6	309.7
2009	27.6	17.9	23.9	36.9	125.9	43.5	79.7	114.7	79.2	94.9	57.9	35.3	737.3
2010	36.6	24.9	35.3	58.5	59.8	59.7	46.5	76.3	125.1	121.8	67.8	51.5	763.8
2011	44.0	35.0	39.7	37.8	34.7	25.2	42.5	40.9	43.2	64.5	56.1	31.0	494.6
2012	18.3	13.4	18.3	13.5	15.5	22.8	28.2	16.7	58.2	50.8	45.3	27.6	328.7
2013	34.1	19.3	21.7	26.7	23.9	89.4	112.5	47.7	75.0	105.7	61.5	38.1	655.7
2014	30.1	18.2	21.4	24.9	50.5	40.8	46.5	122.1	55.8	58.9	39.0	26.0	534.3
2015	21.7	14.6	18.6	25.2	66.7	82.2	68.5	68.2	46.2	59.8	36.9	16.1	524.7
2016	10.2	18.8	11.2	19.2	29.8	18.9	37.5	27.6	24.0	46.5	36.0	34.4	314.0
2017	33.2	22.7	20.5	22.8	22.0	19.2	20.2	26.7	31.5	28.2	19.5	9.0	275.3
2018	6.5	17.9	15.5	28.2	76.0	28.2	130.2	66.3	72.6	66.3	82.5	48.4	638.6
2019	27.3	17.4	21.4	41.7	65.7	56.7	43.7	32.6	28.5	31.3	31.8	76.0	474.0
2020	36.6	58.2	22.0	24.6	33.8	20.1	177.0	41.5	141.9	93.9	41.1	22.9	713.7
2021	37.2	14.6	17.1	20.7	21.7	21.3	136.4	118.1	129.3	70.4	48.9	32.2	667.8
2022	14.9	17.4	12.7	–	–	–	–	–	–	–	–	–	45.0 *

Table H-2: **Monthly estimate of NNN load.** Derived from LOADEST model using Fish Trap data. * = incomplete year.

Year	Load per month (kg)												Annual Total (kg)
	Jan.	Feb.	June	Mar.	Apr.	May	Aug.	July	Sep.	Oct.	Nov.	Dec.	
2001	418.8	290.1	358.7	398.1	413.9	445.5	451.4	513.1	522.6	443.9	359.7	342.2	4957.9
2002	340.1	226.2	320.2	314.4	320.5	492.3	499.1	616.9	822.6	870.5	684.0	519.6	6026.4
2003	350.0	245.8	293.9	323.7	374.8	399.3	465.6	426.3	584.7	623.4	504.9	355.3	4947.6
2004	256.7	263.2	248.9	265.5	324.0	492.3	526.1	704.9	745.2	638.6	545.7	539.7	5550.8
2005	430.3	350.3	439.3	437.1	403.0	425.1	465.3	527.6	502.8	459.7	384.9	301.0	5126.4
2006	296.1	200.8	228.8	303.6	300.7	378.6	371.7	428.7	491.1	504.1	531.6	505.0	4540.7
2007	356.2	265.7	292.0	270.0	397.7	414.6	450.1	530.1	527.4	837.9	545.7	307.8	5195.3
2008	280.6	225.1	266.0	285.6	307.8	301.8	367.7	342.9	417.3	466.9	355.8	352.2	3969.5
2009	293.0	221.5	274.7	342.9	529.2	470.1	554.6	732.2	647.7	656.6	472.8	355.9	5551.0
2010	331.7	257.6	323.3	402.9	480.2	531.3	541.6	647.3	768.6	713.9	507.0	401.1	5906.5
2011	354.6	292.0	338.8	354.0	386.0	379.2	502.2	532.0	522.0	556.8	471.0	340.7	5029.3
2012	246.8	191.5	243.0	231.0	274.7	347.7	385.0	368.0	566.4	514.0	434.1	325.2	4127.3
2013	310.0	229.0	262.3	307.5	331.4	506.4	703.1	570.7	614.4	659.4	492.0	372.3	5358.5
2014	307.8	229.3	262.9	300.0	415.4	442.8	538.5	758.3	579.9	555.5	413.1	321.2	5124.6
2015	266.6	205.5	252.0	297.9	481.4	569.4	625.0	657.5	543.3	561.7	408.9	262.6	5131.8
2016	197.2	232.7	204.9	273.0	367.0	342.6	477.1	465.3	418.5	485.5	401.4	361.5	4226.6
2017	321.5	253.7	264.7	294.3	324.9	345.6	393.1	450.4	467.4	425.6	312.6	208.6	4062.4
2018	165.9	207.5	235.3	306.3	425.6	405.6	677.0	656.0	603.6	589.3	541.2	414.5	5227.7
2019	298.8	230.7	267.5	349.2	439.9	533.1	537.5	504.7	452.7	447.0	386.7	470.3	4918.2
2020	341.3	292.9	280.2	308.4	361.5	350.4	612.9	561.1	737.7	669.0	436.2	313.4	5265.0
2021	332.3	218.1	253.0	291.3	330.8	360.6	641.7	741.8	767.1	609.8	465.0	363.9	5375.4
2022	244.9	219.2	225.4	–	–	–	–	–	–	–	–	–	689.5*

Table H-3:   Monthly estimate of TSS load. Derived from LOADEST model using Fish Trap data. * = incomplete year.

Years	Load per month (t)												Annual total (t)
	Jan.	Feb.	June	Mar.	Apr.	May	Aug.	July	Sep.	Oct.	Nov.	Dec.	
2003	7.3	4.4	5	5.2	5.9	5.8	9.8	5.9	12.3	14.5	11.9	6.8	94.8
2004	4.4	4.7	3.9	3.9	4.6	10.1	7.8	32.4	26.3	14.9	13.7	16.9	143.5
2005	11.4	7.6	9.9	8.2	6	5.9	6.2	7.8	7.8	7.7	6.7	5	90.4
2006	5.4	3.1	3.2	4.8	3.9	5.2	4.7	7.8	10.8	13.1	25.4	13.5	101
2007	6.9	4.5	4.4	3.8	6.3	7.5	7.5	23.7	11	35.1	13.7	5.2	129.5
2008	4.8	3.6	4	4	4	3.7	4.7	4.3	8.6	8.1	6.2	6.7	62.5
2009	5.1	3.5	4.2	5.5	19.6	6.8	15.1	19.8	13.8	16.6	10.4	6.6	126.9
2010	6.2	4.3	5.5	8	8.4	8.9	8.1	13.6	21.9	21.8	12.3	9.3	128.3
2011	7.4	5.7	6.1	6.2	6.2	5.5	7.9	8.3	9	12.8	10.9	6.5	92.6
2012	4.2	3.2	3.8	3.2	3.7	4.9	6.6	4.9	12.1	11	9.6	6.2	73.6
2013	6.8	4.1	4.4	5	5	18.6	20.7	10.3	16.9	23.1	13.2	8.4	136.3
2014	6.4	4.2	4.6	5.1	9.3	8.3	9.9	27.7	13.1	14	9.6	6.7	118.9
2015	5.5	3.9	4.5	5.5	12.3	16.9	14.8	15.9	12.1	15.4	10	5.3	121.9
2016	3.7	3.8	3.6	4.9	7	5.6	10	8.5	8	14.1	10.7	9.7	89.6
2017	8.6	6	5.5	5.9	6.2	6.1	7	9.1	10.8	10	7.4	4.4	87.1
2018	3.6	5.8	5.1	7.7	25.9	8.6	52.9	20.7	26.3	22.8	28.1	15.7	223.3
2019	9.2	6	7	11.9	19.8	16.5	14.9	12.8	12.3	13.5	13.2	28	165.2
2020	12.9	26.7	7.9	8.5	12.9	8.6	178.7	17.5	75.6	41.3	18.4	11	420
2021	15.2	6.7	7.5	8.5	9.3	10	95.4	64.8	70.9	35.5	24.7	16.3	364.9
2022	8.5	8.8	7	–	–	–	–	–	–	–	–	–	24.4*

Table H-4: Summary statistics for monthly TP load for two 19 year periods – 1984-2002 and 2003-2021 inclusive.

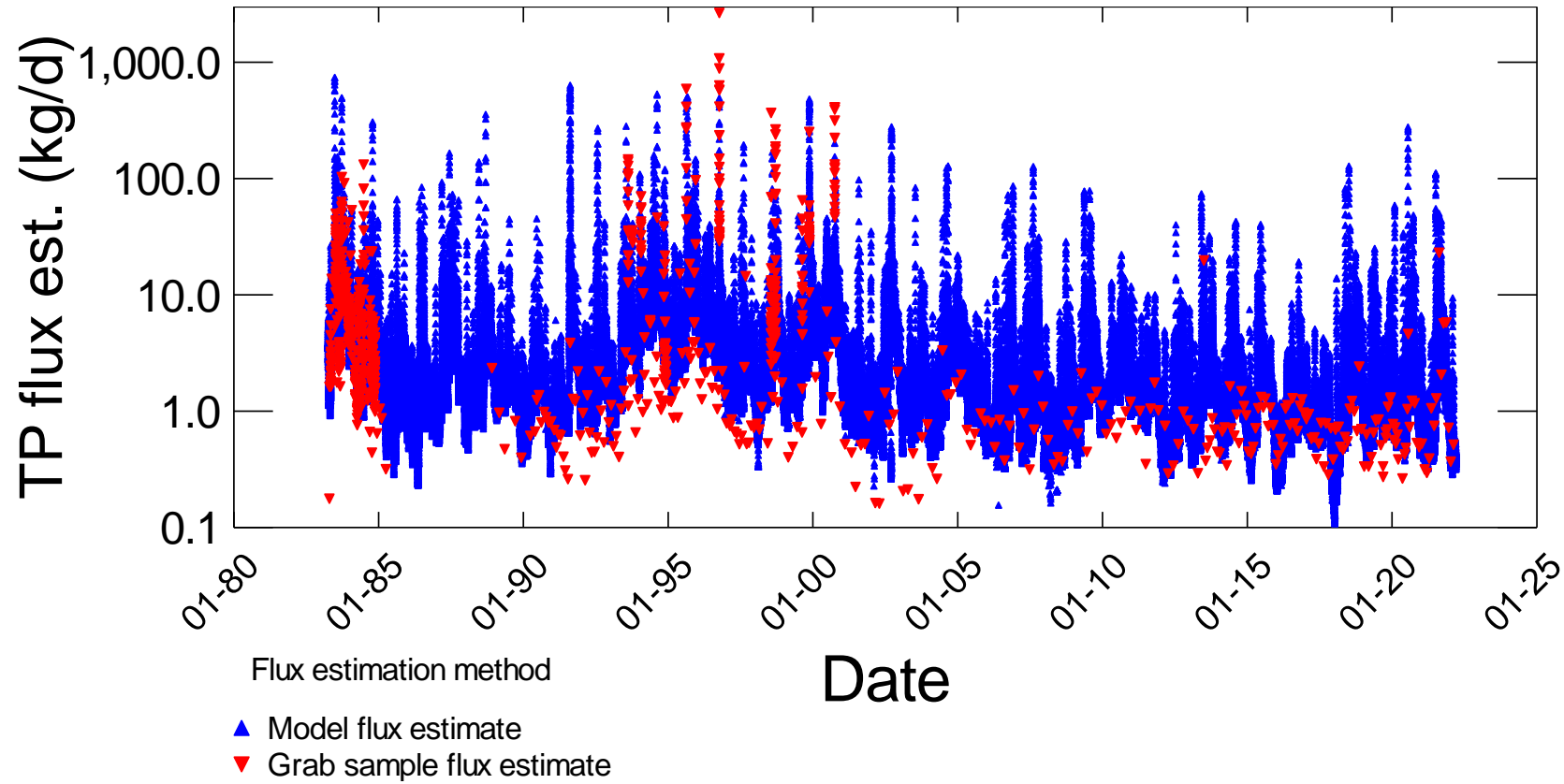| Statistic	TP load/month (kg)	
	1984-2002	2003-2021
N of Cases	228	228
Minimum	17.6	6.5
Maximum	1227	204.6
Arithmetic Mean	116.8	46.2
Standard Deviation	139.5	32.8
Percentile		
1.00%	20.1	10.0
5.00%	26.9	15.5
10.00%	31.2	18.4
20.00%	38.5	21.4
25.00%	42.8	23.2
30.00%	46.2	25.2
40.00%	58.2	30.1
50.00%	72.8	35.7
60.00%	91.8	41.3
70.00%	116.9	50.6
75.00%	141.7	58.9
80.00%	157.6	66.3
90.00%	240.2	88.1
95.00%	350.9	122.3
99.00%	770.8	157.9

Figure H-1: **Comparison of instantaneous and modelled total phosphorus (TP) loads for the Fish Trap site.** Note that the Y axis of the plot has log10 scale.

Table H-5: Summary statistics for monthly NNN load for two 19 year periods – 1984-2002 and 2003-2021 inclusive.

Statistic	NNN load/month (kg)	
	1984-2002	2003-2021
N of Cases	228	228
Minimum	226.24	165.85
Maximum	1360.8	837.93
Arithmetic Mean	593.4	415.1
Standard Deviation	223.3	141.6
Percentiles		
1.00%	258.7	195.9
5.00%	314.3	228.4
10.00%	331.5	252.3
20.00%	396.8	292.0
25.00%	422.5	301.4
30.00%	445.4	320.4
40.00%	494.9	351.6
50.00%	548.5	389.9
60.00%	611.3	436.5
70.00%	689.1	486.0
75.00%	719.0	510.5
80.00%	790.9	537.1
90.00%	907.6	620.7
95.00%	994.2	679.6
99.00%	1237.2	767.4
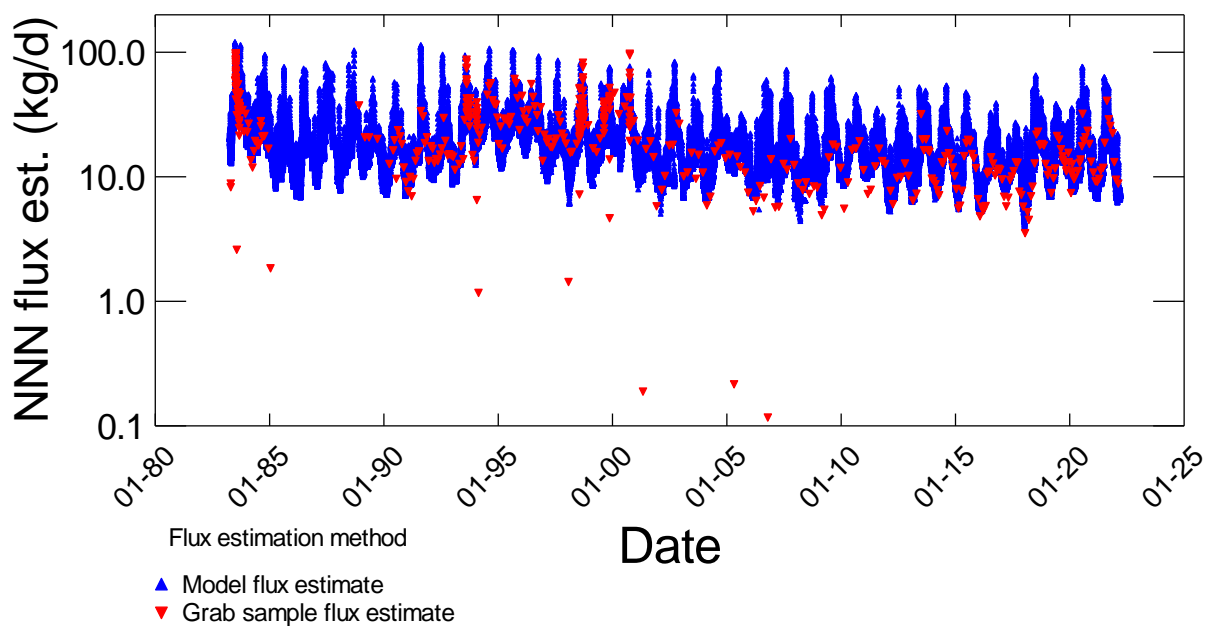
Figure H-2: **Comparison of instantaneous and modelled nitrate-nitrite N (NNN) loads for the Fish Trap site.** Note that the Y axis of the plot has log10 scale.
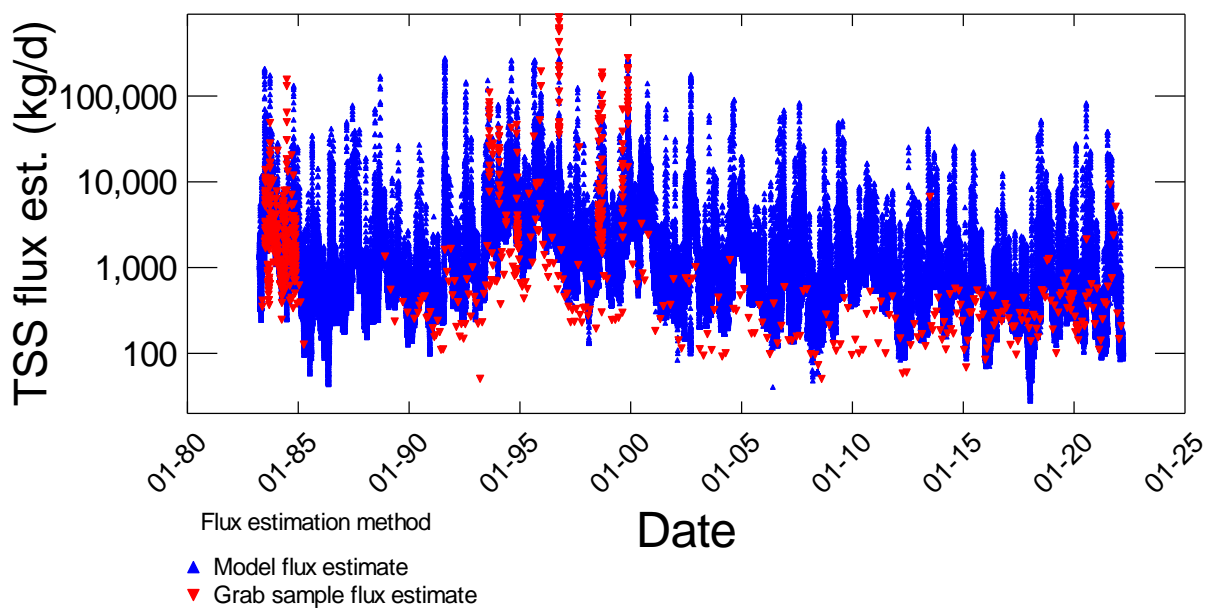
Figure H-3: **Comparison of instantaneous and modelled total suspended solids (TSS) loads for the Fish Trap site.** Note that the Y axis of the plot has log10 scale.
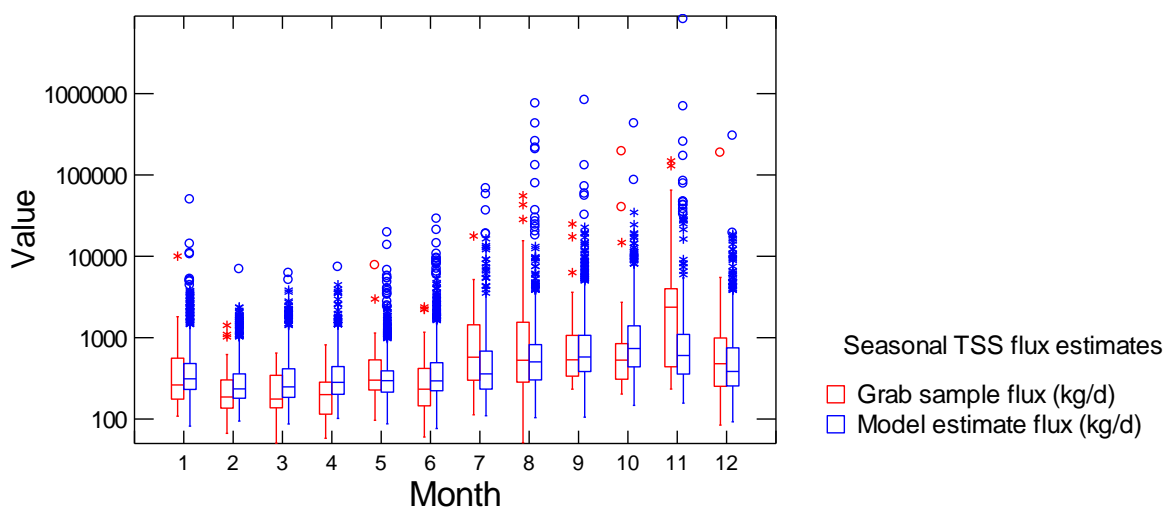
Figure H-4: **Comparison of seasonal grab sample instantaneous and modelled TSS loads for the Fish Trap site.** See Figure 3-6 for explanation of box plot components.

Table H-6: **Summary statistics for monthly TSS load for two 19 year periods – 1984-2002 and 2003-2021 inclusive.**

Statistic	TSS load/month (t)	
	1984-2002	**2003-2021**
N of Cases	228	228
Minimum	6.3	2.1
Maximum	931.2	167.6
Arithmetic Mean	75.6	26.5
Standard Deviation	104.1	22.8
Percentiles		
1.00%	7.7	3.9
5.00%	11.1	6.4
10.00%	14.5	7.3
20.00%	19.5	9.6
25.00%	20.9	10.8
30.00%	22.4	12.0
40.00%	29.9	15.8
50.00%	42.6	19.1
60.00%	52.0	23.6
70.00%	71.0	28.7
75.00%	86.9	33.5
80.00%	106.5	38.8
90.00%	171.6	59.9
95.00%	255.1	70.4
99.00%	527.9	103.4